Role of Snx9 in the Regulation of Mitochondrial Morphology

LERATO ELAINE MAGOSI

Thesis submitted to the Faculty of Graduate and Postdoctoral Studies
In partial fulfillment of the requirements
For the degree of

MASTER OF SCIENCE

Department of Biochemistry, Microbiology and Immunology
Faculty of Medicine, University of Ottawa
Ottawa, Ontario, Canada

Abstract

Mitochondria are dynamic; they alter their shape through fission, fusion and budding of vesicles. Mitochondrial vesicles serve as a quality control mechanism enabling these organelles to rid themselves of damaged lipids and proteins. Dysregulation in mitochondrial dynamics and quality control have been linked to Parkinson's Disease, making the identification of molecules requisite for these processes a priority. We identified the endocytic protein, Sorting nexin 9 (Snx9) through a genome wide siRNA screen for genes which substantially alter mitochondrial morphology and therefore are important for its maintenance. In this work, the role of Snx9 in mitochondrial morphology is examined. Ultrastructural imaging of mitochondria within cells silenced for Snx9 revealed unbudded vesicles along a hyperfused mitochondrial reticulum suggesting a role for Snx9 in the release of these vesicles. The vesicular profiles contained concentric membranous whorls enriched for neutral lipids. Localization studies suggest the Parkinson's disease genes, Parkin and Vps35 localize to the unbudded profiles.

Acknowledgements

I would like to thank my supervisor Dr. McBride for her guidance throughout this project. Furthermore, I would like to thank my family, friends and fellow lab members for their support.

Table of Contents

List of Abbreviations.

AMD	Actinomycin D
BAR	Bin amphyphisin rvs domain
Caf4	Caffeine resistant 4
CCCP	Carbonyl cyanide m-chlorophenyl hydrazone
CME	**C**lathrin **M**ediated **E**ndocytosis
DMEM	Dulbecco's modified Eagles medium
Dnm1	Dynamin 1
Dnm2	Dynamin 2
Drp1	Dynamin related protein 1
DRP3A	Dynamin related protein 3A
DRP3B	Dynamin related protein 3B
D. Melanogaster	Drosophila melanogaster
E. Coli	Escherichia coli
ECFP	Enhanced cyan fluorescent protein
EGFP	Enhanced green fluorescent protein
EYFP	Enhanced yellow fluorescent protein
EPS15	Epidermal growth factor receptor substrate 15
GST	Glutathione S transferase
FBS	Fetal Bovine Serum
Fis1	Fission protein 1
hFis1	human Fission protein 1
Ftsz	Filamentous temperature sensitive Z
Fzo	Fuzzy onion
HeLa	Henrietta Lacks culture cells
HEK293	Human embryonic kidney culture cells
H_2O_2	Hydrogen peroxide
LC	Low complexity domain
LC3	Light chain 3
LRRK2	Leucine-rich repeat kinase
MAPL	Mitochondrial anchored sumo E3 ligase
mCherry	monomeric Cherry
Mdm33	Mitochondrial distribution and morphology
Mdv1	Mitochondrial division protein 1
MDVs	Mitochondrial derived vesicles
Mff	Mitochondrial fission factor
Mfn1	Mitofusin 1
Mfn2	Mitofusin 2
Mgm1p	Mitochondrial genome maintenance protein 1
mtDNA	Mitochondrial DNA
NAO	Nonyl acridine orange
NEAA	Non-essential amino acids
NT	Non-targeted small interfering RNA
OCT	Ornithine carbamyl transferase
OsO_4	Osmium tetroxide

ORF	Open reading frame
Opa1	Optic atrophy protein 1
PBS	Phosphate buffered saline
PCR	Polymerase chain reaction
pCMV	Cytomegalovirus
PFA	Paraformaldehyde
PX	Phagocytic oxidase domain
PRDX3	Peroxiredoxin3
PVDF	Polyvinylidene fluoride
Pink1	PTEN induced putative kinase proteins
ROS	Reactive oxygen species
S. Cerevisiae	Saccharomyces Cerevisiae
SDS-PAGE	Sodium dodecyl sulfate polyacrylamide gel electrophoresis
SENP5	Sentrin-specific protease 5
SH3	Src Homology 3 domain
SMAC	Second mitochondria activator of caspases
SIMH	Stress induced mitochondrial hyperfusion
siRNA	small interfering RNA
Snx9	Sorting nexin 9
TEM	Transmission electron microscopy
tRNA	transfer RNA
Tom20	Translocase of outer membrane 20
Ubl	Ubiquitin ligase
UTR	Untranslated region
UV	Ultra violet
VPS35	Vacoular protein sorting 35
WASP	Wiskott aldrich syndrome protein
WAVE	WASP family Verprolin-homologous protein
Yme1	Yeast mitochondrial inner membrane protease

List of Figures.

1. *Introduction*

2.*Methods*

No figures

3. *Results*

4. *Discussion*

1. Introduction

1.1 A brief history highlighting the milestones in mitochondrial morphology research.

Mitochondria are double membrane organelles which house their own DNA and serve as power stations for the cell **(Figure, 1.1)**. They use the process of oxidative phosphorylation to generate ATP for the cell's energy needs. These organelles were discovered in the mid and late 1800s, first by the Swiss anatomist and physiologist Kolliker who observed granule-like structures with their own membrane, lined up between striated myofibrils of muscle. He named the structures sarcosomes (Fawcett, 1966; Leisa et al, 2009). A subsequent observation was made by Flemming in 1880, who identified granule-like structures that he called "filaments" in the cytoplasm of other cell types. A decade later, Altmann would use fuchsin to stain these organelles making it feasible to reveal their presence in a wide variety of cell types. He (Altmann) named the structures bio-blasts and likened them to bacteria, speculating that they could exist independently (Altmann, 1890). Carl Benda later renamed the bio-blasts, mitochondria (derived from the Greek terms, mitos and khondrion which mean thread and granule respectively) describing their thread-like granular form (Benda, 1898).

The early 1900s brought attention to mitochondrial dynamics, as work done by Lewis in 1914 and studies by Strangeways and Canti in 1921 would reveal that mitochondria were motile structures (Fawcett, 1966). This was evidenced by the on-going sinuous movements, and the quick twists and turns of these organelles in living cells. Moreover, Lewis noted

Figure 1.1: A colourized transmission electron micrograph of a HeLa cell illustrating the four mitochondrial compartments. These include: the outer and inner mitochondrial membranes, inter-membrane space and the matrix. Source: Lerato Magosi (McBride Lab).

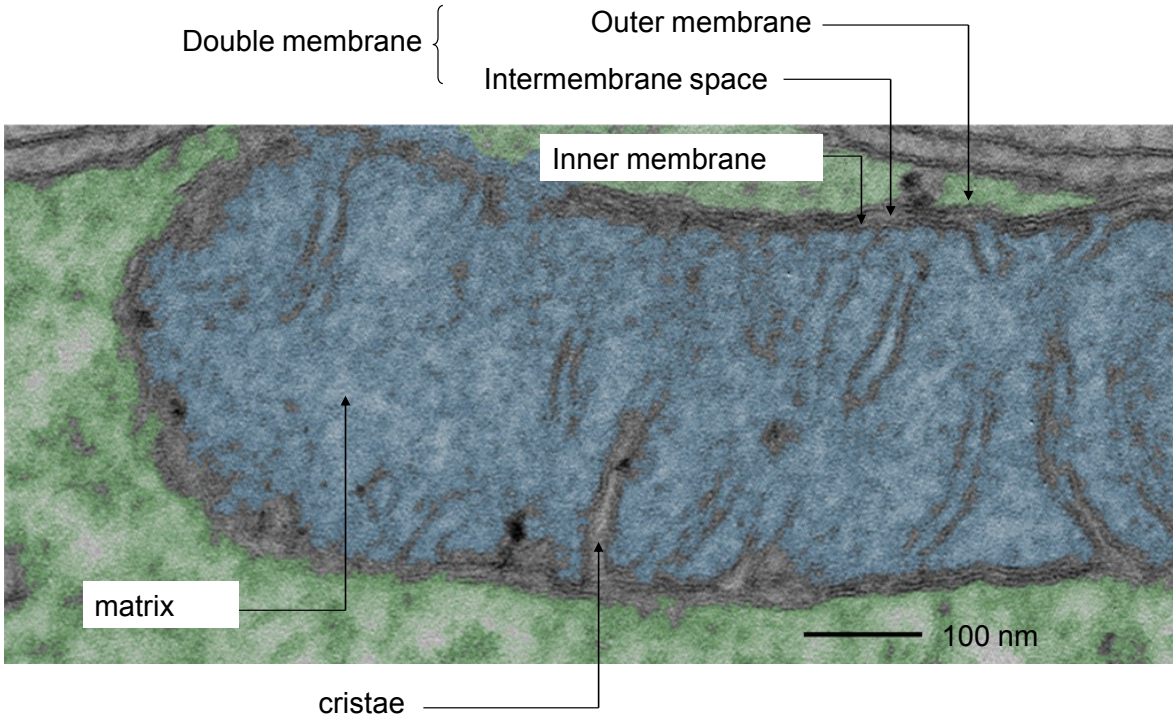
Double membrane
Outer membrane
Intermembrane space
Inner membrane
matrix
100 nm
cristae

from chick fibroblasts that mitochondria had the ability to significantly change shape, in particular he pointed out:

> We find in the living that, granules can be seen to fuse together into rods or chains, and these to elongate into threads, which in turn anastomose with each other and may unite into a complicated network, which in turn may again break down into threads, rods, loops and rings. (Lewis and Lewis, 1914: 332)

These observations highlighted that mitochondria have a plastic physique. We now know from time lapse imaging of fluorescently tagged proteins targeted to the mitochondria that these changes in shape occur through the opposing processes of mitochondrial fusion and fission (Bereiter-Hahn and Voth, 1994) **(Figure, 1.2)**.

1.2 A concise summary of the current status of mitochondrial dynamics research.

Mitochondrial fission

Fission is described as the division/fragmentation of the chondriome (total population of mitochondria in the cell) in to small spherical organelles. Mitochondria are descendents of α-proteobacteria hence it is not surprising that the machinery used to facilitate mitochondrial fragmentation in lower eukaryotes e.g. the slime mould *Dictyostelium discoideum* bears similarity to that used in bacteria such as *Escherichia coli* (Gilson et al, 2003). In *E. coli*, the GTPase and bacterial tubulin homologue FtsZ (filamentous temperature sensitive Z) localizes to the cytoplasmic side of the cell membrane at division sites to facilitate cytokinesis. Specifically, FtsZ forms a Z ring which allows for constriction

Figure 1.2: An illustration of mitochondrial dynamics. Mitochondria divide via fission and come together to form a network through fusion (Image inspired by: Modzy and Shaw, 2003).

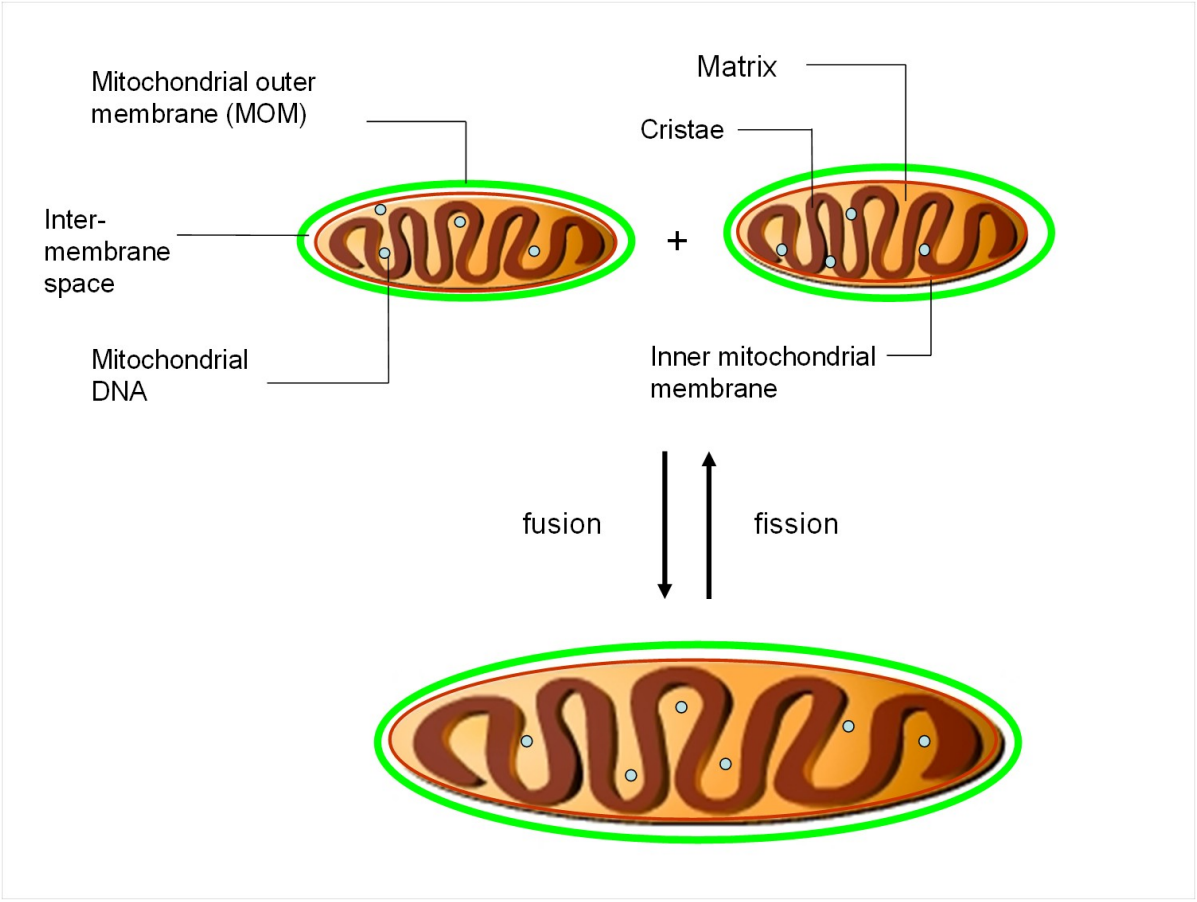
Mitochondrial outer membrane (MOM)
Matrix
Cristae
Inter-membrane space
+
Mitochondrial DNA
Inner mitochondrial membrane
fusion
fission

and eventual scission of the parent to yield two daughter cells (Dajkovic et al, 2008; Scott and Logan, 2010) **(Figure, 1.3)**.

In contrast, the fission machinery in eukaryotic cells resembles that found at the cell surface for clathrin mediated endocytosis (CME). During CME, dynamin2 (a classical dynamin) translocates from the cytosol to the cell surface where it forms rings, wrapping around the narrow neck of the budding vesicle. Additionally, dynamin 2 acts as a mechanoenzyme, using the energy obtained from the hydrolysis of GTP to cleave the enclosed membranes at the neck, freeing the nascent vesicle for fusion with the early endosome (Lundmark and Carlsson, 2003) **(Figure, 1.4)**. Mitochondrial fission events in eukaryotic cells are orchestrated by dynamin related GTPases.

In yeast e.g. *Saccharomyces cerevisiae*, the cytosolic GTPase Dnm1 (Dynamin 1) can be recruited to the mitochondrial outer membrane in two ways. The first involves the adaptor proteins mitochondrial division protein 1 (Mdv1) and fission protein 1(Fis1) **(Figure, 1.5)**. It has been postulated that the mitochondrial outer membrane protein Fis1 recruits cytosolic Mdv1 to the mitochondria. Once anchored on the outer membrane, Mdv1 interacts with GTP-bound Dnm1. This association would then promote the spiral assembly of GTP-Dnm1 oligomers around the mitochondrial outer membrane culminating in a scission event which would divide the mitochondrial tubule in two (Lackner et al, 2009; Westermann, 2010). The second involves the substitution of Mdv1 by the adaptor protein, Caffeine-resistant 4 (Caf4). Whereby, Dnm1 would be recruited to the mitochondrial outer membrane through an interaction with Caf4 rather than Mdv1, forming a Dnm1-Caf4-Fis1 fission complex. Although a substitution is possible, it would be important to note that the cardinal complex for mitochondrial fission in yeast is Dnm1-Mdv1-Fis1.

Figure 1.3: An illustration of the assembly of Ftsz (Filamentous temperature sensitive z) proteins into a ring structure (the Z ring) in *E.coli* so as to facilitate the division of the parent cell to yield two daughter units (Image inspired by: Lutkenhaus and Addinall, 1997).

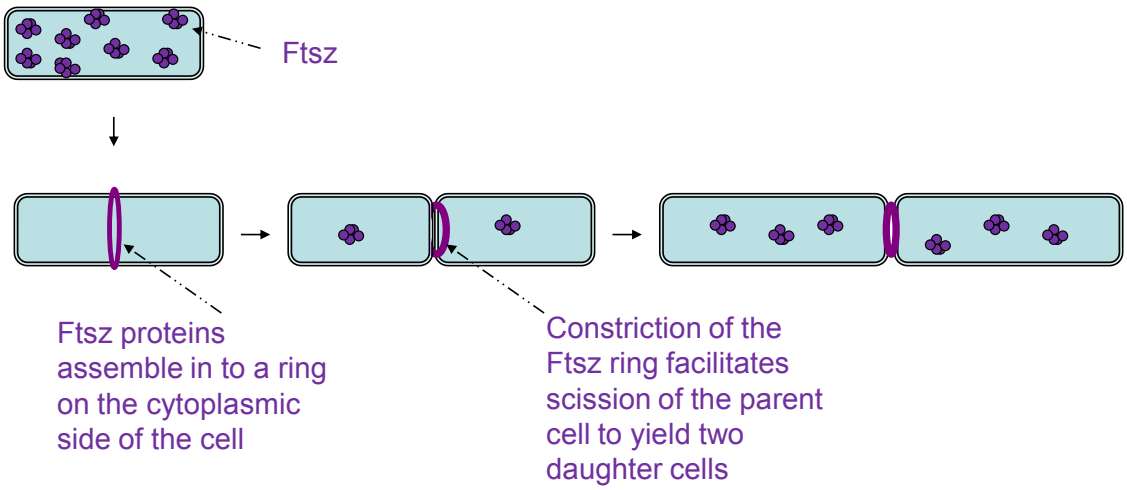
Ftsz
Ftsz proteins assemble in to a ring on the cytoplasmic side of the cell
Constriction of the Ftsz ring facilitates scission of the parent cell to yield two daughter cells

Figure 1.4: An illustration of the machinery involved in clathrin mediated endocytosis at the cell surface. Dynamin molecules gather at the neck of the budding vesicle (via Snx9 recruitment), assemble into ring structures and facilitate the scission and release of the nascent vesicle, aided by the torsion generated from actin polymerization. Actin polymerization is facilitated by the actin regulator, N- WASP (neural- Wiskott Aldrich Syndrome Protein) (Image inspired by: Lundmark and Carlsson, 2009).

Endocytosis model

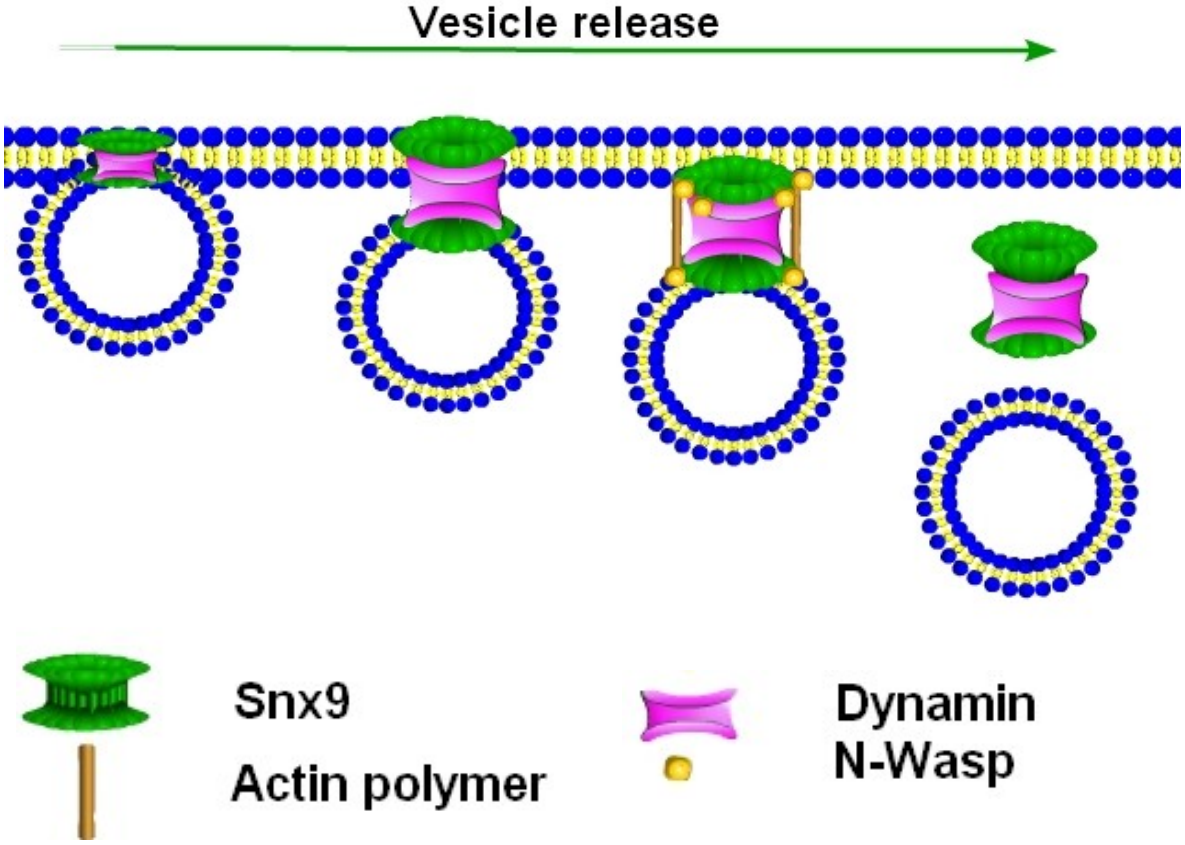

Figure 1.5: An illustration of the core mitochondrial fission machinery in yeast and mammals. Dnm1 (Dynamin 1), Mdv1 (Mitochondrial division protein 1) and Fis1 (fission protein 1) form the major mitochondrial fission complex in yeast. These proteins govern outer membrane fission whilst Mdm33 (mitochondrial distribution and morphology 33) may be important for division of the inner membrane. In mammals, the main regulators of mitochondrial fission include: Drp1 (Dynamin related protein 1), MFF (mitochondrial fission factor) and hFis1 (human fission protein 1). A sumoylation- desumolyation cycle mediated by MAPL and SENP5 respectively; stabilizes Drp1on the outer mitochondrial membrane. **Note:** SUMO = small ubiquitin like modifier; MAPL = mitochondrial anchored sumo E3 ligase; SENP5 = Sentrin specific protease 5. (Images inspired by Westermann, 2010).

Fission machinery

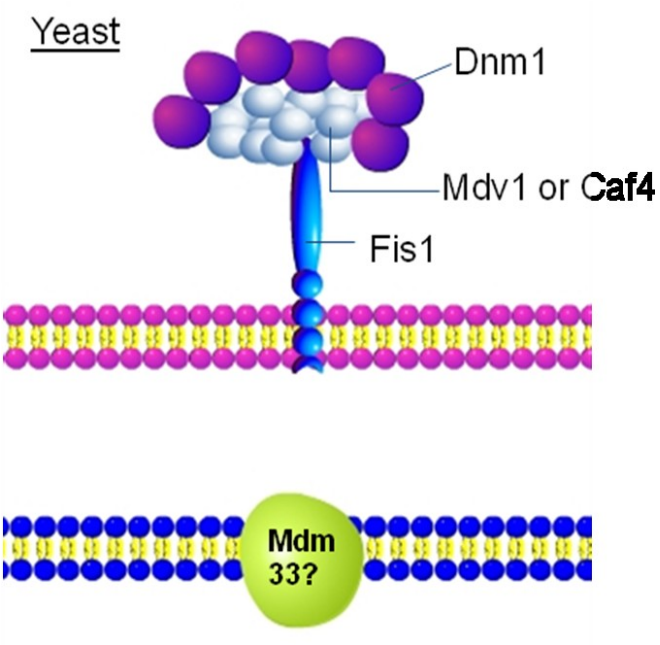

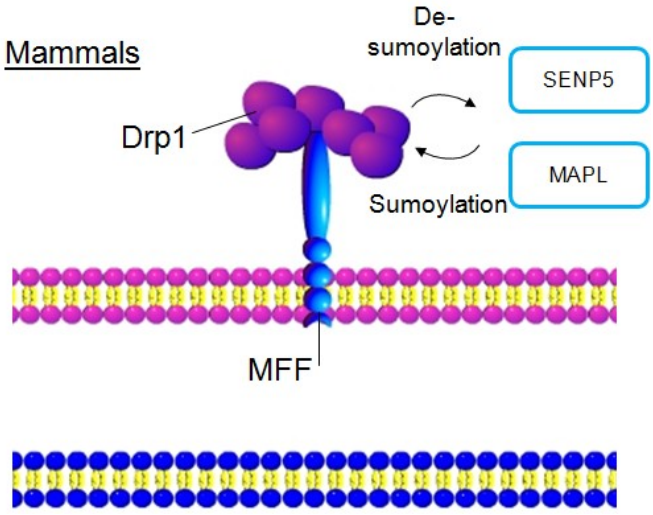

Live cell imaging studies in yeast and round worms have shown that the inner membrane bound compartments i.e. the matrix can divide in the absence of Dnm1 (Griparic and Van der Bliek, 2001; Westermann, 2010). Leading to the hypothesis that the molecular machinery which governs inner membrane fission differs from that at the outer membrane. So far, Mdm33 (mitochondrial distribution and morphology 33) has been suggested as a potential candidate for yeast inner mitochondrial membrane fission (Messerschmitt et al, 2003). Nonetheless, further enquiry into Mdm33's interacting partners at the inner membrane will be required in order to better understand its role in fission.

In mammals, mitochondrial division is primarily regulated by the human Dnm1 homolog i.e. Drp1 (Dynamin related protein 1) aided by the proteins MFF (mitochondrial fission factor) and hFis1 (human fission protein 1) as adaptors **(Figure, 1.5)**. The GTPase Drp1 is mainly cytosolic where it is diffusely distributed. In order to partake in fission events, Drp1 translocates to the mitochondrial surface forming foci "dots" on the outer membrane. The series of events during mammalian mitochondrial division have not been as clearly delineated as in yeast; however the presiding hypothesis is that Drp1 is recruited to mitochondria through MFF and hFis1 (Gandre-Babbe and van der Bliek, 2008; Westermann, 2010). Once at the outer membrane Drp1 is thought to be stabilized through a sumoylation cycle (on and off) by MAPL (Mitochondrial anchored sumo E3 protein ligase) and SENP5 (sumo protease for mitochondrial proteins) (Braschi et al, 2009; Zunino et al, 2009; Zunino et al, 2007; Wasiak et al, 2007).

Although there is evidence for a direct interaction between Drp1 and MFF both in vivo and in vitro, the same is yet to be confirmed for Fis1. MFF has been shown to be essential for mitochondrial Drp1 localization, making it the main adaptor for Drp1 at the

mitochondria (Gandre-Babbe and van der Bliek, 2008; Otera et al, 2010). To date, there has been no confirmed interaction between MFF and hFis1 further suggesting that they may be acting as independent adaptors (Gandre-Babbe and van der Bliek, 2008).

Interestingly, plant mitochondrial division utilizes fission machinery, similar to that found in yeast and mammals. In plants e.g. *Arabidopsis thaliana*, the two dynamin related GTPases, termed DRP3A and DRP3B (Dynamin related proteins 3A and 3B) generate the forces of constriction for mitochondrial fission (Arimura et al, 2004; Scott and Logan, 2010). The molecules described above represent the core fission machinery in yeast, mammals and plants.

Mitochondrial fusion

The ability of individual mitochondria to unify into an interconnected network is described as mitochondrial fusion **(Figure, 1.2)**. This process of fusion is not unique to mitochondria, for instance it (fusion) is used to merge gametes during fertilization. Additionally, enveloped viruses utilize it as a gateway to enter the host's cytosol (Martens and McMahon, 2008). However, the fact that mitochondria are double membrane structures makes their fusion events far more intricate as they involve a merger of four different membrane bilayers, rather than the typical two **(Figure, 1.6)**. Fusion proteins lower the energy barrier that must be overcome for fusing organelles to become apposed and ultimately fused. The process of mitochondrial fusion is comprised of four sequential steps including: tethering, docking, priming and fusion (Meeusen and Nunnari, 2004; Schauss et al, 2010). Moreover, mitochondrial fusion has been studied in various organisms including:

Figure 1.6: An illustration of single membrane and double membrane fusion events in neurons and mitochondria. The process of fusion in the cell is typically characterized by the merger of two different bilayers. An example would be in neurons, where the release of neurotransmitters is facilitated by a fusion event between the vesicle and plasma membranes. However, there are some instances in the cell (e.g. during mitochondrial fusion) where fusion events involve a merger of four different bilayers. (Images inspired by: Modzy and Shaw, 2003).

Single membrane fusion in neurons

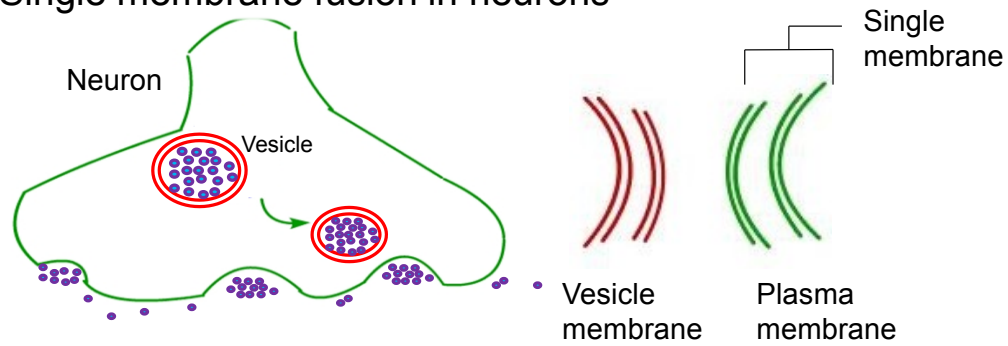

Double membrane fusion in mitochondria

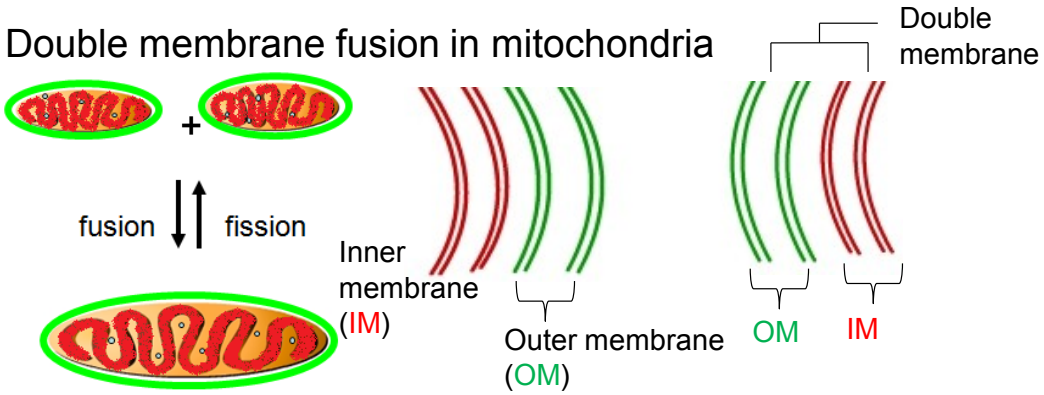

fruit flies, round worms, yeast and mammals; the consensus being that fusion is principally regulated by three GTPase related proteins.

In mammals these are: Mfn1 (mitofusin 1), Mfn2 (mitofusin 2) and Opa1 (Optic atrophy protein 1). Where, Mfn1 and Mfn2 govern outer mitochondrial membrane fusion while Opa1 mediates inner membrane fusion **(Figure, 1.7)**. The mitofusins represent the human orthologues of the *D. melanogaster* mitochondrial outer membrane GTPase, fuzzy onions (earliest gene identified as having a role in mitochondrial fusion) (Hales and Fuller, 1997). During spermatogenesis (process whereby male germ cells undergo a series of divisions finally giving rise to mature sperm cells) of fruit flies, the mitochondria fuse in to two onion- ring shaped organelles which are collectively described as a Nebenkern. However, *D. melanogaster* males with a mutation in the fuzzy onion (Fzo) gene are unable to undergo mitochondrial fusion. Similarly, mutations in the GTPase domains of the mitofusins impair fusion and have been found to be embryonic lethal (Chen et al, 2003).

In the yeast *S. cerevisiae*, outer membrane fusion is mediated by the GTPase Fzo1p whilst inner membrane fusion is regulated by Mgm1p (mitochondrial genome maintenance protein 1) **(Figure, 1.7)**. The GTPase related protein Mgm1p, has one end inserted and anchored within the inner membrane and the other exposed to the inter-membrane space (space between the inner and outer mitochondrial membranes) in order to associate with the adaptor Ugo1p. The protein Ugo1p, forms part of the mitochondrial transporter family and is believed to couple outer membrane and inner membrane fusion through its interactions with both Fzo1p and Mgm1p. A key difference between mammalian and yeast mitochondrial fusion is that there currently is no identified orthologue for Ugo1 in mammals (Sesaki and Jensen, 2001; Meeusen and Nunnari, 2005).

Figure 1.7: An illustration of the core mitochondrial fusion machinery in mammals and yeast. In mammals, mitofusins 1 and 2 govern outer membrane fusion whilst OPA1(Optic atrophy 1) regulates inner membrane fusion. In yeast, outer mitochondrial membrane fusion in is regulated by Fzo1 (fuzzy onion) whilst inner membrane fusion is mediated by Mgm1 (mitochondrial genome maintenance 1). In addition, yeast have an adapter protein, Ugo1 (Japanese for fusion) which is believed to couple outer membrane and inner membrane fusion events (Images inspired by: Westermann, 2010).

Fusion machinery

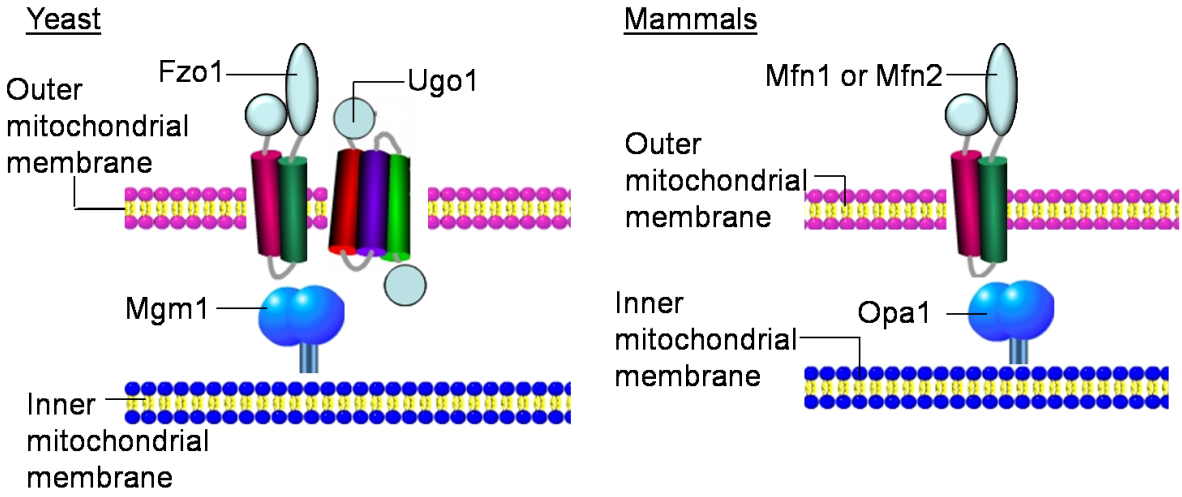

Although mitochondrial fusion events have been observed in live imaging of plant cells such as the onion bulb epidermal cell there has been limited success in identifying the core fusion machinery involved (Arimura et al, 2004).

1.3 Physiological importance of fission and fusion

The merger (fusion) of individual organelles into an interconnected reticulum allows for content mixing, and this has been shown to be important for the inheritance and maintenance of mtDNA (mitochondrial DNA). As demonstrated in DNA complementation experiments performed by Ono et al, 2001; with the aim of combining two respiratory deficient cell lines in order to form hybrids with restored respiratory activity. Each cell line had a pathogenic deletion mutation on a separate tRNA (transfer RNA) gene. Since mitochondria rely on their genomes for production of respiratory chain complexes, these cell lines had inhibited protein synthesis and low cytochrome c oxidase activity. Fusing the two cell lines set the stage for inter- mitochondrial fusion events, where mitochondria from the two respiration incompetent cell lines could share contents allowing for DNA complementation consequently restoring normal respiratory function and cytochrome c oxidase activity (Ono et al, 2001) **(Figure, 1.8)**.

Nakada et al, made similar observations in a transgenic mouse model, where the mixing of mutant and healthy mtDNA (up to 60% mutant DNA) prevented the expression of disease phenotypes including: renal failure and auriculoventricular blockage (Nakada et al, 2001). Mitochondrial fusion is hypothesized to be an important line of defense against cellular ageing. In generating ATP for the cell's metabolic activities, mitochondria produce harmful by-products, such as ROS (reactive oxygen species) which damage their DNA.

Figure 1.8: Mitochondrial fusion facilitates DNA complementation. An illustration of a mitochondrial fusion experiment aimed at restoring normal respiratory function to two respiratory deficient cell lines through the process of DNA complementation (Image inspired by: Nakada et al, 2009).

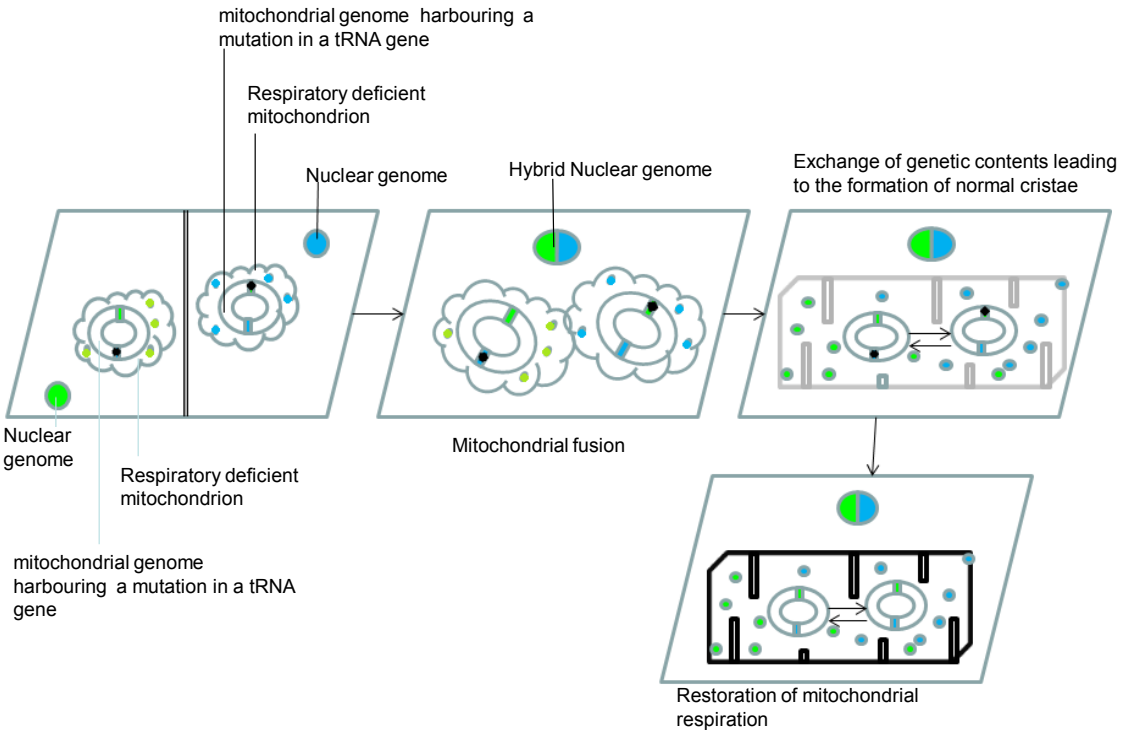
mitochondrial genome harbouring a mutation in a tRNA gene
Respiratory deficient mitochondrion
Nuclear genome
Hybrid Nuclear genome
Exchange of genetic contents leading to the formation of normal cristae
Nuclear genome
Respiratory deficient mitochondrion
mitochondrial genome harbouring a mutation in a tRNA gene
Mitochondrial fusion
Restoration of mitochondrial respiration

These lesions (ROS induced DNA damage) accumulate on the mitochondrial genome over time impeding the ability of the mitochondria to efficiently generate ATP. It's postulated that mitochondrial fusion events may foster trans-complementation of somatic mutations leading to the restoration of optimal respiratory activity (Ono et al, 2001; Westermann, 2002). Furthermore, fusion is speculated to be important for the maintenance of the inner mitochondrial membrane folds (cristae) which mediate metabolism (Olichon et al, 2003; McBride et al, 2006).

In yeast, mitochondria that are unable to fuse due to mutations in their genomes have been shown to gradually lose their genomes with each successive round of cell division. This highlights the importance of fusion in the inheritance of genetic information (Sesaki and Jensen, 2001; Westermann, 2002).

Mitochondria may also fuse in response to cell stressors. One of the first reports noting this effect was made in the late 1960's by Deitch and Godman. Upon subjecting HeLa cells to moderate (0.1 μg) doses of Actinomycin D (AMD), they observed a shift in the chondriome's morphology from short rods to an elaborate branched network made up of elongated filaments (Deitch and Godman, 1967). Since AMD (chromopeptide antibiotic produced by soil bacteria of the genus streptomyces), had been previously reported to inhibit both DNA-dependent RNA synthesis and respiration, as well as lower the ATP content of cells (Laszlo et al, 1966); Deitch and Godman postulated that AMD's negative impact on metabolism and ATP synthesis may be involved in the formation of the interconnected mitochondrial networks they observed. This effect has since been observed in cells exposed to other stressors including: serum starvation and UV radiation and is now termed, stress induced mitochondrial hyperfusion (SIMH) **(Figure, 1.9)** (Tondera et al, 2009).

Figure 1.9: Mitochondria fuse in response to stress through the process of stress induced mitochondrial hyperfusion (SIMH). An example of hyperfused mitochondria in HeLa cells stained with anti-PRDX3.

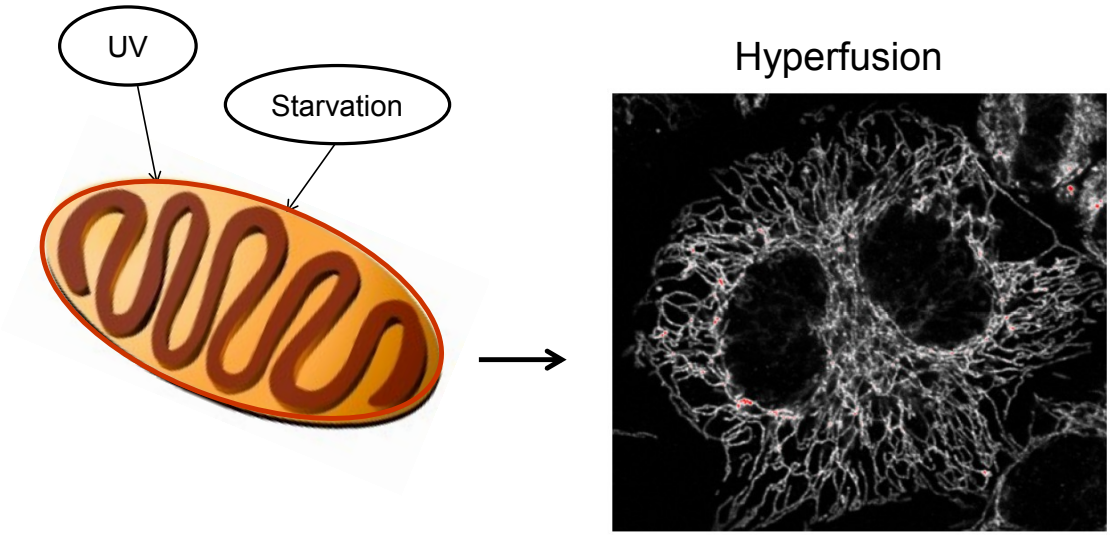
UV
Starvation
Hyperfusion

Furthermore, the mitochondrial fusion factors Mfn1 and Opa1 have been shown to be requisite for SIMH.

Along with the formation of hyperfused mitochondrial networks in response to stress, Tondera and colleagues noted an increase in ATP production (ATP content was measured by a genetically encoded luciferase probe targeted to the mitochondrial matrix) (Tondera et al, 2009). In line with the latter observations, Gomes et al have discovered that the elongated mitochondria in starving cells also have a high density of cristae favouring efficient ATP production (Gomes et al, 2011). Similar observations were made by Rambold et al who not only noted that mitochondria fuse during starvation but that fission was repressed resulting in unimpeded fusion (Rambold et al, 2011).

The role of mitochondrial fission in the maintenance of mtDNA is yet to be clarified. On the other hand, mitochondrial fission is of strategic importance in apoptosis (programmed cell death) and cell division. Apoptosis is a type of programmed cell death utilized in the formation of organs during embryo development **(Figure, 1.10a)**. Additionally, apoptosis is important for the maintenance of homeostasis in cells **(Figure, 1.10b)** (Vander Heiden et al, 1997; Vander Heiden and Thompson, 1999). During apoptosis, mitochondria fragment into small spherical organelles. This action, results in the release of several pro-apoptotic factors including: cytochrome- c and SMAC (second mitochondria-derived activator of caspases), from the inter-membrane space into the cytosol. Upon release into the cytosol, cytochrome-c and SMAC activate the caspases (cysteine family proteases), triggering a protease cascade which may culminate in cell death (Kuwana et al, 2002; Karbowski and Youle, 2005). Another role for mitochondrial division in cells is to facilitate the disassembly of the chondriome into individual entities for separation during cell division

Figures 1.10a and b: An illustration of the role of apoptosis (cell death) in embryo development (A) and homeostasis (B). In (A), apoptosis facilitates the controlled killing of cells to allow for the shaping of digits. Apoptosis also helps the cell get rid of ineffective organelles. (B) illustrates the balance (homeostasis) that is maintained such that the growth of new cells is accompanied by the death of old ones (Images inspired by: Walensky, 2006; Danton H. O' Day).

(A)

An illustration of the formation of digits in a human embryo

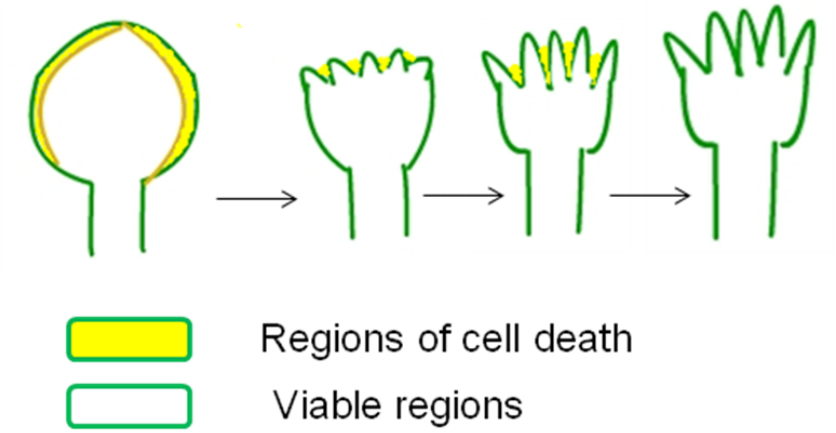

(B)

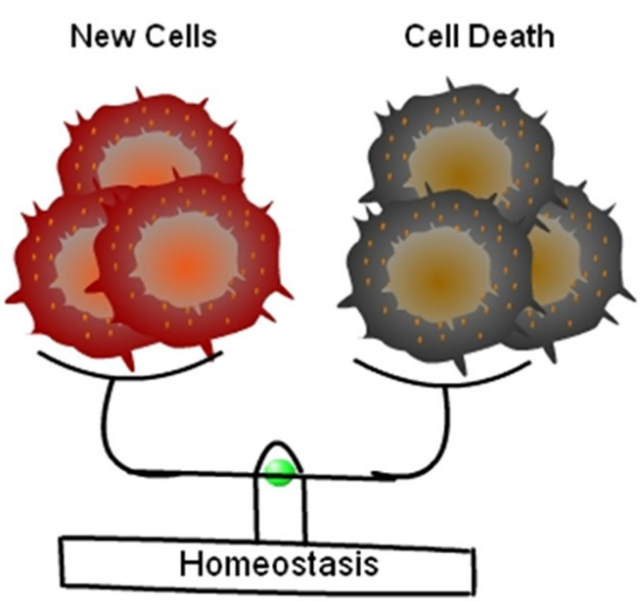

(Gorsich and Shaw, 2004). This has been useful in ensuring that the mitochondrial population of a parent cell undergoing mitosis randomly segregates into roughly equal proportions in the two daughter cells (Birky, 1983; Taguchi et al, 2007; Westermann, 2010).

In summary, fission favours the induction of cell death pathways, whilst fusion protects the cell from degradation by impeding the release of mitochondrial pro-apoptotic factors. Although, mitochondrial hyperfusion may be characterized as a survival response, it would be important to note that there is a price to pay. Mitochondrial hyperfusion has been found to coincide with an increase in damaged protein (Twig et al, 2008). In particular, the indirect stimulation of fusion by inhibiting mitochondrial fission machinery (e.g. Drp1 or Fis1) has been found to lead to the accumulation of oxidized mitochondrial proteins (Twig et al, 2008).

1.4 Mitochondrial derived vesicles

Besides being able to form a unified reticulum or fragmenting into individual organelles, mitochondria also posses the ability to bud vesicles from the outer membrane **(Figure, 1.11)** (Neuspiel et al, 2008; Braschi et al, 2010; Soubannier et al, 2012). This is fascinating, as most structures involved in budding vesicles for intracellular traffic have a single membrane, i.e. they need only shape a single lipid bilayer to form a vesicle e.g. the plasma membrane during endocytosis. Since mitochondria are double membrane organelles they would have to overcome a much larger energy barrier in order to shape and sculpt their two lipid bilayers to form vesicles. Different populations of MDVs (mitochondrial derived vesicles) are distinguished from each other by the mitochondrial proteins which they incorporate. For instance, MDVs targeted to the peroxisome contain the fission protein,

Figure 1.11: Mitochondria bud vesicles. Whilst some mitochondrial vesicles have been found to be targeted to the peroxisomes others have being identified as lysosome bound. **Note**: MAPL = Mitochondrial anchored sumo E3 ligase and Tom20 = Translocase of outer membrane 20 (Image adapted from Heidi McBride, McBride Lab).

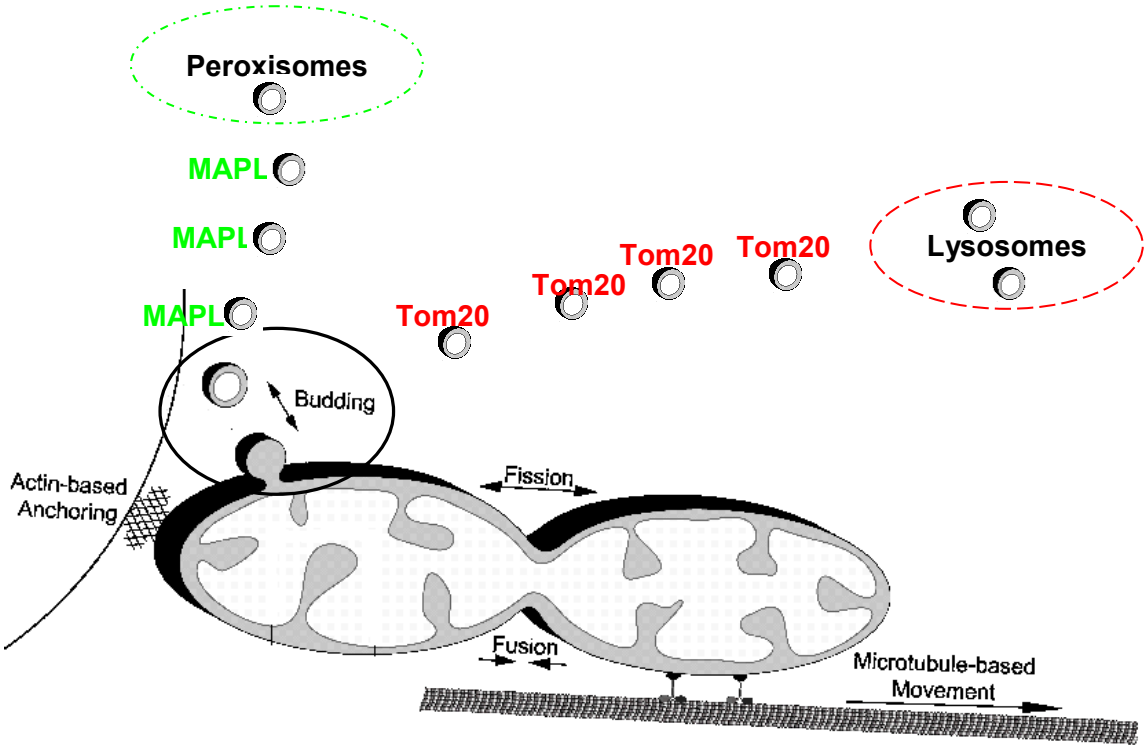
Peroxisomes
MAPL
MAPL
MAPL
Tom20
Tom20
Tom20
Tom20
Lysosomes
Budding
Actin-based
Anchoring
Fission
Fusion
Microtubule-based
Movement

MAPL and can therefore be labeled by an anti-MAPL antibody **(Figure, 1.11)** (Neuspiel et al, 2008). In contrast, some of the vesicles that go to the lysosome contain the outer membrane channel protein, Tom20 (translocase in outer membrane) (Soubannier et al, 2012). Whilst it is known that MAPL containing MDVs are delivered to the peroxisome via the retromer complex, the structure(s) responsible for mediating transport of Tom20-vesicles (i.e. vesicles incorporating Tom20) to the lysosome has yet to be identified (Braschi et al, 2010).

As is common with most new ideas, the discovery of MDVs has been met with rigorous debate. One of the primary questions raised is whether the MDVs represent vesicles or mitochondrial fragments. Neuspiel et al, demonstrated that MDVs have a spherical morphology. Moreover, mitochondria can bud vesicles in the absence of the main fission regulator Drp1. Since MDVs can be generated in the absence of core fission machinery they are unlikely to be mitochondrial fragments (Neuspiel et al, 2008). Other questions have been about the physiological relevance of MDVs. Some mitochondrial derived vesicle (MDV) populations serve as a way for the mitochondria to communicate with other organelles e.g. the peroxisomes, while recent work in the McBride laboratory has shown that other vesicles provide a mechanism for mitochondria to rid themselves of damaged parts including, proteins and lipids. To this end, our emerging hypothesis regarding the cardinal function of lysosome bound MDVs in the cell is that, these vesicles serve as a quality control mechanism that mitochondria employ to maintain their integrity (remain in good health).

1.5 A short summary on the principles of mitochondrial quality control

Mitochondria are involved in a myriad of functions which impact the cell's metabolism including: oxidative phosphorylation, heme biosynthesis, beta- oxidation of fatty acids, the citric acid cycle, amino acid and nucleic acid biosynthesis (Zick et al, 2009; Gorsich and Shaw, 2004). Hence it's not surprising that impaired mitochondrial function frequently leads to disease. To counter this, the cell uses many quality control measures " fail –safes" to ensure that the mitochondria remain in good health. At the molecular level, the mitochondria engage their intra-organellar proteolytic system which breaks down damaged proteins into peptides. These peptides would then be degraded to amino acids by oligopeptidases. For, quality control at the organellar level, the process of mitochondrial fusion is thought to bring back functionality to damaged mitochondria since fusion with healthy organelles may buffer, or rescue damage.

Alternatively, extensively damaged mitochondria which have lost their ability to fuse are removed by mitophagy (autophagy of mitochondria) (Narendra et al, 2008; Tatsuta and Langer, 2008). Under the current model for mitophagy, the mitochondrial kinase, Pink1 (PTEN induced putative kinase protein 1) would accumulate at damaged mitochondria due to the inhibition of its (Pink1) proteolysis. Whilst the protease responsible for Pink1 proteolysis in mammalian cells has yet to be identified, the protease Rhomboid 7 has been linked to Pink1 cleavage in fly cells (Whitworth et al, 2008; Youle and Narendra, 2011). The accumulation of Pink1 on the surface of impaired mitochondria would then trigger the translocation of the ubiquitin E3 ligase, Parkin from the cytosol to the mitochondria. Once at the mitochondria, Parkin is believed to ubiquitinate fusion proteins e.g. mitofusin 1 and

mitofusin 2, tagging them for proteosomal degradation. The degradation of these (mitofusin 1 and mitofusin 2) major mitochondrial fusion regulators is mediated by the ATPase, p97 and has been posited to be a step that ensures that extensively damaged mitochondria do not fuse with the rest of the healthy reticulum (Tanaka et al, 2010). Following the accumulation of Parkin molecules, the damaged mitochondria would be engulfed by the autophagosome for degradation in the lysosome **(Figure, 1.12)** (Tanaka et al, 2010; Youle and Narendra, 2011).

It would be important to note that a common assay for the study of mitophagy, has been to impair the mitochondria by inducing global depolarization, whereby uncouplers can be used to cause the entire mitochondrial population to loose membrane potential. However, the induction of mitophagy in response to global depolarization has been shown to be mostly confined to immortalized culture cell lines e.g. HeLa cells. In particular, Sterky and colleagues' studies in the dopaminergic neurons of mice investigated whether Parkin would localize to mitochondria which had impaired respiratory function. They discovered that, the impaired respiratory function was due to a loss of mtDNA expression. Although Parkin localized to impaired mitochondria in HeLa cells, Sterky and colleagues discovered that, Parkin did not get recruited to damaged mitochondria in dopaminergic neurons (Sterky et al, 2011). Tying in with this, recent studies by Van laar et al indicate that mitochondria in primary cells (rat cortical neurons) seldom experience a global loss of potential (Van laar et al, 2011); ergo these (primary cells) cells maybe reliant on an alternative quality control mechanism. Interestingly, Parkin also associates with MDVs that ferry cargo to the lysosomes (EA Fon and McBride, unpublished). Indeed, the generation of at least one class

Figure 1.12: An illustration of the clearance of damaged mitochondria through mitophagy Mitophagy initiates with the E3 ubiquitin ligase, Parkin localizing to mitochondria depolarized by CCCP (carbonyl cyanide m-chlorophenyl hydrazone). Once at the mitochondria Parkin ubiquitinates the fusion regulators mitofusin 1 and mitofusin 2, tagging them for p97 mediated degradation in the proteasome. The depolarized mitochondria are then engulfed by the autophagosome (Image inspired by: Yoshii et al, 2011).

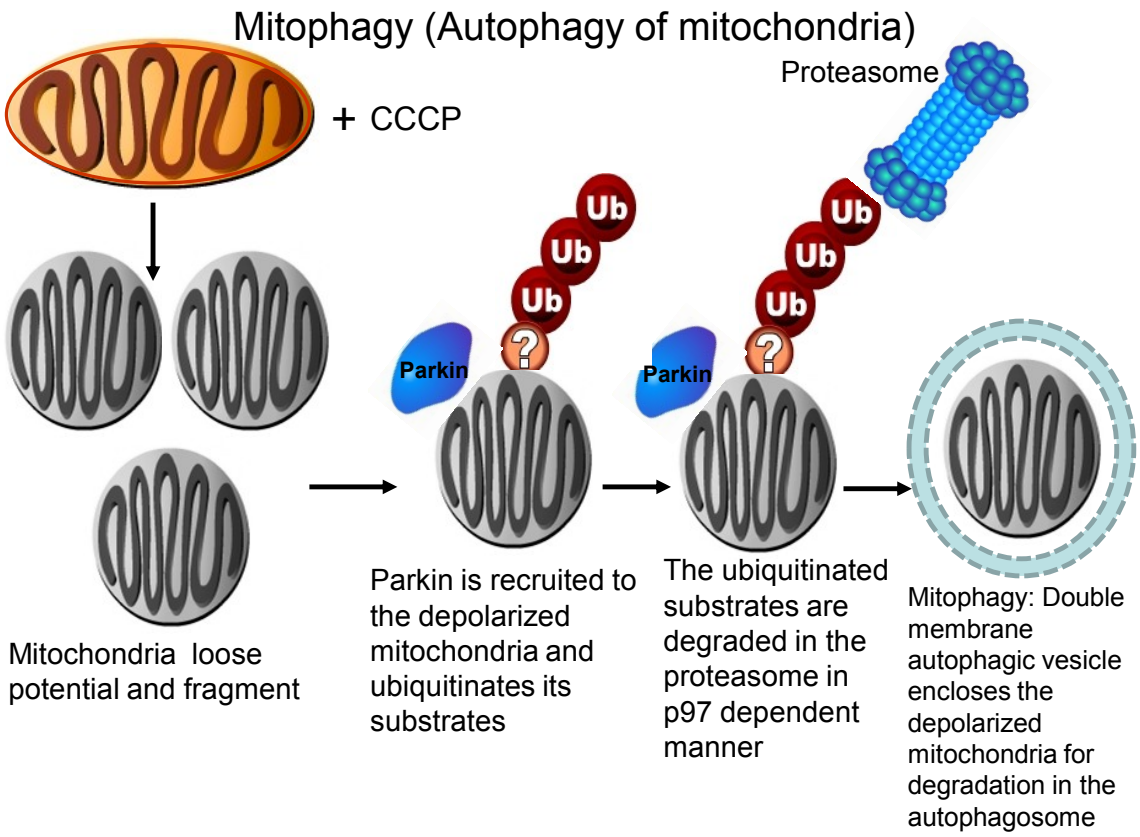
Mitophagy (Autophagy of mitochondria)
+ CCCP
Proteasome
Ub
Ub
Ub
?
Parkin
Ub
Ub
Ub
?
Parkin
Mitochondria loose potential and fragment
Parkin is recruited to the depolarized mitochondria and ubiquitinates its substrates
The ubiquitinated substrates are degraded in the proteasome in p97 dependent manner
Mitophagy: Double membrane autophagic vesicle encloses the depolarized mitochondria for degradation in the autophagosome

of mitochondrial vesicles requires Parkin. Suggesting that, Parkin may have an alternate primary role of targeting MDVs to the lysosome for degradation.

1.6 Turnover of mitochondrial lipids

The reactive oxygen species generated as a toxic by –product of the production of ATP, have been implicated in the destruction of lipids, proteins and nucleic acids (mitochondrial DNA) (Smith et al, 1998; Gutierrez et al, 2006). Current mitochondrial quality control strategies address the degradation of proteins (through proteases), organelles (through mitophagy) or whole cells (through apoptosis), but little is known about the clearance of damaged mitochondrial lipids. This gap in the cell's mitochondrial quality strategy may be filled by mitochondrial derived vesicles. In an attempt to avoid accumulating damaged lipids, MDVs would enable these (mitochondria) organelles to export the damaged lipids to the lysosome for degradation.

Dysregulation of mitochondrial dynamics and quality control has been linked to neurodegenerative diseases including: Charcot-Marie-Tooth type 2A, dominant optic atrophy, Alzheimer's and Parkinson's **(Figure, 1.13)** (Chen and Chan, 2009). In contrast to other cell types which engage in both glycolysis and oxidative phosphorylation to meet their energy needs, neurons are heavily reliant on mitochondria for the production of ATP (Knott et al, 2008). This dependency may explain why neurons can be hard hit by mitochondrial dysfunction.

Mutations in the gene encoding the outer mitochondrial membrane protein, Mfn2 bring about Charcot-Marie-Tooth disease type 2A. This disease is characterized by a

Figure 1.13: Dysregulation of mitochondrial dynamics and quality control have been linked to neurodegenerative diseases including: Charcot-Marie-Tooth type 2A, dominant optic atrophy, Alzheimer's and Parkinson's. The regions of the nervous system targeted by these diseases have been illustrated (Image inspired by: Chen and Chan, 2009).

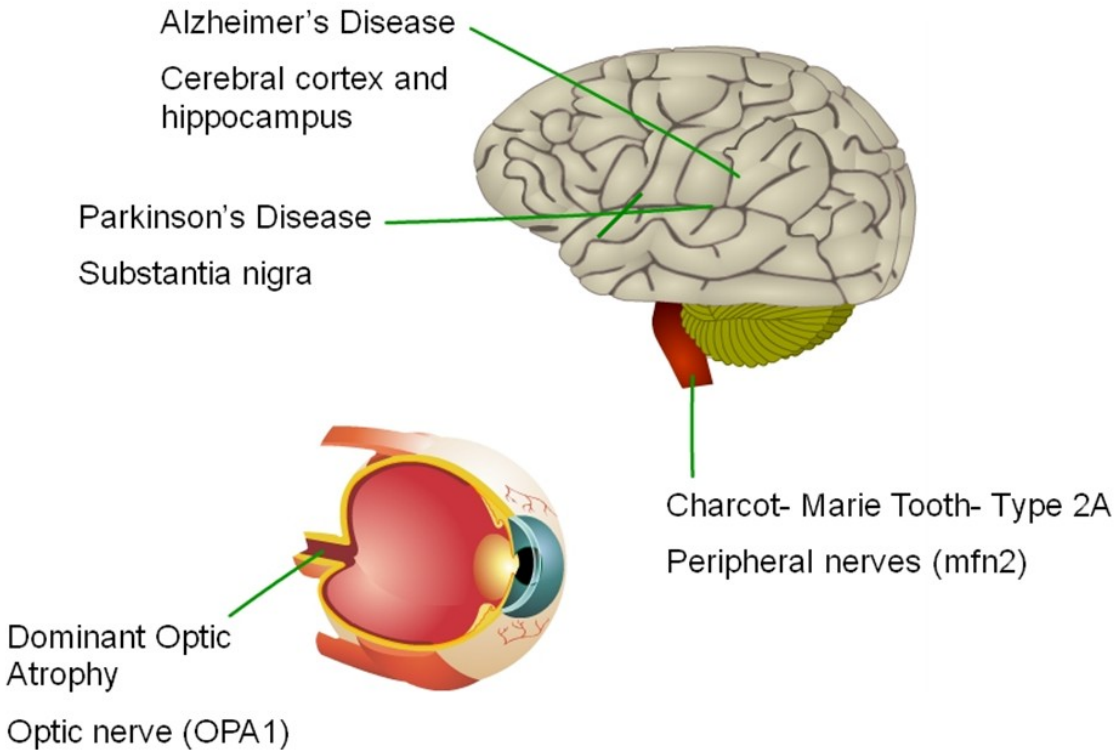
Alzheimer's Disease
Cerebral cortex and hippocampus
Parkinson's Disease
Substantia nigra
Charcot- Marie Tooth- Type 2A
Peripheral nerves (mfn2)
Dominant Optic Atrophy
Optic nerve (OPA1)

deterioration of long peripheral nerves leading to injury of the distal sensory and motor neurons (Zuchner et al, 2004; Westermann, 2010). Mutations in the gene encoding the inner mitochondrial membrane protein, Opa1 cause dominant optic atrophy (a form of inherited childhood blindness). This disease is marked by a gradual decline in eyesight due to a destruction of retinal ganglion cells. Whereby, the axons of retinal ganglion neurons make up the optic atrophy nerve (Delettre et al, 2000; Westermann, 2010).

Alzheimer's is one of the most prevalent forms of neurodegenerative disease and is associated with memory loss and cognitive dysfunction due to the deterioration of neurons in the cerebral cortex (Chen and Chan, 2009). This condition is marked by excessive production of beta-amyloid (peptide originating from the amyloid precursor protein) in the presence of mitochondrial dysfunction (increased ROS generation) (Manczak et al, 2006; Knott et al, 2008). Parkinson' s disease is another common neurodegenerative disorder owing to the loss of dopaminergic neurons in the substantia nigra and the build up of Lewy bodies in nerve cells (Dauer and Przedborski, 2003) . Moreover, the oxidative damage observed when mitochondrial dysfunction arises from the poisoning of complex I of the electron transport chain has been associated with the loss of dopaminergic neurons, further demonstrating links between mitochondrial impairment and Parkinson's Disease (Sherer et al, 2002; Chen and Chan, 2009). The protein targets for mutations in Parkinson's disease localize or translocate to the mitochondrial outer membrane and include: the kinases Pink1 and LRRK2, the E3 ligase Parkin, Dj1 and VPS35 (Knott et al, 2008; Zimprich et al, 2011). The implication of mitochondrial dynamics in the various forms of neurodegenerative disease has made the identification of core fusion and fission molecules and their interacting partners a top priority to many in the cell biology arena.

1.7 Research needs

So far the core fusion components that have been discovered include: the three dynamin related GTPases Mfn1, Mfn2 and Opa1. On the fission side, the core machinery currently includes: Drp1, MFF and hFis1 (Westermann, 2010). **The intricate nature of mitochondrial dynamics would suggest that there are many more components, governing the processes of mitochondrial fusion, fission and budding that have yet to be discovered.**

In an attempt to identify proteins that would significantly alter mitochondrial morphology and therefore be required for its maintenance i.e. core fission and fusion molecules, an independent genome wide siRNA screen of 18 000 genes was performed (in collaboration with Rob Screaton, Children's Hospital of Eastern Ontario- Research Institute) **(Figure, 1.14)**. In addition to the positive and negative controls (silencing either Drp1 or both Mfn1/Mfn2 concurrently), the screen was internally validated through the identification of most of the known players regulating mitochondrial morphology. These included the regulators of mitochondrial fission: Drp1 and MFF; and fusion: Mfn1, Yme1 (mitochondrial protease), and Opa1. In addition, novel, unexpected proteins were identified, including the endocytic BAR-domain containing protein Snx9 (sorting nexin 9).

This endocytic protein (Snx9) had previously come up in a smaller screen focused on identifying fission factors. Specifically, an affinity column approach had been adopted where

Figure 1.14: Genome wide siRNA morphology screen in HeLa cells to identify genes that could substantially alter mitochondrial morphology and therefore be requisite for its maintenance. Following the silencing of genes, the mitochondrial length to width ratio was measured. Genes with a mitochondrial length-to-width ratio > 2 had a hyperfused mitochondrial phenotype whilst those with a length-to-width ratio < 2 had fragmented mitochondria.

GWsiRNA screen to identify genes which would alter mitochondrial morphology and therefore be required for its maintenance

Genome-wide siRNA plot of all 18,739 genes silenced.

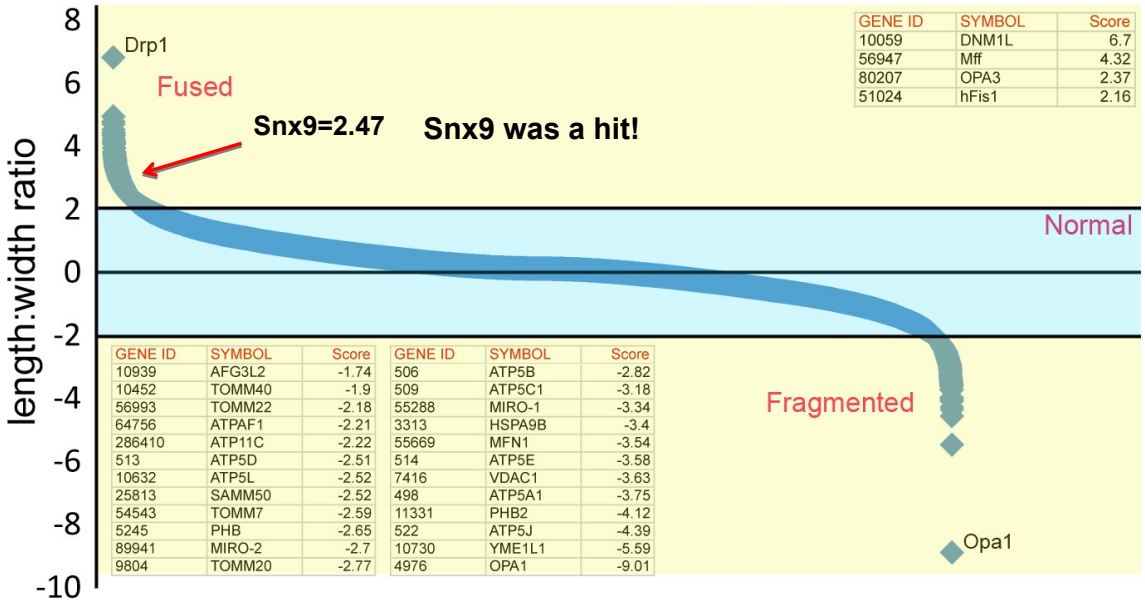

GENE ID	SYMBOL	Score
10059	DNM1L	6.7
56947	Mff	4.32
80207	OPA3	2.37
51024	hFis1	2.16

GENE ID	SYMBOL	Score
10939	AFG3L2	-1.74
10452	TOMM40	-1.9
56993	TOMM22	-2.18
64756	ATPAF1	-2.21
286410	ATP11C	-2.22
513	ATP5D	-2.51
10632	ATP5L	-2.52
25813	SAMM50	-2.52
54543	TOMM7	-2.59
5245	PHB	-2.65
89941	MIRO-2	-2.7
9804	TOMM20	-2.77

GENE ID	SYMBOL	Score
506	ATP5B	-2.82
509	ATP5C1	-3.18
55288	MIRO-1	-3.34
3313	HSPA9B	-3.4
55669	MFN1	-3.54
514	ATP5E	-3.58
7416	VDAC1	-3.63
498	ATP5A1	-3.75
11331	PHB2	-4.12
522	ATP5J	-4.39
10730	YME1L1	-5.59
4976	OPA1	-9.01

a GST (Glutathione S – transferase) tagged form of the ring domain for MAPL (a fission protein), was used to " fish out" targets from placental cytosol.

Snx9 is a 66 kDa protein whose larger role in the cell has been to facilitate clathrin mediated endocytosis at the cell surface (Lundmark and Carlsson, 2003). Snx9 has six structural domains which it uses to recruit and activate endocytic molecules **(Figure, 1.15)**. Specifically, it has an SH3 (Src homology 3) domain which binds polyproline rich sequences such as those found in dynamin 1, dynamin 2, and the WASP (Wiskott Aldrich Syndrome protein)/WAVE actin regulator. Moreover it hosts an LC (Low complexity) domain which may interact with Arp 2/3 (actin nucleating complex), clathrin (coat protein) and the alpha and beta appendages of AP-2 (plasma membrane protein). In addition, Snx9 has two yoke domains (n-terminal yoke and c-terminal yoke), which flank either side of the PX (Phox homology) domain. The yoke domains link the PX and BAR domains together to form a PX-BAR super domain which is involved in membrane binding and sculpting (Lundmark and Carlsson, 2003; Lundmark and Carlsson, 2009).

The prevailing model for Snx9's involvement in clathrin mediated endocytosis is as follows: clathrin would oligomerize on the cytoplasmic side of the cell. AP2 would then bind and concentrate the molecules to be imported into the cell at clathrin coated areas forming an invaginated bud with a narrow neck. Snx9's role would be to bind and recruit dynamin 2 to the site of endocytosis at the cell surface and activate it. In addition, Snx9 would activate the actin regulator WASP. Actin polymerization would further constrict the narrow neck allowing dynamin 2 to facilitate scission and release of the vesicle from the plasma membrane for fusion with the early endosome **(Figure, 1.4)** (Lundmark and Carlsson, 2009).

Figure 1.15: An illustration of Snx9's domain structure and interacting partners. The numbers indicate the last amino acid. (Image inspired by: Lundmark and Carlsson, 2009).

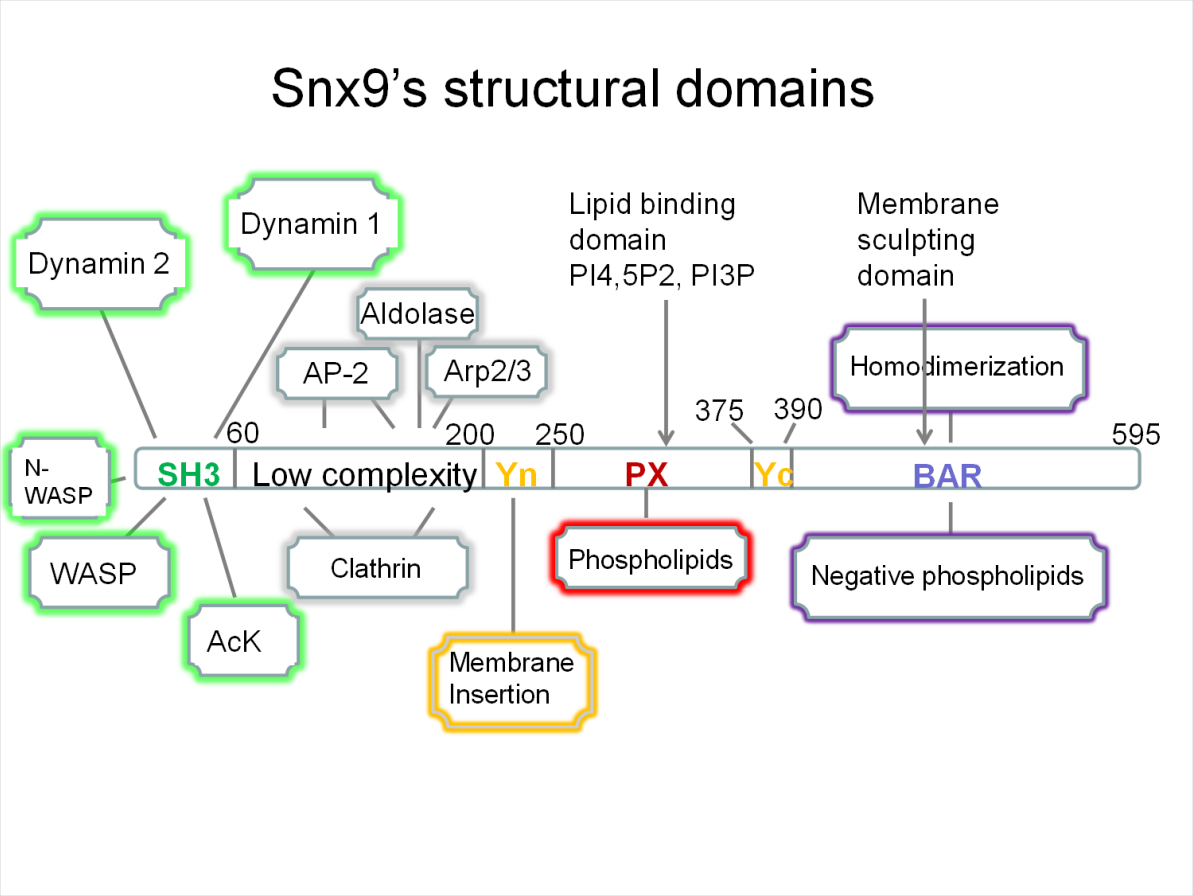
Snx9's structural domains
Dynamin 2
Dynamin 1
Lipid binding domain PI4,5P2, PI3P
Membrane sculpting domain
Aldolase
AP-2
Arp2/3
Homodimerization
60
200
250
375
390
595
N-WASP
SH3
Low complexity
Yn
PX
Yc
BAR
WASP
Clathrin
Phospholipids
Negative phospholipids
AcK
Membrane Insertion

The principle goal of this research program has been to characterize Snx9's role in mitochondrial morphology. The identification of Snx9 from two independent screens (the first an affinity column performed to find potential interactors of the mitochondrial fission protein, MAPL and the second a mitochondrial morphology screen), when put together with its roles in membrane binding and sculpting and associations with constrictors e.g. dynamin, made Snx9 a compelling investigative target. In order to tackle the set goal of characterizing Snx9's role in mitochondrial morphology, this research program focused on achieving three specific aims:

1.8 Specific aims of this research:

1.8.1 Aim 1: Investigate how silencing Snx9 alters mitochondrial morphology

1.8.2 Aim 2: Characterize Snx9's association with the mitochondria

1.8.3 Aim 3: Define the role of snx9 at the mitochondria

2. Methods

2.1 Plasmids

Constructs generated in this research program:

The pmCherry-C1-Snx9 construct was prepared by means of PCR (polymerase chain reaction).

Briefly, the human Snx9 cDNA which codes for the 595 amino acid protein, Snx9 was amplified from a pEYFP-C3-Snx9 DNA template using oligonucleotide primers which had EcoRI and BamHI sites. The oligonucleotide sequences were as follows:

Forward primer: 5' ACG**GAATTC**TATGGCCACCAAG 3'

Reverse primer: 5' GTT**GGATCC**CTACATCACTGG 3'

Following PCR amplification, the Snx9 cDNA was inserted (sub-cloned) into the unique EcoRI/BamHI sites located downstream of the mCherry fluorescent protein gene in the pmCherry-C1 mammalian expression vector (Clontech). The pmCherry-C1-Snx9 construct was confirmed by restriction digests (at the EcoRI/BamHI sites) and DNA sequencing (carried out by Stemcore Laboratories,Ottawa Hospital Research Institute, http://www.stemcore.ca).

The pCMV-Flag Tag 2A-Snx9 construct was prepared by means of PCR in a manner similar to the pmCherry-C1-Snx9 construct.

Briefly, Snx9 cDNA was amplified from a pEYF-C3-Snx9 (DNA template) using oligonucleotide primers with EcoRI and BamHI sites. The oligonucleotide sequences were as follows:

Forward primer: 5’ ATT**GGATCC**CATGGCCACCAAG 3’

Reverse primer: 5’ CCT**GAATTC**CTACATCACTGG 3’

Following PCR amplification, the Snx9 cDNA was inserted (sub-cloned) into unique EcoRI/BamHI sites downstream of the Flag gene in the mammalian expression vector, pCMV-Tag2A (Agilent Technologies).

The pCMV-Flag Tag 2A-Snx9 construct was confirmed by restriction digests (at the EcoRI/BamHI sites) and DNA sequencing (carried out by Stemcore Laboratories, Ottawa Hospital Research Institute, http://www.stemcore.ca).

Other constructs:

The mitochondrial matrix markers fused to cyan (CFP) and yellow fluorescent proteins (YFP): pOCT-CFP& pOCT-YFP were previously described in (Harder et al, 2004). OCT comprises the first 32 amino acids of the enzyme, ornithine carbamyl transferase. The retromer complex fusion protein, YFP-VPS35 was previously described in (Braschi et al, 2010). CFP-VPS35 was generated from YFP-VPS35 by Emelie Braschi (McBride lab). pmCherry-Parkin was provided by E. Fon (Montreal Neurological Institute, Canada) whilst GFP-LC3 was obtained from Z. Yao (University of Ottawa, Canada). YFP-Parkin was sourced from M. Schlossmacher (Ottawa Hospital Research Institute, Canada). YFP-C3-Snx9 was generated by Emelie Braschi (McBride lab).

2.2 Antibodies

Monoclonal antibodies

The monoclonal antibodies used in this research program were sourced from the following providers:

Anti-Snx9 (H00051429-M03) antibody from Abnova (Walnut, CA. USA), anti-β-tubulin (556321) from BD Bioscience (Mississauga, ON, Canada), anti-Flag (F3165-1MG) from Sigma-Aldrich (Oakville, ON, Canada), and anti-FP (632381) from Clontech (Burlington, ON, Canada).

Dilutions: anti-Snx9, anti-β-tubulin, and anti-Flag were used at a dilution of 1:500 overnight, whilst anti-FP was used at 1:1000 overnight.

Polyclonal antibodies

The polyclonal antibodies used in this research program were sourced from the following providers:

Primary antibodies:

Anti-Tom20 (FL-145) and anti-EPS15 (H-896) from Santa Cruz Biotechnology (Santa Cruz, CA, USA), anti-Dynamin2 (ab3457) from Abcam (Cambridge, MA, USA), anti-MFF (17090-1-AP) from Protein Tech Group (Chicago, IL, USA), anti-PRDX3 described in (Jeyaraju et al, 2006). **Note**: The above polyclonal antibodies were raised in rabbit.

Dilutions: Anti-EPS15, anti-Dynamin2 and anti-MFF were used at a 1:500 dilution overnight whilst anti-Tom20 and anti-PRDX3 were used at a dilution of 1:1000 for 1h.

Secondary antibodies:

Alexa Fluor goat anti-rabbit (647 nm) from (Invitrogen), 800IRDye goat anti-mouse and 800IRDye goat anti-rabbit from (Li-cor Biosciences).

Dilutions: Alexa Fluor goat anti-rabbit (647) was used at a dilution of 1:1000 for 30 mins, whilst 800IRDye goat anti-rabbit and 800IRDye goat anti-mouse were used at 1: 10 000 for 30 mins.

2.3 Chemicals:

CCCP was obtained from (Sigma-Aldrich).

2.4 Cell culture and Transfection assays:

Cell culture

HeLa and HEK293 cells were procured from the American Type Culture Collection, ATCC (Manassas, VA). Cells were grown in high glucose Dulbecco's modified Eagle's Medium, DMEM (Invitrogen) supplemented with 10% (v/v) fetal bovine serum, FBS (GIBCO Invitrogen), 2mM L-glutamine (Invitrogen), 0.1mM non-essential amino acids, NEAA (Invitrogen). The cells were maintained at 37 °C and 5 % CO_2.

Immunofluorescence Transfection assay

HeLa or HEK 293 cells at 70-90 % confluency were transfected overnight with plasmids (0.8 μg DNA/ well for a 24 well plate) using Lipofectamine 2000 (Invitrogen) according to the manufacture's instructions.

With regard to fixed cell imaging, the cells were washed 3 times with Phosphate Buffered Saline (PBS) and fixed in 4% paraformaldehyde (PFA, cross-linking reagent) in PBS for 15

minutes at 37 ° C. Subsequent to fixation, the cells were quenched with 50mM ammonium chloride in PBS for 10 minutes at room temperature. Note: This is done in order to bind the free aldehydes left over after fixation. After quenching, the cells were washed 3 times with PBS and were either mounted onto slides using fluorescent mounting medium from Dako (Carpinteria, CA) or permeabilized with 0.1% Triton X-100 in PBS for 10 minutes, in order to stain the mitochondria with antibodies. Following permeabilization, the cells were washed 3 times in PBS and blocked with 10 % FBS in PBS for 30 minutes to prevent non-specific antibody binding. The cells were then incubated in primary antibody (either anti-Tom20 or anti-PRDX3) in 5% FBS in PBS for 1h at room temperature. The cells were then washed in 5% FBS in PBS to remove excess primary antibody and incubated in goat anti-rabbit (Alexa-Fluor 647) secondary antibody for 30 minutes. Finally, the antibody stained cells were washed 3 times in PBS to remove excess secondary antibody and mounted with fluorescent mounting medium.

For live cell imaging, the cover slips were mounted on an aluminium coverslip mount (chamber), containing 10mM HEPES buffer (to maintain pH at ~ 7.4) in DMEM (supplemented with 10 % FBS, 2mM L-Glutamine, 0.1mM NEAA). Following this, the cells were examined with a confocal microscope fitted with a heated environmental chamber in order to maintain the temperature at 37 ° C (physiological temp.).

2.5 Small interfering RNA (siRNA) mediated knock down

siRNA treatments were carried out according to the Thermo scientific Dharmafect siRNA transfection protocol. HeLa or HEK293 cells seeded on glass coverslips were transfected with siRNA duplexes to a final concentration of (100 nM) using Dharmafect 1 as

the transfection reagent (Dharmacon). Cells were either fixed for microscopy (immunofluorescence or electron microscopy) or harvested for immunoblotting after 72h. The following siRNA duplex **ON-TARGETplus SMARTpools** were used:

#L-017335-00-0005 (Snx9)

#L-004005-00-0005 (EPS15)

#L-004007-00-0005 (DNM2)

#L-018261-00-0005 (MFF)

#D-001810-10-20 (non-targeted).

With regard to **individual siRNA oligonucleotides** for silencing Snx9, the following siRNA duplexes were used:

5' CGAGGAAACAGUCGUGCUA 3' (oligo1)

5' GGACAGAACGGGCCUUGAA 3' (oligo2)

5' GAGUCAGCAUCAUGUCUUA 3' (oligo3)

5' GUAACCGGAUCUAUGAUUA 3' (oligo4)

2.6 Fluorescence staining for cholesterol and neutral lipids

HeLa cells previously transfected with Snx9 siRNA duplexes were transfected with OCT-YFP 24h prior to the 72h time point. After the 72 h time point, the cells were rinsed 3 times in PBS to remove the culture medium and fixed in 4 % paraformaldehyde for 15 mins at 37 ° C. Subsequently, the paraformaldehyde was quenched with 50mM glycine at room temperature over a 10 minute period. The cells were then stained with 0.025 μg/ul filipin (Sigma) in PBS or 0.001μg/ul Nile Red (Sigma) in PBS for 30 minutes at room temperature. Thereafter, the cells were rinsed 3 times in PBS to remove excess stain. Finally, the

coverslips were mounted on slides and visualized using the 405nm laser for filipin or the 515 nm for Nile red on an Olympus FV1000 confocal microscope.

2.7 Microscopy

Confocal Microscopy

An Olympus FV1000 confocal microscope fitted with an environmental chamber (for live imaging) was used to determine the localization of the fluorescently tagged proteins. Images were collected using a 100X, 1.4 Numerical aperture plan apochromat objective. The microscope was controlled using Fluoview 2.1c edition software.

Transmission Electron Microscopy

Snx9 silenced cells on glass coverslips were fixed in 5 % PFA/ 0.1 glutaraldehyde in PBS for 15 minutes at 37°C. Following this, the cells were washed 3 times in PBS and quenched in 50 mM glycine in PBS (pH 7.4) for 15 minutes at room temperature. The cells were then washed 3 times in PBS and stored in 1.6 % glutaraldehyde in PBS. Subsequently, cells were postfixed in 1% OsO4 in PBS buffer, dehydrated in ascending concentrations of ethanol and embedded in Spurr's epoxy resin. Coverslips were removed from the cured resin by a quick immersion into liquid nitrogen. Thin sections were cut on a Reichart OMU 3 Ultramicrotome, mounted on copper grids and counterstained with lead citrate and uranyl acetate. Samples were viewed on a JEOL 1230 transmission electron microscope at 60kV adapted with a 2000 x 2000 pixel bottom mount CCD digital camera (Hamamatsu, Japan) and digital images taken using AMT software.

2.8 *Western blotting*

The whole cell lysates of HeLa and HEK293 cells were obtained in the following manner: the cells seeded on 6 well plates were firstly washed twice in PBS to remove residual culture medium. Thereafter, the cells were incubated in 200 µl/well of cold RIPA buffer (Composition: 20mM Tris pH 8.0, 150 mM NaCl, 0.1 % SDS (vol/vol), 1 % deoxycholic acid (wt/vol), 1 % Triton X-100 (vol/vol)) and protease inhibitors in order to lyse the cells. The cell lysate was then centrifuged at 4° C for 15 minutes at 16 000 x g in order to separate the solubilized protein from undissolved material. Following this, the cell lysates were size fractionated on a 4 – 20 % Tris-glycine SDS-PAGE gel (Invitrogen) and transferred to a polyvinylidene difluoride membrane, PVDF (Millipore, Bedford, MA) for immunoblotting. Near infrared fluorescence detection (Li-COR Biosciences, Lincoln, NE) of the following infra red secondary antibodies: 800IRDye goat anti-mouse and 800IRDye goat anti-rabbit was used to visualize the blotted proteins. A SeeBluePlus2 Pre-stained molecular weight marker (Invitrogen) was used as a size standard.

3. Results

3.1 Aim 1: Investigating how silencing Snx9 alters mitochondrial morphology

3.1.1 Validation, verification and rescue of the siSnx9 mitochondrial phenotype from the genome wide siRNA morphology screen.

The endocytic protein, Snx9 was identified as a hit in a genome wide siRNA screen monitoring mitochondrial shape in HeLa cells. Specifically, the silencing of Snx9 altered the chondriome's morphology to yield a hyperfused mitochondrial phenotype. The first step of this research program was to validate the siSnx9 phenotype from the morphology screen. To this end, an " ON-TARGET plus" smart pool (used to minimize off-target effects) of four synthetic small interfering RNA duplexes targeted at the Snx9 gene, was introduced into HeLa cells via lipid mediated transient transfection. Silencing Snx9 over 72h (chosen to reflect the design of the siRNA screen which was done at 72h) led to a 12.5% increase in the number of cells with fused mitochondria compared to the non-targeted controls. This indicated a mild but substantial hyperfused (elongated) mitochondrial phenotype in siSnx9 cells **(Figure, 3.1)**. In addition, this result was in line with the fused mitochondrial phenotype obtained from siSnx9 cells in the morphology screen. Interestingly, silencing other endocytic proteins like EPS15 (adaptor which recruits clathrin) or dynamin2 (cell surface dynamin) did not result in hyperfusion **(as shown in Figure, 3.1)**, suggesting that the siSnx9 phenotype affecting mitochondria was not due to global effects of suppressed endocytosis.

Following the validation of the screen's siSnx9 fused phenotype, it was imperative to perform a rescue experiment as a control for silencing Snx9.This involved a deconvolution of the pooled siRNAs by testing whether each individual siRNA could silence Snx9.

Figure 3.1: Silencing of the endocytic protein Snx9 affords a hyperfused mitochondrial phenotype. (A and B) siRNA mediated transfection was employed to silence Snx9 over 72h in HeLa cells. The mitochondria were then labeled with anti-PRDX3 (mitochondrial matrix marker) to enable scoring of cells exhibiting fused mitochondria. The level of hyperfusion observed upon silencing Snx9 was greater than that obtained from silencing its endocytic partners (Dynamin2 and EPS15). Therefore, signaling that the siSnx9 mitochondrial phenotype was unlikely a result of the global effects of suppressed endocytosis. The bar graph is a plot of the mean of the % of cells with hyperfused mitochondria over three experiments ± SD. In each experiment, a minimum of 100 cells were counted per siRNA condition. (C) Western blots were used to verify the silencing of Snx9, EPS15 and Dynamin2 (dyn2) in HeLa cells.

How does silencing Snx9 alter mitochondrial morphology?

A

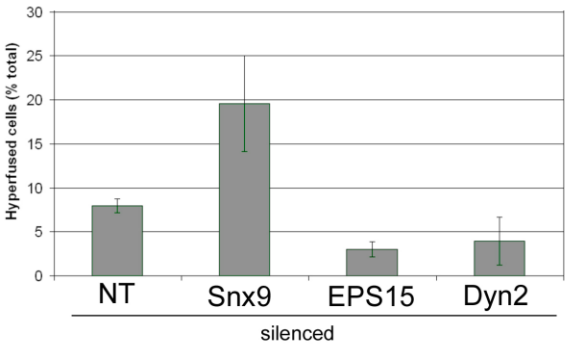

C

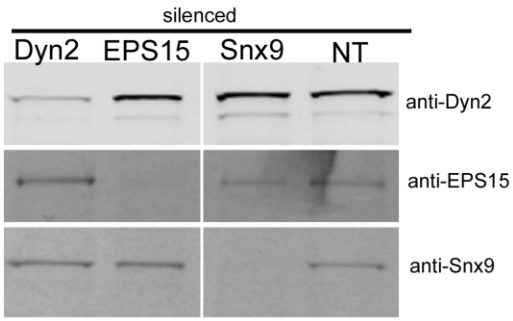

B

siSnx9 HeLa cells labeled with anti-PRDX3 antibody

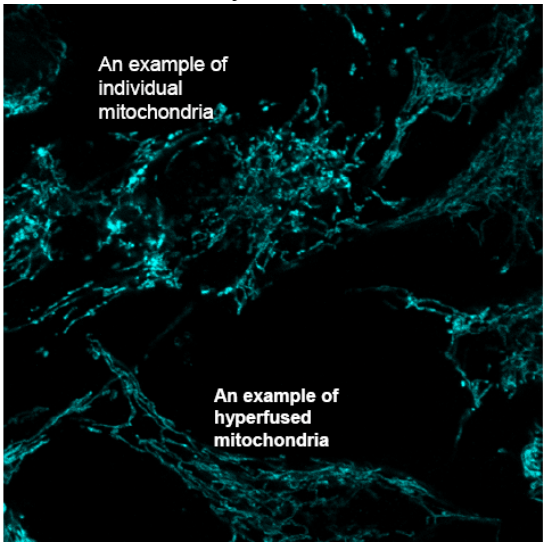

siNT HeLa cells labeled with anti-PRDX3 antibody

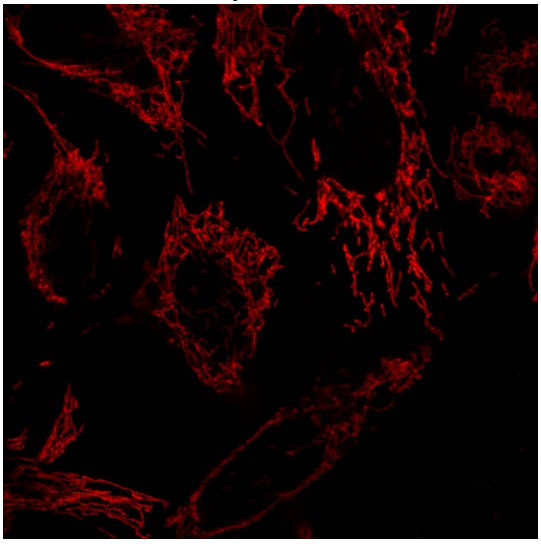

Indeed, all four individual siRNAs successfully silenced Snx9 gene expression **(as shown in Figure, 3.2a)**. Importantly, the deconvolution of siRNA pools is a key step in ruling out off-target effects which may arise from non-specific silencing of the genome. Since one of the four siRNAs in the pool was complementary to Snx9's 3'-untranslated region (3-UTR), gene expression could be restored by overexpressing either the YFP-Snx9 or Flag-Snx9 plasmids **(as shown in Figure, 3.2b)**. Notably, plasmids are typically designed to include the target gene's ORF (open reading frame) but not its 3'UTR, thereby making this type of rescue possible.

3.1.2 Interpreting the hyperfusion phenotype displayed by mitochondria in siSnx9 HeLa cells.

A hyperfused mitochondrial phenotype heralds two possibilities, either an inhibition of fission or an activation of fusion. The silencing of a molecule with a role in fission, allows for unopposed fusion resulting in a hyperfused mitochondrial phenotype. Conversely, mitochondrial hyperfusion can be activated by subjecting the cell to stress e.g. starvation or uv radiation. In order to test whether the siSnx9 hyperfusion phenotype was an indication that Snx9 was a fission molecule, it was important to check for interactions between Snx9 and known fission players. The overexpression of Snx9 for 24h in HeLa cells and labeling of Drp1 (primary fission regulator) with antibody demonstrated that YFP-Snx9 molecules did not co-localize/associate with Drp1, rather they were juxtaposed **(Figure, 3.3)**. In addition, the observation of YFP-Snx9 in living HeLa cells by time lapse imaging analysis did not reveal any convincing localization to active fission sites (not shown). Rather, YFP-Snx9 generally appeared to be in foci along-side mitochondrial tubules (see below).

Figure 3.2: A rescue experiment for silencing Snx9 gene expression. In order to select an individual siRNA to use in the rescue experiment, the Snx9-siRNA pool was deconvolved by testing whether each individual siRNA oligo in the pool could silence Snx9. (A) All four siRNAs silenced Snx9 gene expression as evidenced by the loss of the Snx9 protein. Note: Oligo2 targets the 3' UTR whilst the rest of the oligos target Snx9's ORF. (B) The restoration of Snx9 gene expression was done by overexpressing either a YFP-Snx9 or a Flag-Snx9 plasmid over an siSnx9 (oligo2) background.

a

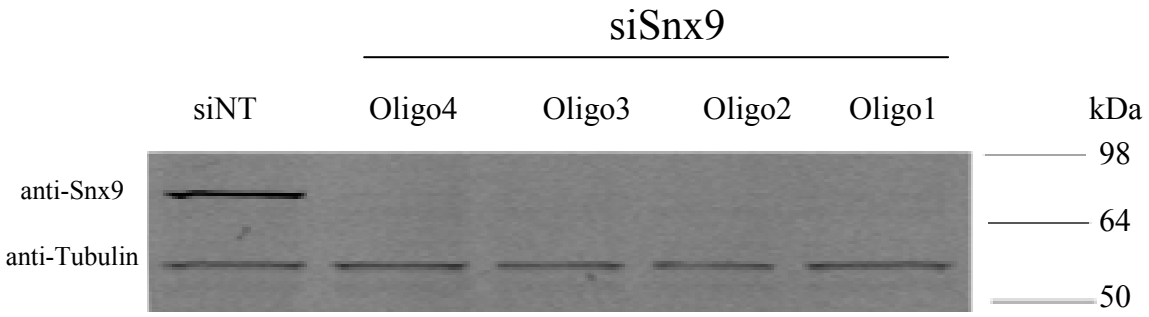
siSnx9
siNT
Oligo4
Oligo3
Oligo2
Oligo1
kDa
anti-Snx9
anti-Tubulin
98
64
50

b

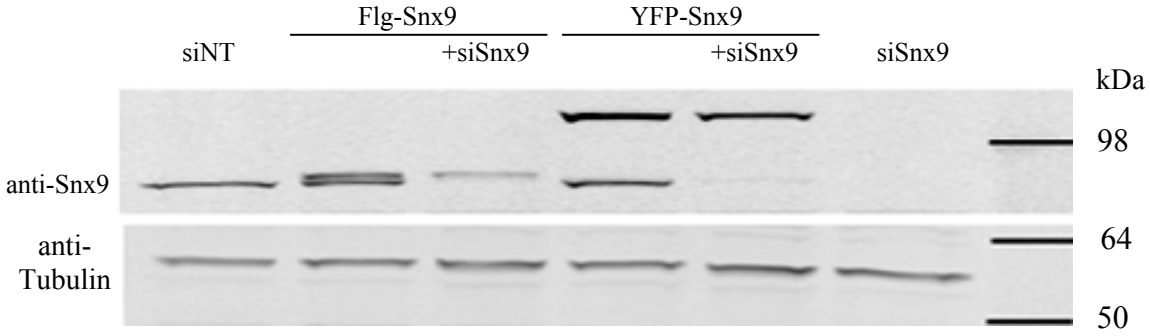
Flg-Snx9
YFP-Snx9
siNT
+siSnx9
+siSnx9
siSnx9
kDa
anti-Snx9
anti-
Tubulin
98
64
50

Figure 3.3: Colocalization experiment to test whether Snx9 may interact with known fission players. In order to test whether Snx9 co-localized with Drp1 (main mitochondrial fission regulator), HeLa cells were transfected with YFP-Snx9 (green) and Drp1 (red) labeled with anti- Drp1 antibody. The cells were also transfected with the mitochondrial matrix protein OCT-CFP (cyan) in order to mark the mitochondria. YFP-Snx9 did not co-localize with the fission GTPase Drp1, rather they were juxtaposed. The lack of colocalization between YFP-Snx9 and Drp1, signaled that the mitochondrial hyperfusion phenotype in siSnx9 cells was less likely to be an indication that Snx9 was a mitochondrial fission molecule.

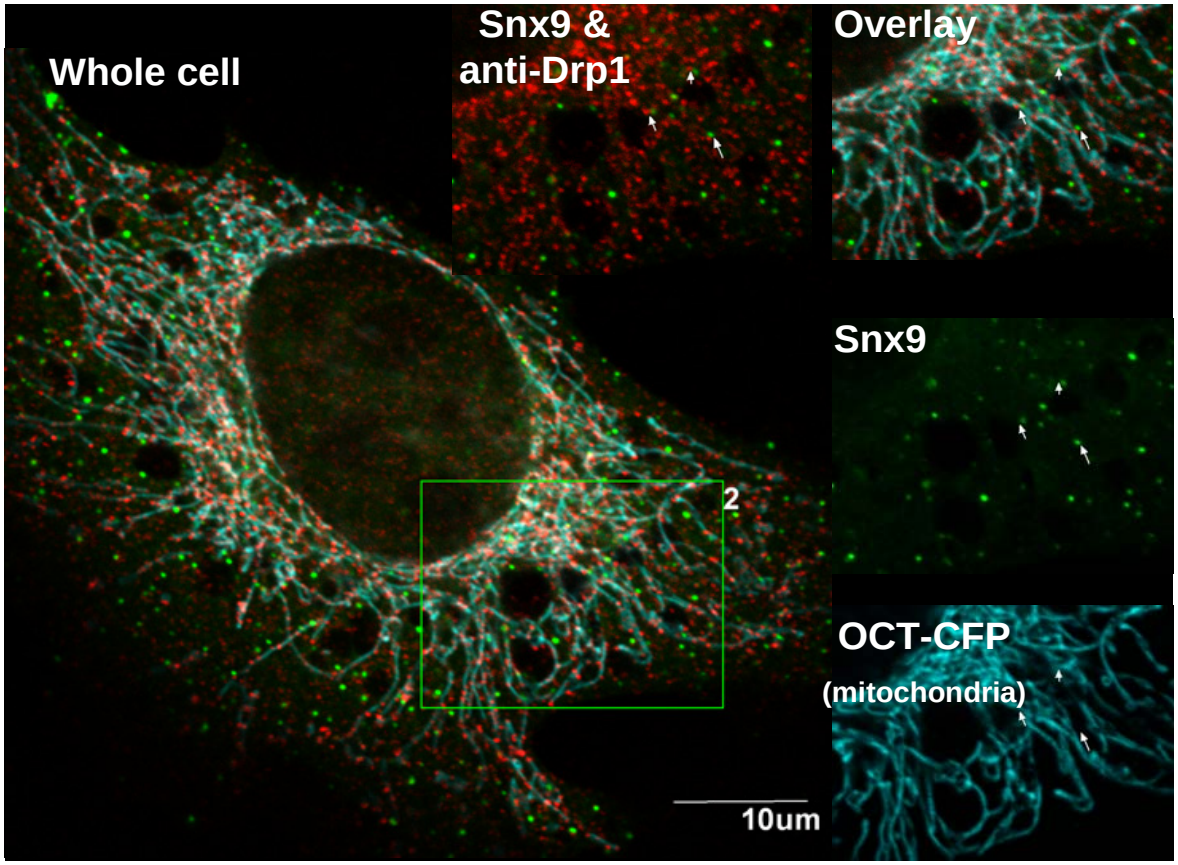
Whole cell
Snx9 &
anti-Drp1
Overlay
Snx9
OCT-CFP
(mitochondria)
2
10um

An explanation for this became more evident upon an ultrastructural analysis of the hyperfused phenotype. Electron microscopy of siSnx9 HeLa cells revealed concentric membranous whorls, between 80-200nm in width, accumulating under the mitochondrial outer membrane **(Figure, 3.4).** Moreover, the membranes had a smooth surface, and were arranged in a coil resembling an Archimedean "simple" spiral **(Figure, 3.4)**. Noticeably, the whorls were spherical in structure as opposed to being tubular/cylindrical suggesting their morphology could be vesicular **(Figure, 3.5).** Together, the above results imply that, the mitochondrial hyperfusion in cells silenced for Snx9 may be a stress response due to a dysfunction in the budding of mitochondrial derived vesicles.

An alternative hypothesis for the hyperfused mitochondrial phenotype in the siSnx9 cells could be that silencing Snx9 impinged on the cells ability to acquire nutrients, thereby triggering SIMH. Notably, Soulet et al have shown that silencing Snx9 decreases the rate of clathrin mediated endocytosis by almost half (evidenced by the 45 % decline in the rate of transferrin internalization in Snx9 silenced HeLa cells) (Soulet et al, 2005). This hypothesis is based on the body of literature which demonstrates that mitochondria of cells subjected to starvation fuse in order to be protected from autophagic degradation (Rambold et al, 2011). However, silencing of the other endocytic proteins including dynamin2 and EPS15 did not prompt fusion, indicating that the hyperfusion response in the mitochondria of siSnx9 cells was specific. In order to further clarify this point it would have been important to include starvation controls (e.g. cells kept on 5 % FBS in serum free media over 72h) and confirm that MDVs were not stalled in this case. This would show that nutrient deprivation leads to hyperfusion that is distinct from the Snx9 phenotype of stalled MDV formation.

Figure 3.4: Ultrastructural analysis of Snx9 silenced HeLa cells reveals whorls accumulating along the mitochondria. Long mitochondria were observed, consistent with mild hyperfusion, however most prominent was the appearance of concentric membranous whorls. This transmission electron micrograph of siSnx9 HeLa cells reveals concentric membranous whorls, between 80 – 200 nm accumulating under the mitochondrial outer membrane. Note: the arrows point out the whorls. The coiled arrangement of membranes in the Snx9-dependent whorls resembles an Archimedean " simple" spiral.

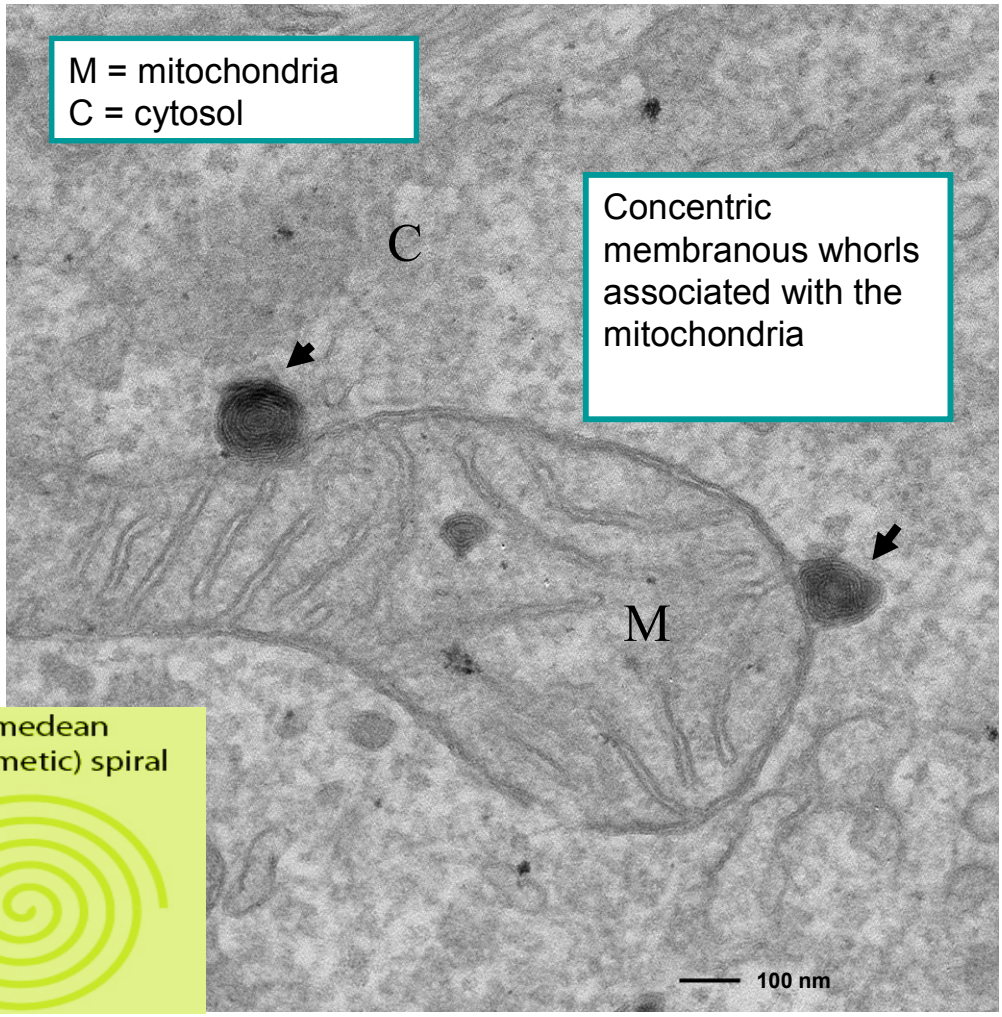

Archimedean (arithmetic) spiral

Direct magnification: 15 000x

Figure 3.5: Snx9-dependent whorls are consistent with mitochondrial derived vesicles. Transmission electron micrograph of Snx9 silenced HeLa cells. The Snx9- dependent multi-membrane whorls have a spherical shape suggesting a vesicular morphology.

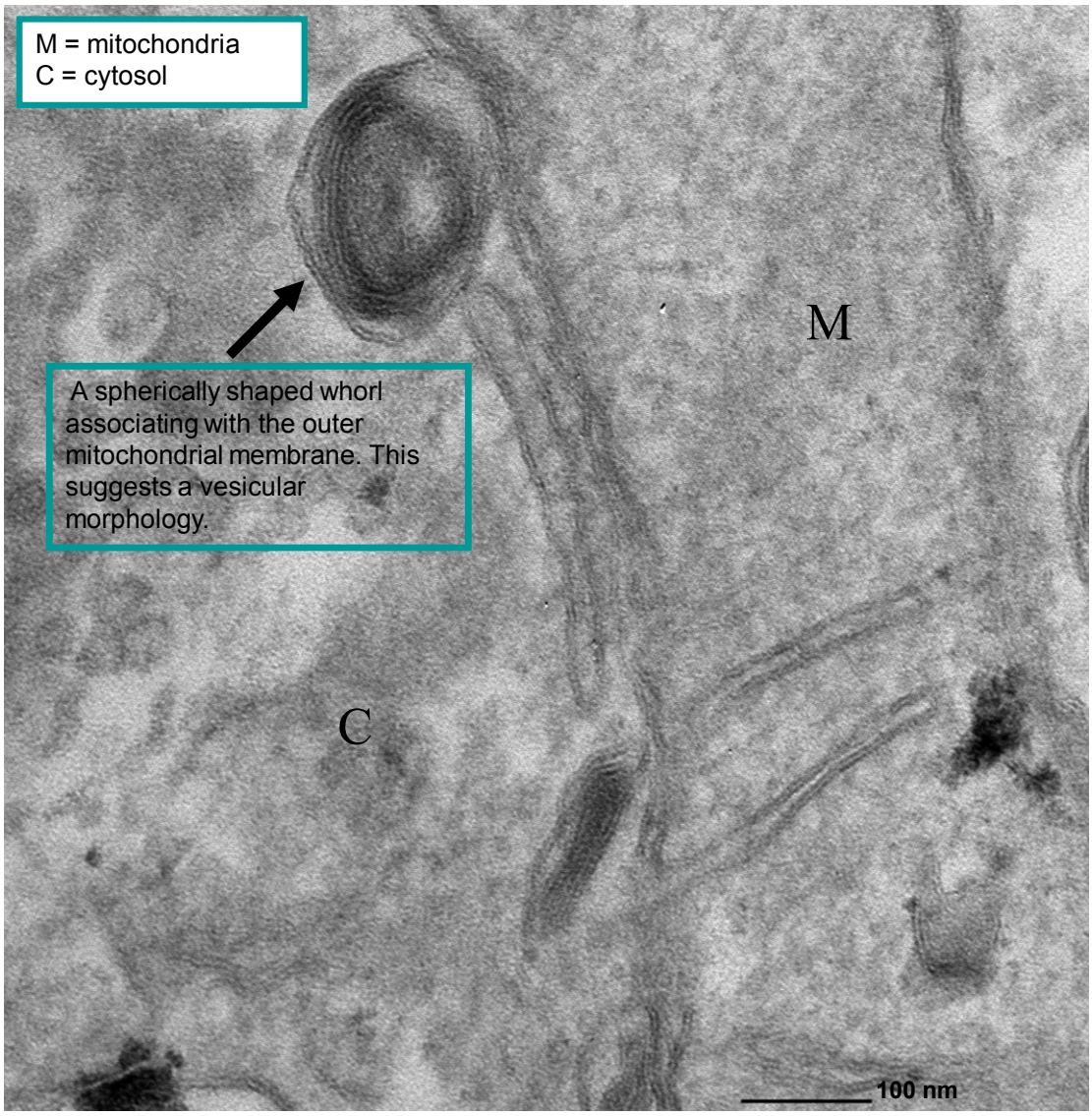

Direct magnification: 30 000x

3.1.3 Quantification of the number of whorls in siSnx9 cells.

In addition, to observing whorls at the mitochondria, multi-membrane structures similar in morphology to the Snx9-dependent MDVs were noted in both the cytosol and the lysosome **(Figures, 3.6 and 3.7)**. This suggested that the whorls seen budding from mitochondria may have been destined for the lysosome. In fact, a comparison of the siSnx9 cells to the controls (non-targeted siRNA) revealed that most of the whorls in the siSnx9 cells were associated with the mitochondria whilst those in the siNT were free in the cytosol **(Figure, 3.8).** One interpretation could be that Snx9 is important for the release of MDVs from the mitochondria into the cytosol **(Figure, 3.6)**. These results provide evidence that Snx9 may form part of the molecular machinery required to bud mitochondrial vesicles.

Snx9-dependent MDVs are lipid rich

Ultrastructural imaging of Snx9-dependent MDVs revealed membranous structures suggesting they may be lipid rich. To determine whether these structures could be followed by confocal microscopy, Snx9 silenced HeLa cells were labeled with the neutral lipid marker nile red. This lipid soluble lysochrome (fat stain) becomes strongly fluorescent in non-polar environments. Confocal imaging revealed punctate structures on the mitochondria which were labeled with nile red but were devoid of the mitochondrial matrix protein marker OCT-CFP **(Figure, 3.9).** This result was in agreement with the ultrastructural imaging which depicted Snx9-dependent MDVs as compact membranous structures, confirming neutral lipids (triglycerides and cholesteryl esters) as a primary cargo of these MDVs. Furthermore, it could be deduced from the ultrastructural imaging that the Snx9-dependent whorls were forming from the inner mitochondrial membrane. If this was true, it could be hypothesized

Figure 3.6: Cytosolic multi-membrane whorls appear to have originated from the mitochondria. (a) The transmission electron micrograph of Snx9 silenced HeLa cells illustrates concentric membranous whorls associated with the mitochondria (i), exiting the mitochondria (ii) and free in the cytosol (iii). (b) The multi-membrane whorls are surrounded by cristae, this further supports the suggestion that the whorls are within and originate from the mitochondria.

A

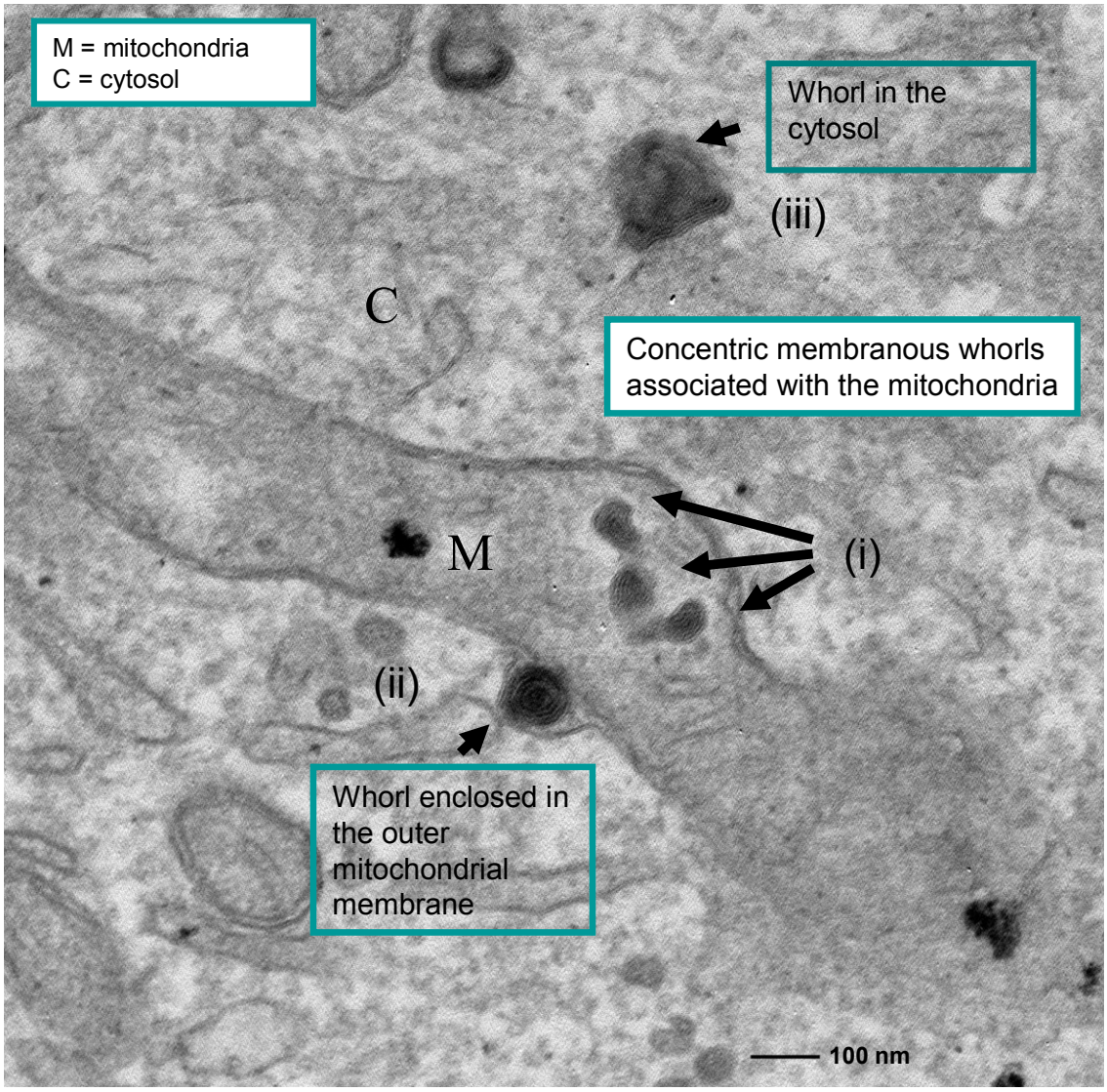

Direct magnification: 15 000x

B

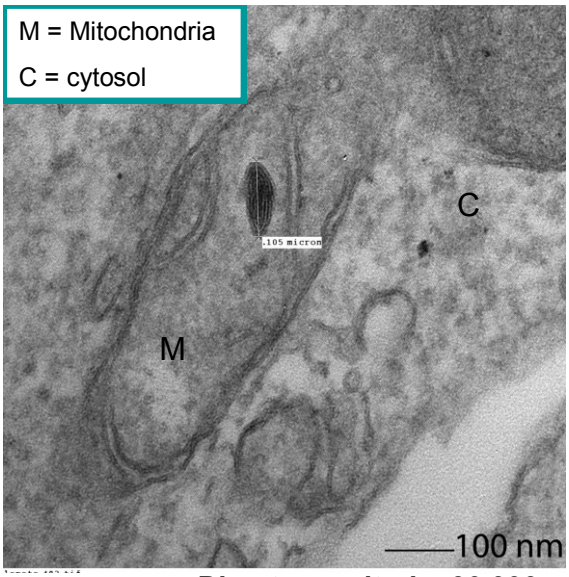

Direct magnitude: 30 000x

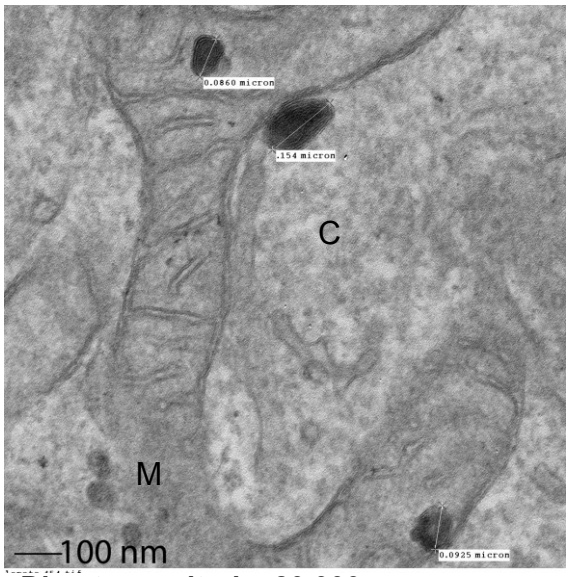

Direct magnitude: 20 000x

Figure 3.7: Membranous structures consistent with the Snx9-dependent whorls appear within the lysosome. Transmission electron micrograph of Snx9 silenced HeLa cells illustrates multi-membrane whorls akin to the Snx9- dependent mitochondrial whorls unraveling in the lysosome.

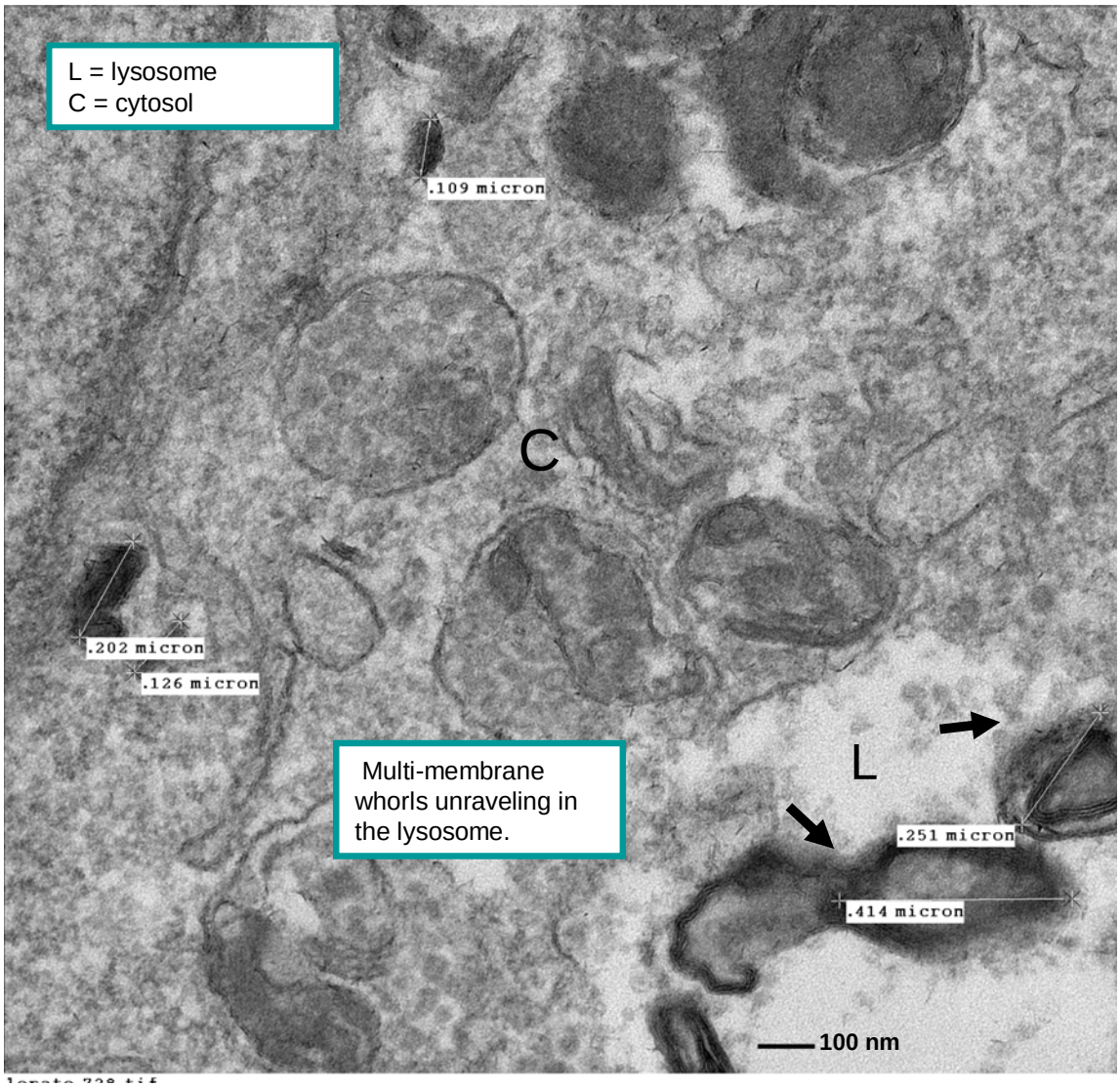

Direct magnification: 12 000x

Figure 3.8: Snx9 is important for the release of mitochondrial derived vesicles.
The number of whorls within the mitochondria, budding from the mitochondria, in the cytosol or in the lysosome in Snx9 silenced HeLa cells and the non-targeted siRNA controls were counted. The bar graph shows that a larger number of whorls remain associated (within or budding) with the mitochondria in Snx9 silenced HeLa cells, rather than free in the cytosol as in the non-targeted controls. This suggests that silencing Snx9 in HeLa cells may stall the release of mitochondrial derived vesicles. The scoring was done by counting the no. of whorls in 150 images (10 images per cell for 15 cells) for siSnx9. The same was done for the non-targeted controls. Scale bars on the transmission electron microscopy images represent 100 nm.

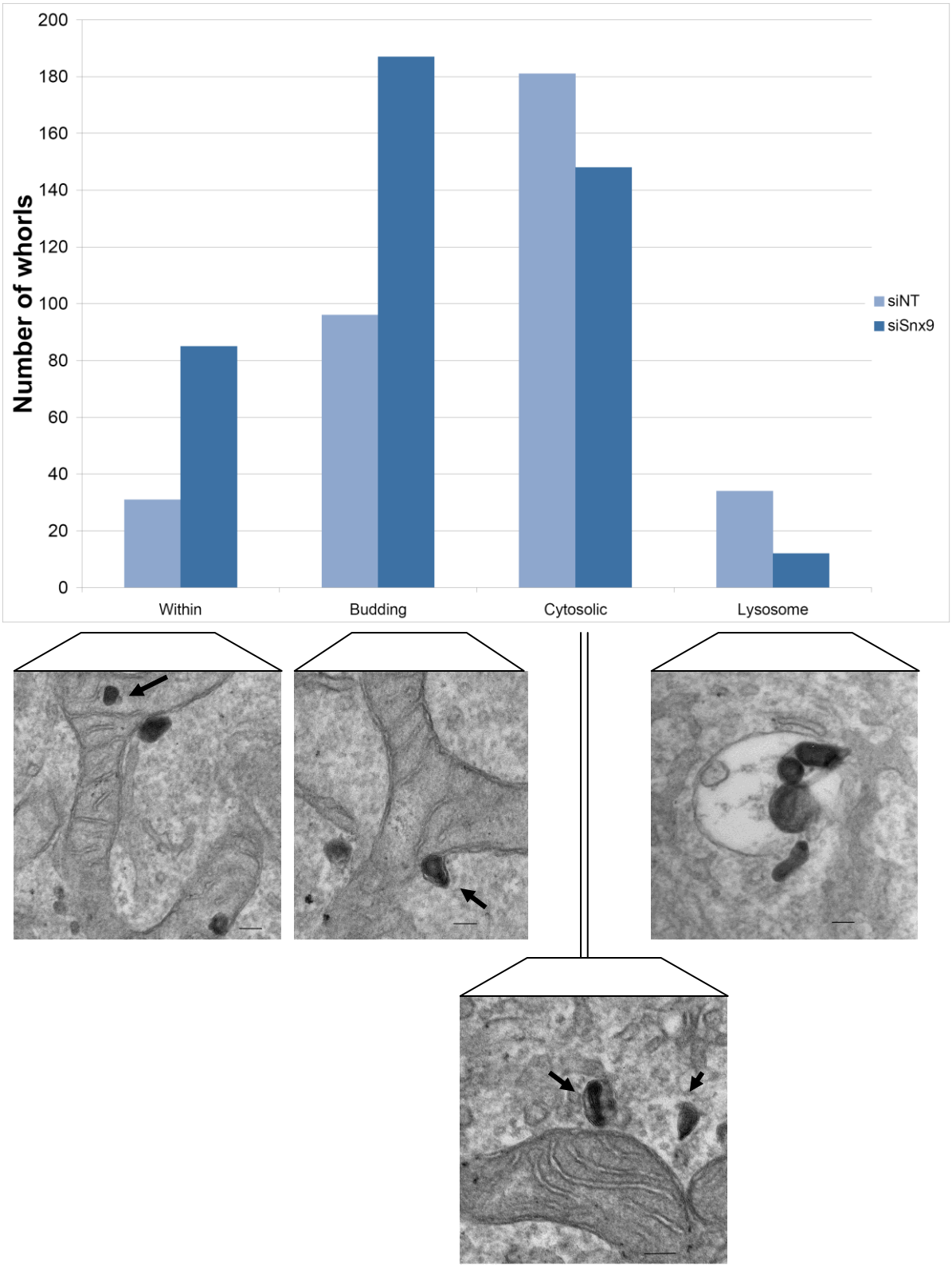
Number of whorls
200
180
160
140
120
100
80
60
40
20
0
Within
Budding
Cytosolic
Lysosome
siNT
siSnx9

Figure 3.9: Snx9-dependent whorls are enriched for neutral lipids. Confocal image of Snx9 silenced HeLa cells stained for the fluorescent neutral lipid marker, nile red (green). The cells were also transfected with the mitochondrial matrix protein OCT-CFP (cyan) in order to label the mitochondria. Accumulation of nile red into punctuate structures "dots" at the mitochondria suggests that the Snx9-dependent whorls (vesicles) are rich in neutral lipids (triglycerides and cholesteryl esters). The regions of nile red accumulation are devoid of the mitochondrial matrix marker OCT-CFP consistent with the Snx9-dependent whorls being compact membranous structures.

Neutral lipid accumulates within mito foci.

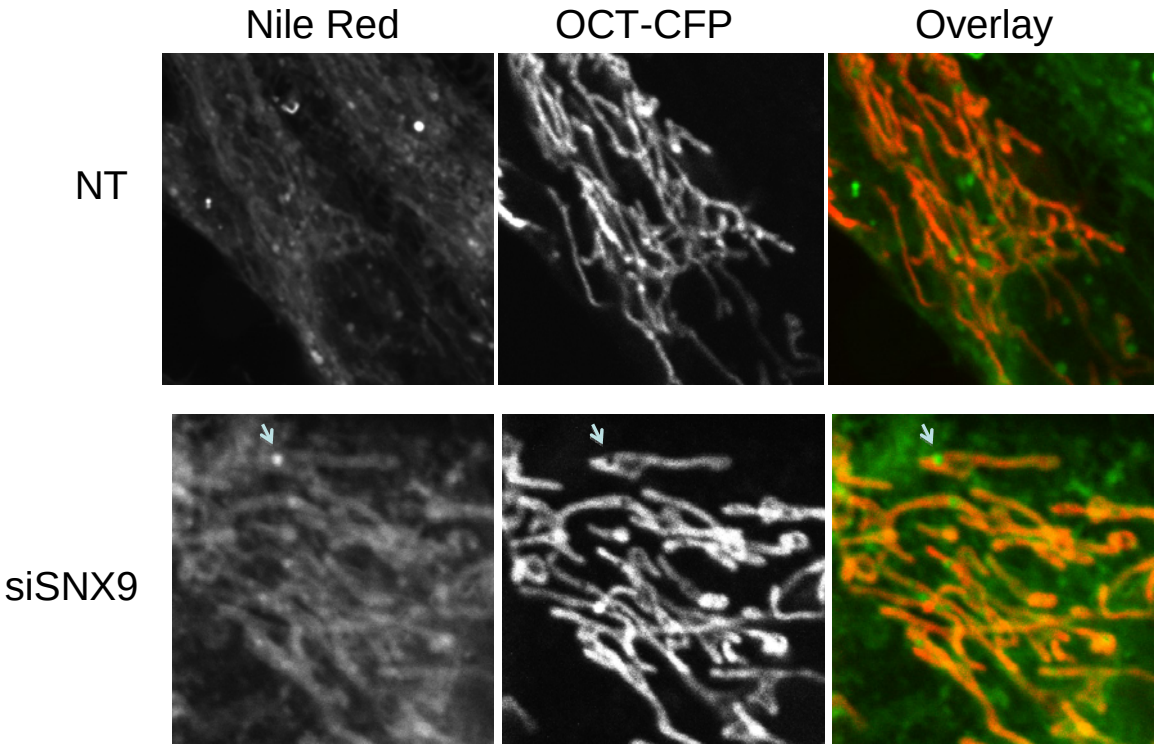

that the Snx9-dependent whorls would not accumulate free cholesterol since the inner mitochondrial membrane lacks cholesterol. Filipin staining of Snx9 silenced HeLa cells was employed to test for the accumulation of unesterified (free) cholesterol in the Snx9-dependent MDVs. However, there was no noticeable modification of the fluorescent cholesterol marker, filipin in Snx9 silenced cells **(Figure, 3.10)**. Together, these results may signify that the concentric membranous whorls originate from the inner mitochondrial membrane and are enriched for triglycerides and cholesteryl esters. Mitochondria are renowned for their rich cardiolipin deposits, therefore it was important to test whether the composition of Snx9-dependent MDVs included cardiolipin. The fluorescent dye, 10-nonyl acridine orange (NAO) was used to detect cardiolipin enrichment. However, NAO was not modified by silencing Snx9 in HeLa cells, suggesting that it was excluded from the MDVs (not shown).

Figure 3.10: Snx9-dependent mitochondrial whorls are not enriched for cholesterol. Confocal image of Snx9 silenced HeLa cells stained for filipin (fluorescent marker for un-esterified cholesterol), in order to test for cholesterol accumulation. The cells were also transfected with the mitochondrial matrix protein OCT-YFP (purple) in order to label the mitochondria. No noticeable modification of the fluorescent cholesterol marker was observed at the mitochondria. This suggested that the Snx9-dependent mitochondrial vesicles were not composed of unesterified cholesterol.

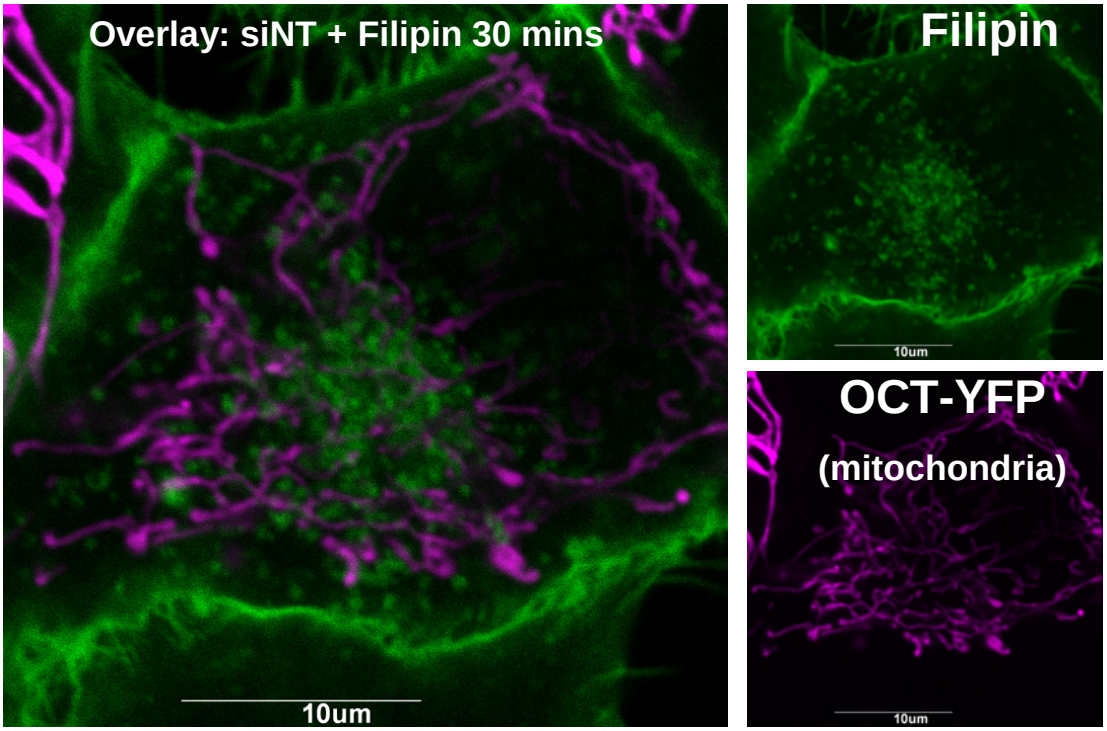
Overlay: siNT + Filipin 30 mins
10um
Filipin
10um
OCT-YFP
(mitochondria)
10um

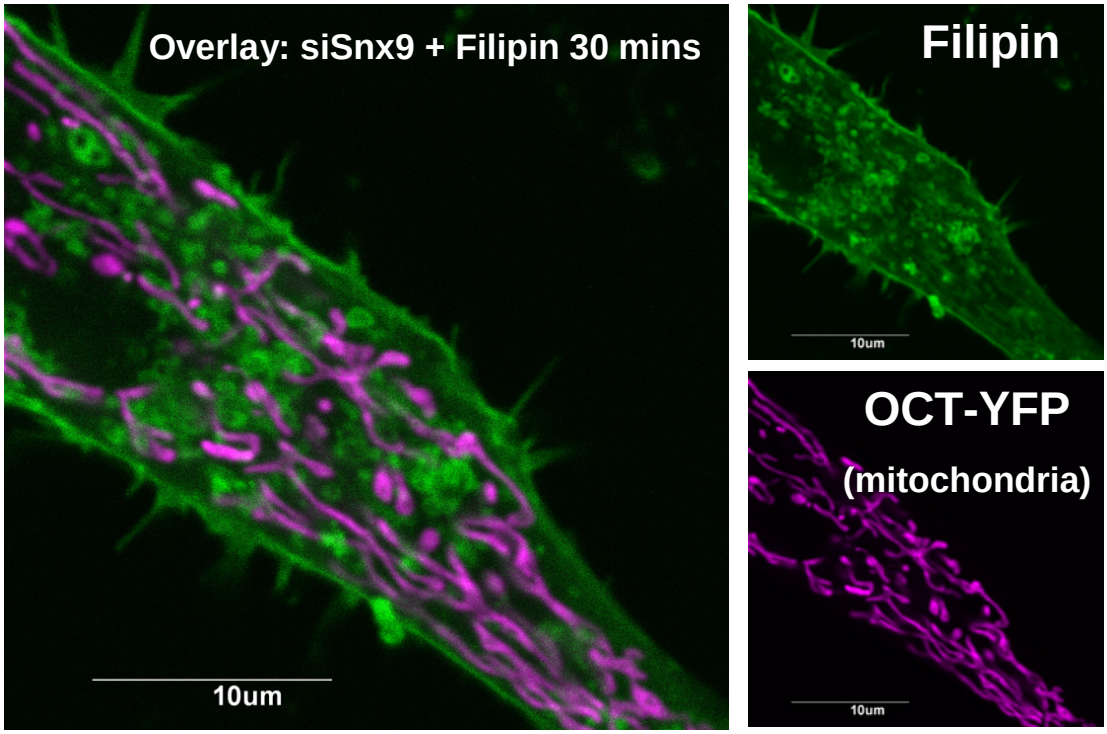
Overlay: siSnx9 + Filipin 30 mins
10um
Filipin
10um
OCT-YFP
(mitochondria)
10um

The experimental outcomes of the first aim, made a case for the recognition of the endocytic protein, Snx9 as molecular machinery requisite for the budding and release of mitochondrial derived vesicles. Following this, the next important step was to examine the regulation of Snx9's association with the mitochondria.

3.2 Aim 2: Regulation of Snx9's association with the mitochondria

The first step towards characterizing Snx9's association with the mitochondria was to test whether it localized to the mitochondria. To this end, YFP-Snx9 was over-expressed over 24h in HeLa cells and the mitochondria labeled with anti-Tom20 (outer membrane marker). Snx9 was largely cytosolic as expected from previous publications (Lundmark and Carlsson, 2003); however a sub-population of Snx9 molecules in the form of foci "dots" partially localized with the edges of the mitochondrial outer membrane. As demonstrated by the partial colocalization between YFP-Snx9 and anti-Tom20 **(Figure, 3.11).** The accumulation of Snx9 at the mitochondria was not always robust as some cells only showed modest recruitment **(Figure, 3.12).** This result suggests that the amount of Snx9 which localizes to mitochondria in HeLa cells is variable.

Snx9 transiently associates/co-localizes with mitochondria in live HeLa cells.

When looking at Snx9's localization to the mitochondria in a single image, it may not be clear whether Snx9 foci specifically colocalize with the mitochondria, or whether the image may reflect a random intersection with the mitochondria. To better characterize the apparent recruitment of Snx9 to the mitochondria, confocal live imaging was used to

Figure 3.11: Snx9 localizes to the mitochondria. Confocal imaging illustrates a partial colocalization between YFP-Snx9 (green) and the mitochondrial outer membrane marker, anti- Tom20 (red) in HeLa cells.

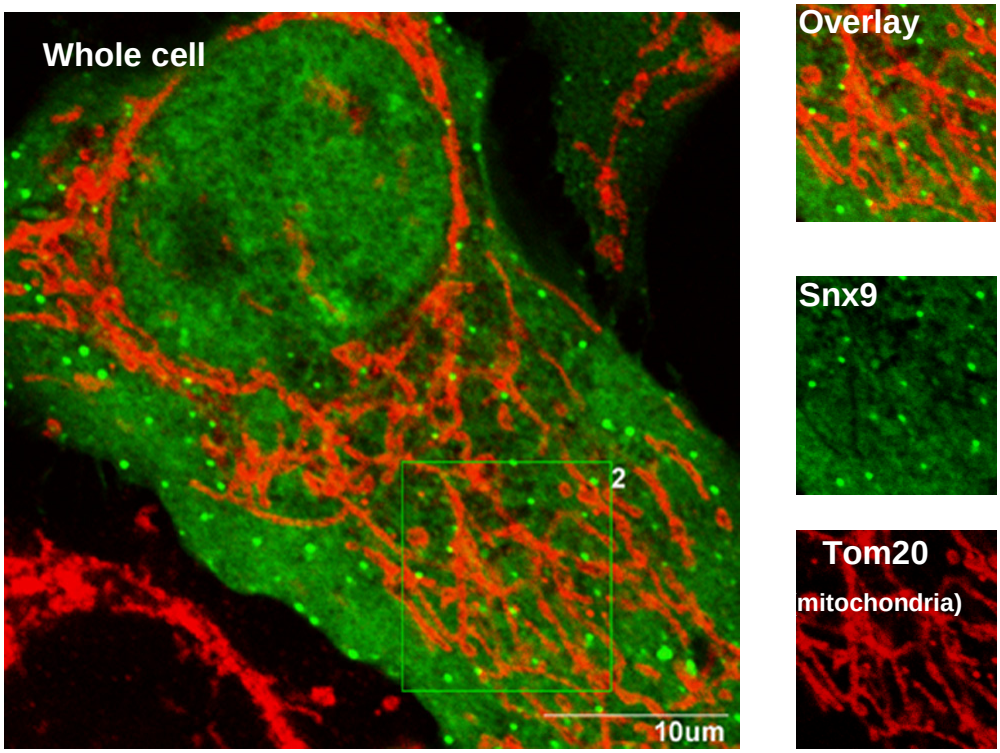
Whole cell
2
10um
Overlay
Snx9
Tom20
mitochondria)

Figure 3.12: The level of Snx9 localization to the mitochondria is variable. Confocal imaging illustrates modest accumulation of YFP-Snx9 at the mitochondria compared to the robust recruitment of YFP-Snx9 previously noted in Figure 3.11. The experiment was carried out in HeLa cells. YFP-Snx9 is indicated in green and the mitochondrial outer membrane marker, anti- Tom20 is shown in red.

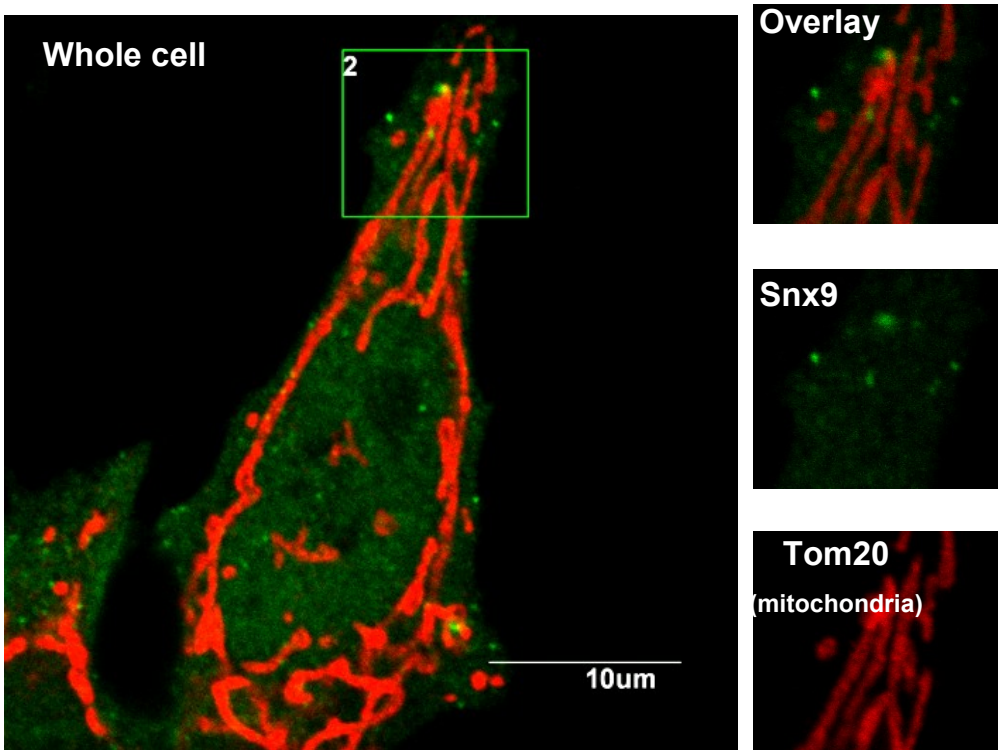
Whole cell
2
10um
Overlay
Snx9
Tom20
(mitochondria)

examine Snx9's behavior in living HeLa cells. Snx9 molecules in the form of foci were found to colocalize with mitochondria. The approximate resident time of Snx9's recruitment to the mitochondria was about 1 min 15 seconds and outlasted that of the flashes of Snx9 observed at the cell surface/cell boundary (30 seconds) **(Figure, 3.13)**. **(Also refer to the accompanying video entitled: YFP-Snx9 OCT-CFP video thesis).** Studies on the transient recruitment of Snx9 to clathrin coated vesicles during endocytosis indicate Snx9 molecules lasting at the cell surface for a brief period of about 27 seconds (Soulet et al, 2005). This is consistent with the quick flashes of Snx9 foci (puncta) seen appearing and disappearing at the cell boundary/ plasma membrane.

Although the majority of Snx9 molecules translocate to the cell surface for clathrin mediated endocytosis. The above evidence demonstrates that there is a sub-population of Snx9 molecules which transiently associates with the mitochondria.

Figure 3.13: YFP-Snx9 transiently associates with the mitochondria in HeLa cells. Confocal video imaging of live HeLa cells transfected with YFP-Snx9 (red) reveals foci of Snx9 at the mitochondria and boundary of the cell (cells surface). The cells were also transfected with OCTCFP in order to mark the mitochondria. In contrast to YFP-Snx9 foci at the cell periphery (cyan arrow), which appear and disappear rapidly “flashes”, YFP-Snx9 foci at the mitochondria (white arrow) depict a more stable association. Over the course of about a minute, the time series of still images illustrates that mitochondria-lly localized YFP-Snx9 remains in contact with the mitochondria for the entire period whilst foci at the cell boundary stay on for ~ 30 seconds.

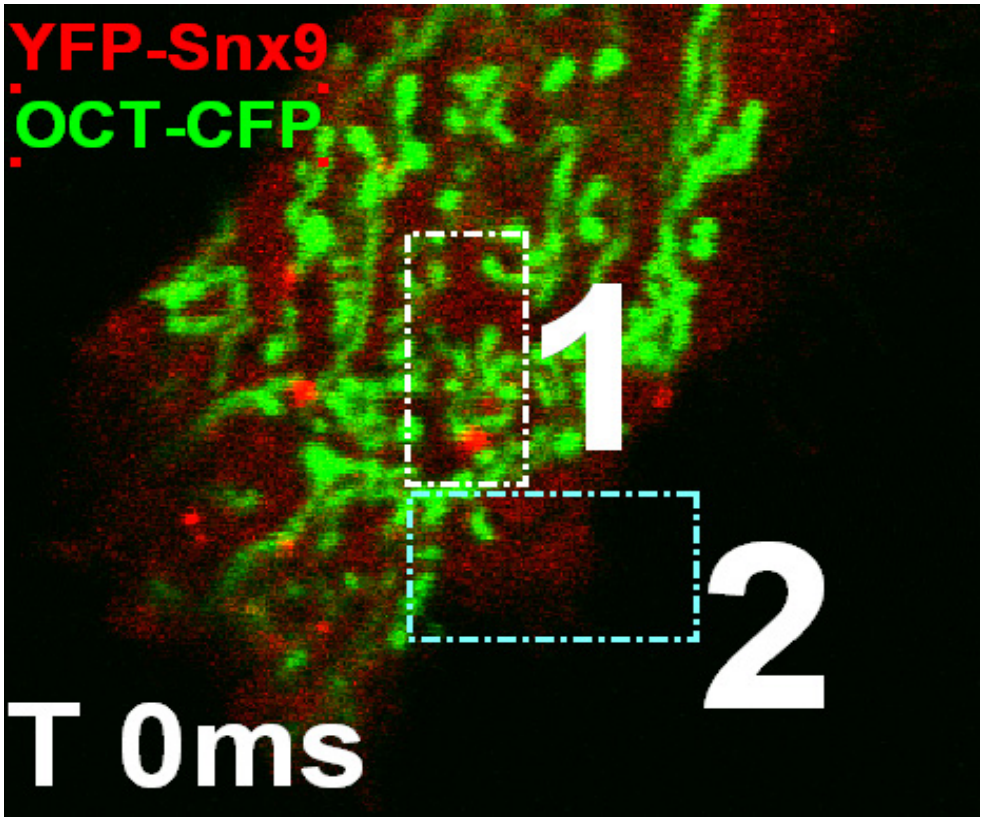
YFP-Snx9
OCT-CFP
1
2
T 0ms

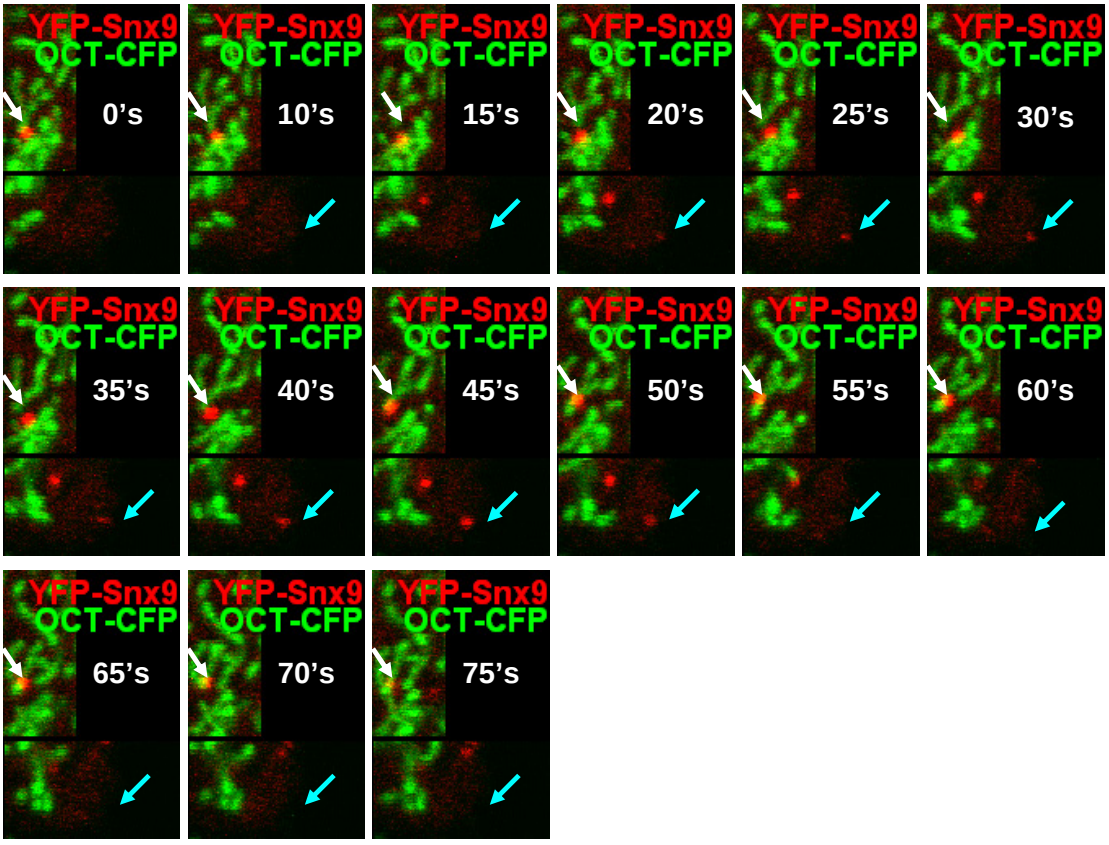
YFP-Snx9
OCT-CFP
0's
10's
15's
20's
25's
30's
35's
40's
45's
50's
55's
60's
65's
70's
75's

Having demonstrated Snx9's role in the release of MDVs and its (Snx9) transient localization to mitochondria, the next major step was to further dissect Snx9's function at the mitochondria by characterizing the cargo in Snx9-dependent MDVs.

3.3 Aim 3: Define the role of snx9 at the mitochondria

Parkinson Disease related proteins label the cargo in Snx9-dependent MDVs

In an attempt to characterize molecular function of Snx9 in the generation of the concentric membranous whorls, we took advantage of ongoing studies within the McBride laboratory. Work done with collaborators (Ted Fon) at the Montreal Neurological Institute has shown that Parkin is selectively recruited to vesicles triggered by oxidative damage (unpublished). We therefore already had an indication that the ubiquitin E3 ligase Parkin was involved in the generation of MDVs. Upon silencing of Snx9 in HeLa cells, we observed a robust enrichment of YFP-Parkin foci on the outer mitochondrial membrane **(Figure, 3.14)**.

Importantly, this recruitment occurred in the absence of mitochondrial depolarization or any other induced stress. The decoration of YFP-Parkin foci on the outer mitochondrial membrane was consistent with the Snx9-dependent MDVs which were seen budding from the mitochondria in the TEM (transmission electron microscopy) images**.** This recruitment was perhaps even better demonstrated in HEK293 cells which, unlike HeLa cells, contain endogenous Parkin **(Figure, 3.15).** Up until now, Parkin foci were only known to localize to mitochondria which had lost potential (depolarized mitochondria) (Narendra et al, 2008).

Realizing that the mitochondrial localization of Parkin could be modulated not only

Figure 3.14: YFP-Parkin localizes to mitochondria in siSnx9 HeLa cells. Over-expression of YFP-Parkin (green) in Snx9 silenced HeLa cells and the siNT controls reveals a robust enrichment of YFP-Parkin foci at the mitochondria (labeled with anti-Tom20: red). The decoration of YFP-Parkin foci along the mitochondrial outer membrane is consistent with the Snx9 –dependent whorls seen budding from the mitochondria (previously shown by transmission electron microscopy). This suggests that YFP-Parkin could be label the cargo in Snx9-dependent mitochondrial derived vesicles.

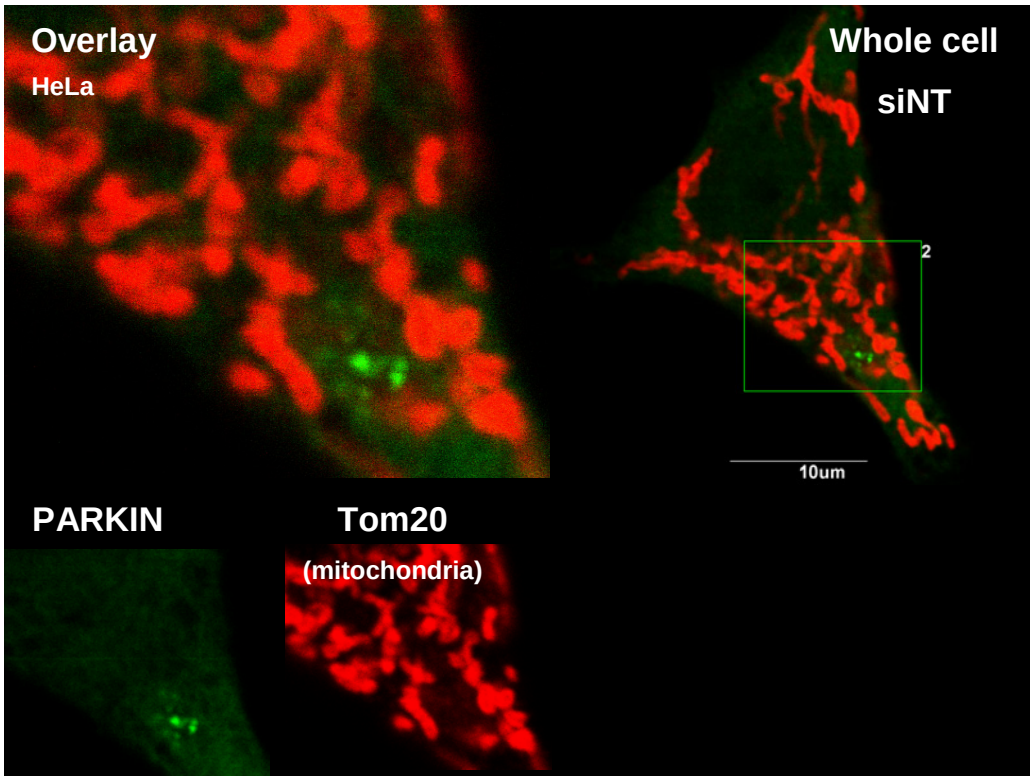
Overlay
HeLa
Whole cell
siNT
2
10um
PARKIN
Tom20
(mitochondria)

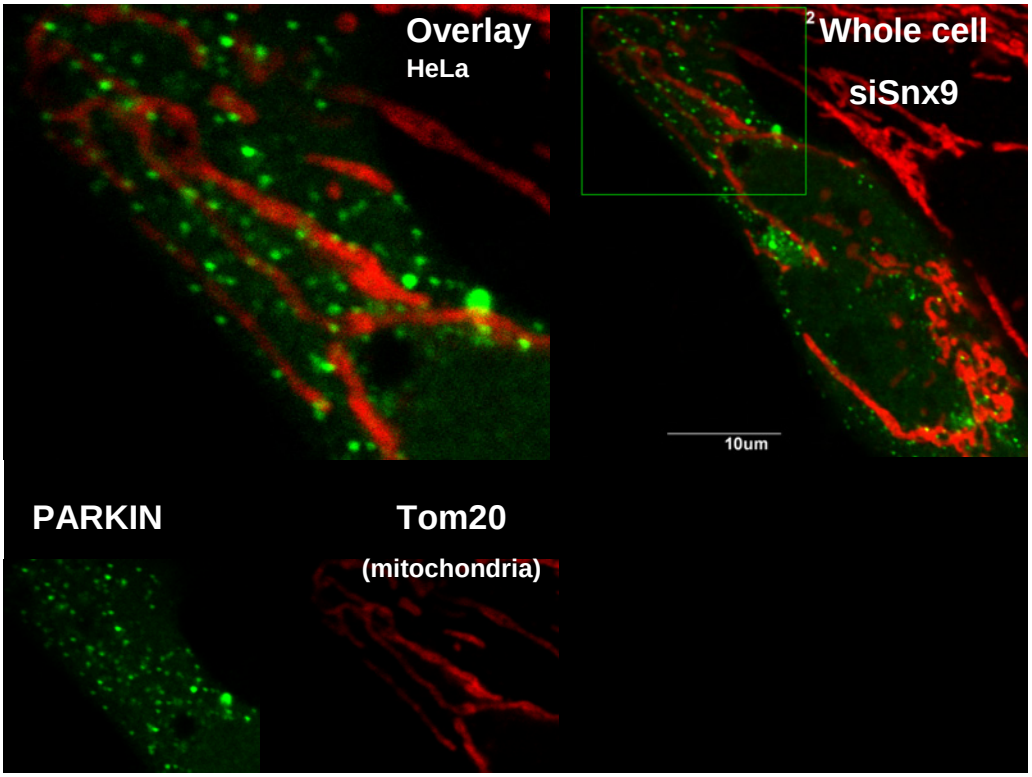
Overlay
HeLa
2
Whole cell
siSnx9
10um
PARKIN
Tom20
(mitochondria)

Figure, 3.15: Accumulation of YFP-Parkin at the mitochondria in Snx9 silenced HEK293 cells. Confocal imaging of siSnx9 HEK293 cells over-expressing YFP-Parkin (green), shows an enrichment of YFP-Parkin at the mitochondria. This result demonstrates that YFP-Parkin can accumulate at the mitochondria of Snx9 silenced cells in a cell line which has endogenous Parkin. The cells were also transfected with OCT-CFP (red) to mark the mitochondria.

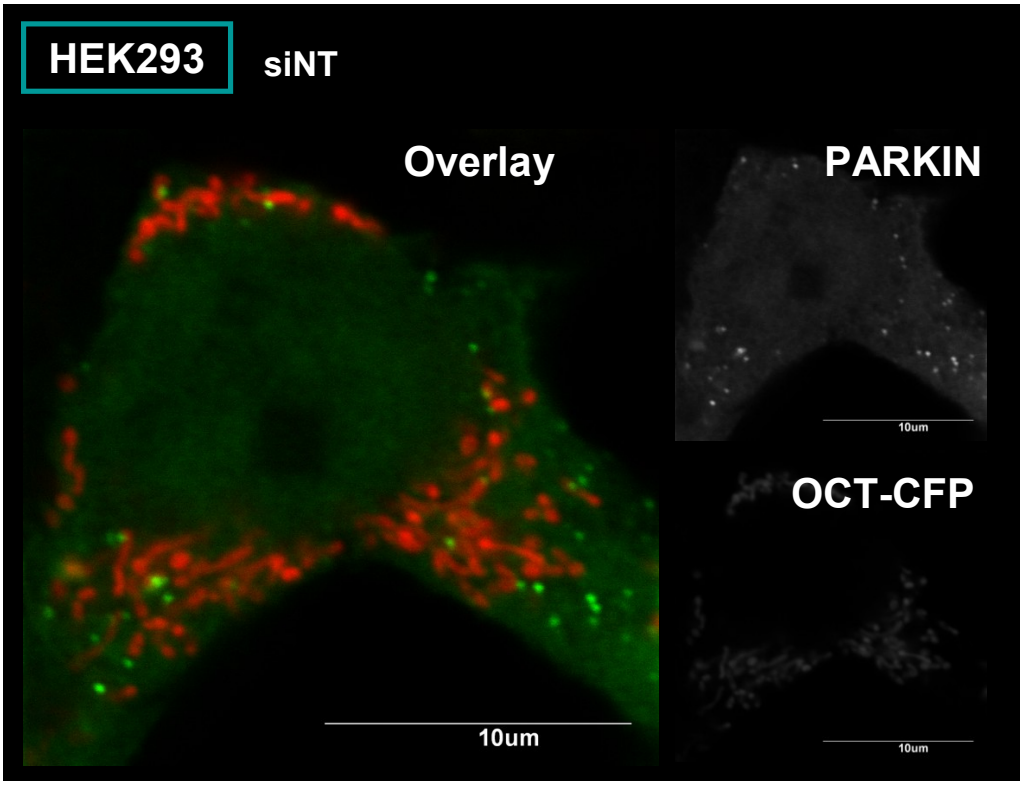
HEK293
siNT
Overlay
PARKIN
10um
OCT-CFP
10um
10um

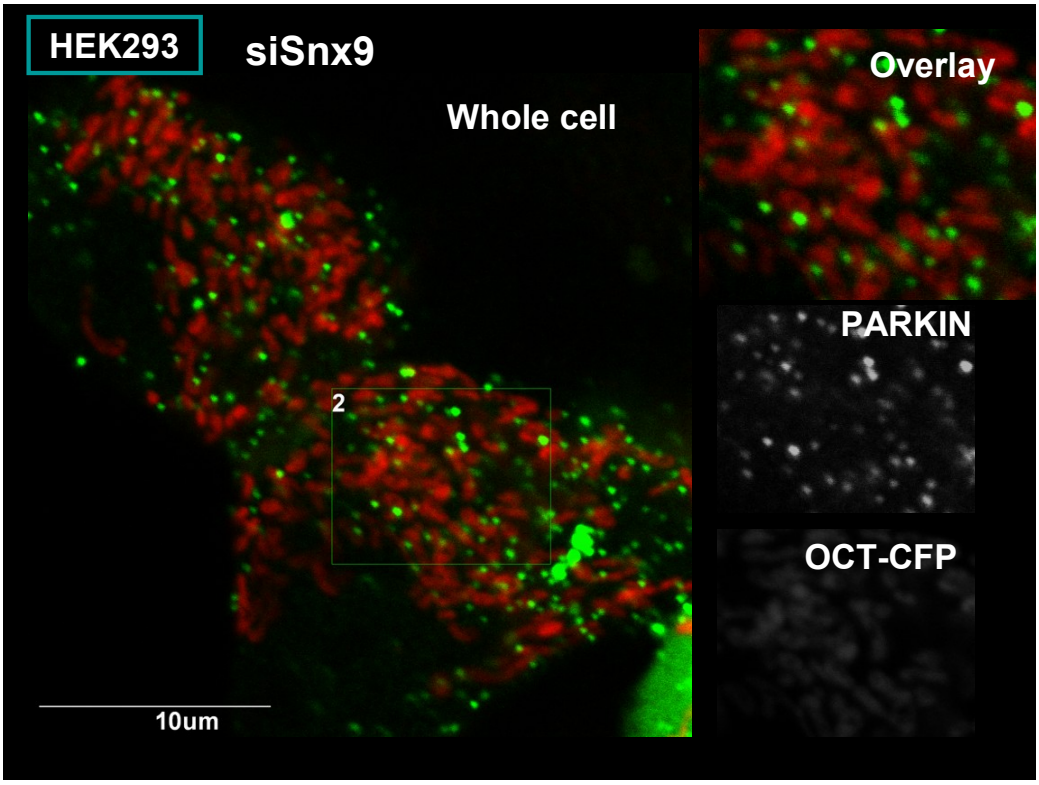
HEK293
siSnx9
Whole cell
2
10um
Overlay
PARKIN
OCT-CFP

by global mitochondrial depolarization but also by silencing Snx9 it was important to test whether there was any interaction between Snx9 and Parkin. Confocal microscopy, demonstrated a co-localization between YFP-Parkin and Cherry-Snx9 consistent with a potential functional interaction between these proteins **(Figure, 3.16).** The Parkin ubiquitin-like domain (ubl) has been shown to directly interact with SH3 (Src homology 3)- domain containing proteins (Trempe et al, 2009). Future work will examine whether Parkin and Snx9 may be associating through a similar Ubl-SH3 interaction **(Figure, 3.17)**.

The evidence that YFP-Parkin accumulates at the mitochondrial surface upon siSnx9 treatment, suggests that Parkin lies upstream of Snx9 (i.e. it does not require Snx9 for its recruitment) in the generation of MDVs. This raised the question of whether Parkin was required for efficient Snx9 recruitment. In order to test whether YFP-Parkin could trigger accumulation of Snx9 at the mitochondria, HeLa cells over-expressing both YFP-Parkin and Cherry-Snx9 were subjected to a CCCP treatment. Notably, the drug CCCP is an uncoupler that is commonly used as a tool to disrupt mitochondrial membrane potential thereby triggering accumulation of Parkin at the mitochondria. Following a 1h treatment with 10 μM of CCCP, confocal imaging revealed robust recruitment of Cherry-Snx9 to the mitochondria **(Figure, 3.18)**. This result indicated that YFP-Parkin might be required for the efficient recruitment of Cherry-Snx9 at the mitochondria.

At this juncture, experiments employing immunogold labeling by EM are currently being finalized in order to confirm that YFP-Parkin is indeed recruited directly to the accumulated mitochondrial whorl-structures seen in siSnx9 treated cells.

Figure 3.16: Cherry-Snx9 colocalizes with YFP-Parkin both along the mitochondria and within cytosolic foci. HeLa cells were co-transfected with Cherry-Snx9 (red) and YFP-Parkin (green). The mitochondria were labeled with anti-Tom20 antibody (purple). (a) Cherry-Snx9 colocalized with YFP-Parkin signifying a potential functional interaction between Snx9 and the Parkinson's Disease related protein, Parkin. Figure (b) has a higher abundance of YFP-Parkin foci compared to figure (a), highlighting the variability observed when imaging YFP-Parkin. Notably, all the Cherry-Snx9 foci colocalize with YFP-Parkin.

a)

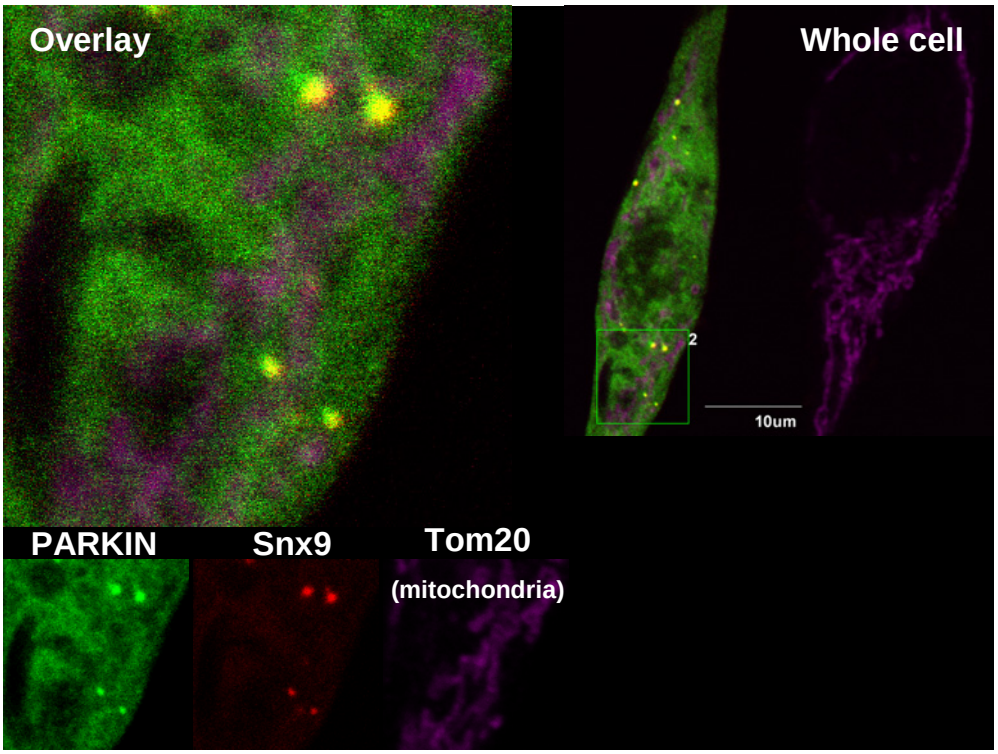
Overlay
Whole cell
2
10um
PARKIN
Snx9
Tom20
(mitochondria)

b)

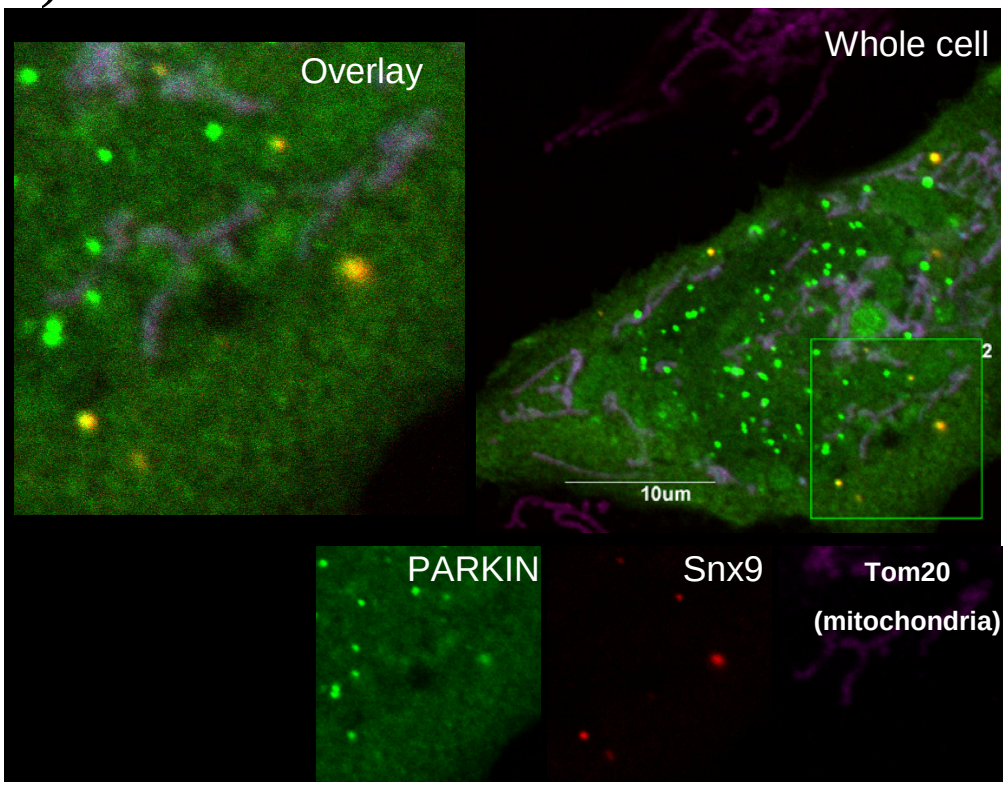
Overlay
Whole cell
2
10um
PARKIN
Snx9
Tom20
(mitochondria)

Figure 3.17: Snx9's domain structure contains a Parkin- interacting motif. Parkin interacts with endocytic BAR domain containing proteins e.g. Endophilin A through (Parkin) Ubl-SH3 (Endophilin A) interaction (Trempe et al, 2009). Similar to Endophilin A, Snx9 is an endocytic BAR domain containing protein which has an SH3 domain. Suggesting that the co-localization observed between Parkin and Snx9 could be mediated by a potential (Parkin)Ubl-SH3(Snx9) interaction (Images inspired by: Suzuki, 2006; Lundmark and Carlsson, 2009).

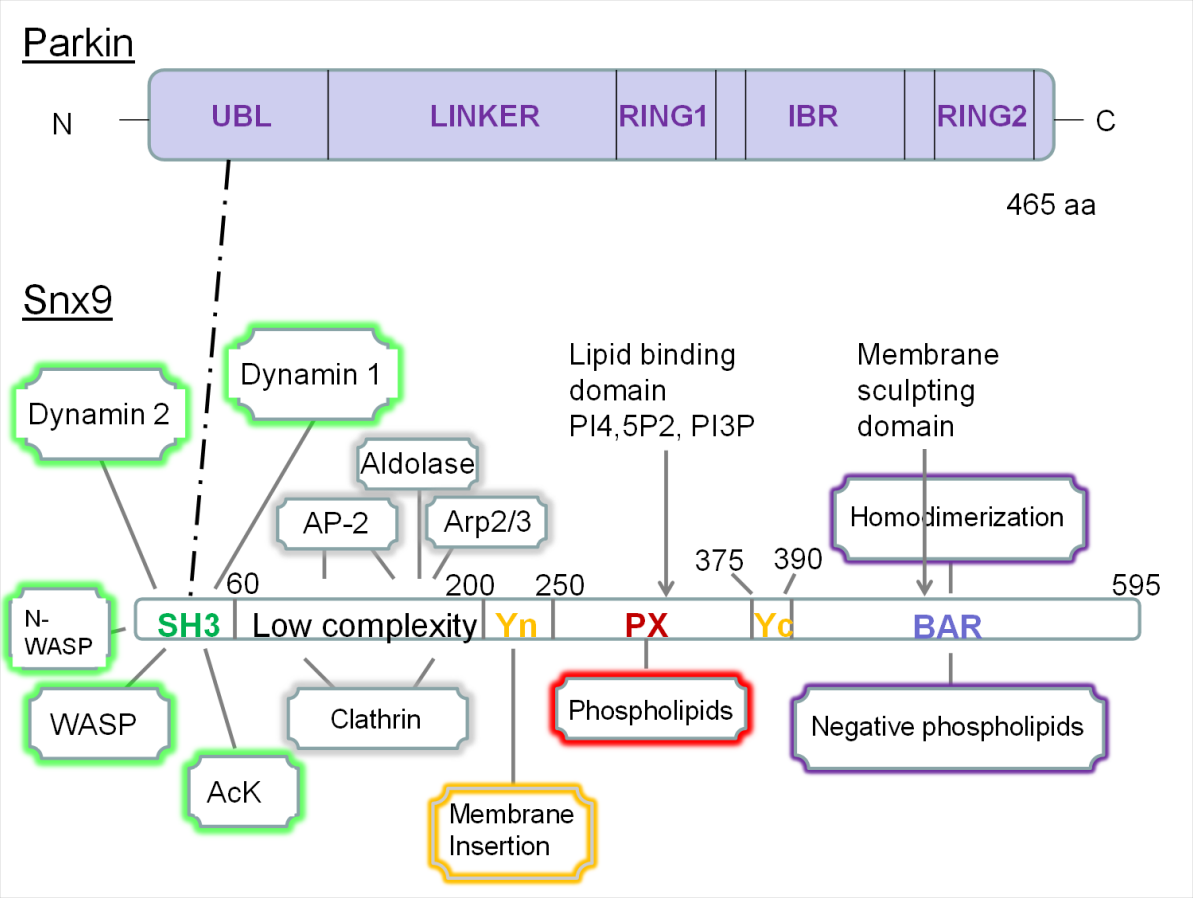
Parkin
N
UBL
LINKER
RING1
IBR
RING2
C
465 aa
Snx9
Dynamin 2
Dynamin 1
Aldolase
AP-2
Arp2/3
Lipid binding domain PI4,5P2, PI3P
Membrane sculpting domain
Homodimerization
60
200
250
375
390
595
N-WASP
SH3
Low complexity
Yn
PX
Yc
BAR
WASP
Clathrin
Phospholipids
Negative phospholipids
AcK
Membrane Insertion

Figure 3.18: Cherry-Parkin is required for the global recruitment of YFP-Snx9 to depolarized mitochondria. HeLa cells over-expressing YFP-Snx9 were subjected to a 10μM CCCP treatment for 1h. The cells were transfected with OCT-CFP in order to label the mitochondria. (a) Some YFP-Snx9 foci localized to the mitochondria. However, the recruitment was not convincing. In figure (b), HeLa cells co-transfected with Cherry-Parkin and YFP-Snx9 were subjected to a 10μM CCCP treatment over 1h. This resulted in the robust recruitment of both Cherry-Parkin and YFP-Snx9 to the mitochondrial surface, suggesting that YFP-Parkin may be required for efficient localization of YFP-Snx9 foci to the mitochondria. The mitochondria were labeled with anti-Tom20.

a)

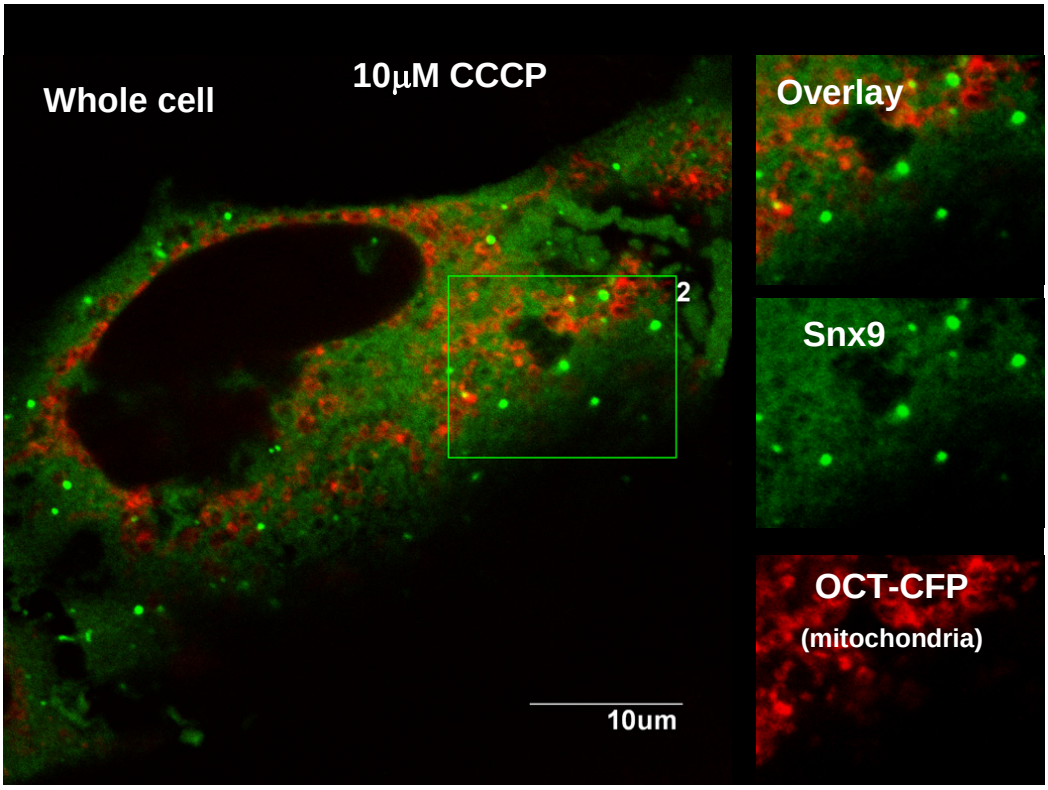
Whole cell
10μM CCCP
2
10um
Overlay
Snx9
OCT-CFP
(mitochondria)

b)

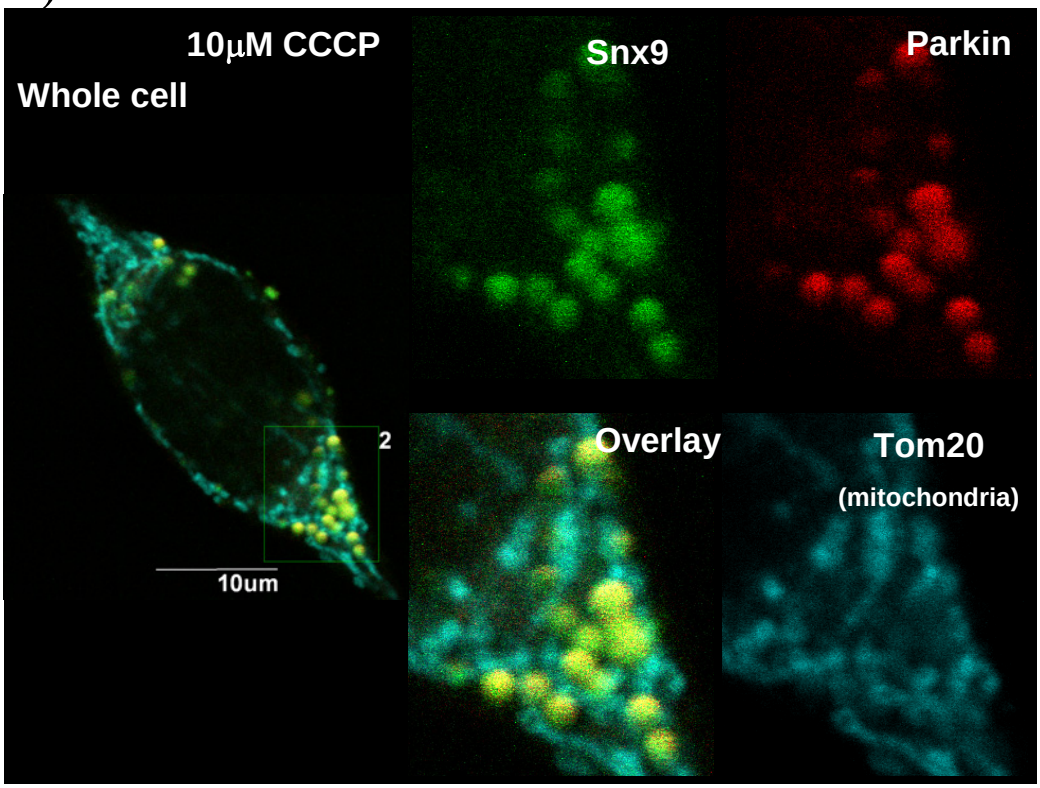
10μM CCCP
Whole cell
2
10um
Snx9
Parkin
Overlay
Tom20
(mitochondria)

It had recently been shown that MDV transport from the mitochondria to peroxisomes required the retromer complex (Braschi et al, 2010). Vacuolar protein sorting VPS35 is a core member of the retromer complex, which binds to the tails (regions of the cargo exposed to the cytosol) of cargo, facilitating their enrichment into vesicles. The retromer complex is known to direct endosome- to -Golgi (retrograde) retrieval of lysosomal hydrolases through vesicular trafficking (Collins, 2008). Importantly, VPS35 was recently identified as a new Parkinson's disease gene (Zimprich et al, 2011), raising the question of whether it could also function along the MDV pathway of mitochondrial quality control, like its counterpart Parkin. To this end, an examination of whether the retromer complex was similarly recruited to the accumulated vesicles upon silencing Snx9 was performed. Indeed, silencing Snx9 in HEK293 cells triggered an enrichment of CFP-VPS35 foci on the outer mitochondrial membrane **(Figure, 3.19),** as it did with Parkin. From the, accumulation of CFP-VPS35 at the mitochondria in siSnx9 cells and the above functions of VPS35 it can be deduced that it (VPS35) might be involved in trafficking of Snx9-dependent MDVs. Future work will be required to determine whether the Parkin and Vps35 labeled structures studding mitochondria in siSnx9 cells are labeling the same, or distinct populations of MDVs.

In summary, the above results demonstrate that Parkin is upstream of Snx9 in the generation of MDVs. Moreover, these results signify a potential interplay between Snx9 and at least two Parkinson Disease genes, VPS35 and Parkin.

Figure 3.19: Silencing Snx9 in HEK 293 cells triggers an accumulation of CFP-VPS35 (green) foci on the outer mitochondrial membrane. CFP-VPS35 was over expressed in siSnx9 cells and the mitochondria, labeled with anti-Tom20 (red). Confocal imaging revealed an enrichment of CFP-VPS35 at the mitochondria.

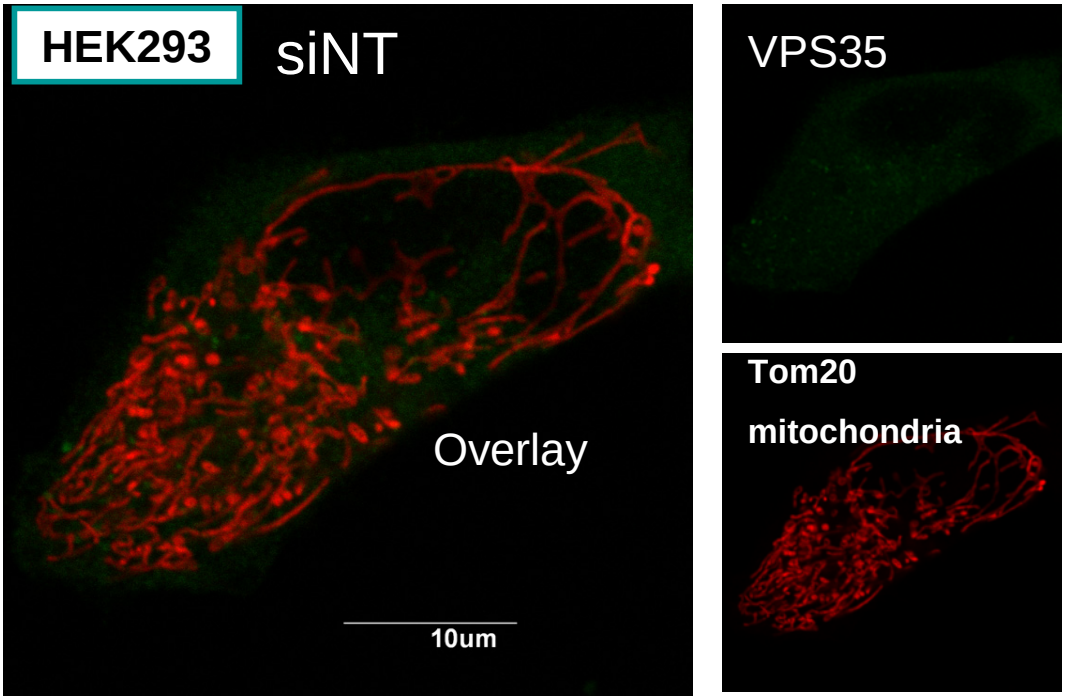
HEK293
siNT
Overlay
10um
VPS35
Tom20
mitochondria

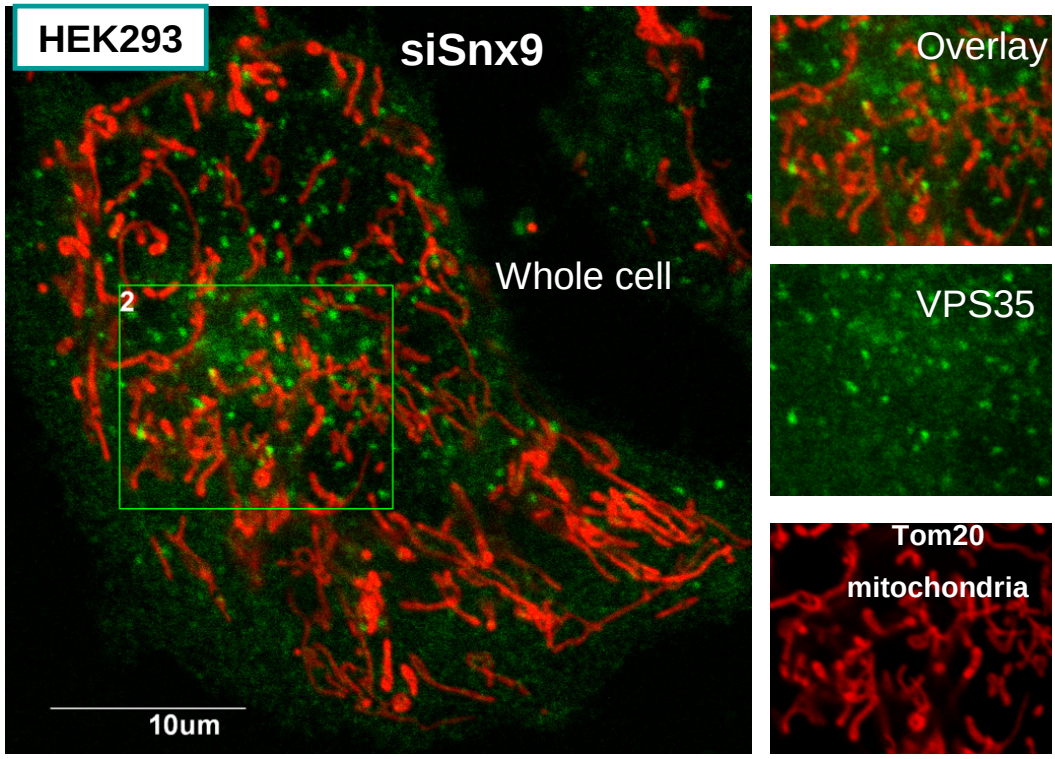
HEK293
siSnx9
Whole cell
2
10um
Overlay
VPS35
Tom20
mitochondria

Discussion

The primary focus of this research program has been to characterize the role of Snx9 in mitochondrial morphology. In doing so, this work has brought to light a novel function for Snx9 in the generation of vesicles at the mitochondria. Furthermore, the arrest of MDVs at the mitochondria in Snx9 silenced cells highlights the extent at which mitochondrial derived vesicles are generated in steady state. It also draws attention to potential functional interactions between Snx9 and two Parkinson's Disease related proteins. Silencing Snx9 in HeLa cells tips the fission- fusion balance in favour of fusion resulting in the mitochondria altering their morphology to form a large interconnected network. Why would silencing an endocytic protein (Snx9) whose major site of action is at the cell surface, upset the fission-fusion balance at the mitochondria? From the results presented under Aim1, it can be deduced that the knockdown of Snx9 created a stressful environment in which the mitochondria were unable to efficiently bud and release vesicles. As highlighted in the introductory section, a typical protective instinct of mitochondria when confronted with stressful stimuli is to fuse through the process of stress induced mitochondrial hyperfusion (Tondera et al, 2009). Up until now, the molecular machinery required for budding and releasing vesicles from the mitochondria was unknown. With the identification of Snx9, we now have the first piece of the puzzle. The Snx9-dependent mitochondrial vesicles represent small sacs of concentric membranous whorls which accumulate under the outer mitochondrial membrane and range in diameter from 80 nm to 200 nm. Interestingly, Pannese (1966) observed similar membranous structures emerging from the mitochondria whilst studying the differentiation of spinal ganglion neuroblasts in chick embryos. Drawing

a parallel between the expansion of the chondriome from the 84th to the 120th hour of incubation and the presence of concentric membranous whorls at the mitochondria; Pannese speculated that the concentric whorls may represent newly forming mitochondria (Pannese, 1966). We now know that mitochondria multiply by growth and division of pre-existing mitochondria through the process of mitochondrial biogenesis (Westermann, 2010). Therefore, it is more likely, that the structures observed by Pannese may have represented vesicles akin to the Snx9-dependent MDVs.

Mitochondrial inclusions reminiscent of Snx9-dependent MDVs were also noted by (Hackenbrock and Caplan, 1969) whilst examining the energized uptake of Ca^{2+} in isolated rat liver mitochondria. Particularly, they pointed out the presence of tightly packed concentrically oriented membranes within the matrix of mitochondria exposed to low concentrations of Ca^{2+} in phosphate free media. These dense (electron-opaque) mitochondrial inclusions were thought to be a result of the Ca^{2+} binding the electron transport membrane (inner mitochondrial membrane). The addition of phosphates liberated the membrane bound Ca^{2+} into the matrix. This diminished the density of the mitochondrial inclusions in the matrix and revealed clearly discernable concentric whorls akin to Snx9-dependent mitochondrial vesicles (Hackenbrock and Caplan, 1969).

Tying in with this, studies of the midgut epithelial cells of *Chaoborus obscuripes* noted the presence of multi-membrane formations (inclusions) at the mitochondria. In particular, they noticed small concentric membranous whorls leaving the mitochondria and appearing in the cytosol over a certain period of functional activity. Based on H_2O_2 treatments of the cells, the authors surmised that the membranous whorls they observed were mainly comprised of lipids. Additionally, they hypothesized that the whorls may play a role

in the lipid metabolism of the midgut epithelial cells (Basurmanova, 1975). As highlighted in the introduction, little is known about the turnover damaged lipids in the mitochondria, therefore there is a possibility that the Snx9-dependent MDVs may be involved in lipid metabolism at the mitochondria. Specifically, Snx9-dependent MDVs might contribute to mitochondrial quality control through the continuous removal of lipids potentially damaged by reactive oxygen species throughout the life of the mitochondria.

Under the current model of quality control, the reactive oxygen species generated by impaired mitochondria are believed to trigger fragmentation of the chondriome; allowing for the sequestration and autophagic clearance of damaged mitochondria (Tatsuta and Langer, 2008). This model is premised on the idea that a fragmentation event of an individual mitochondrial tubule will yield two daughter units, one of which will have lost membrane potential. The mitochondrial kinase, Pink1 would then facilitate the localization of Parkin to the depolarized daughter unit, marking it for degradation by mitophagy.

The findings of this research in Aim3 have demonstrated that Parkin can localize to mitochondria in Snx9 silenced cells. This is an important result as it provides an alternative mechanism for the recruitment of Parkin to the mitochondria without the need to induce global mitochondrial depolarization by CCCP treatment. With the localization of Parkin to steady state mitochondria it stands to reason that Parkin may play a role in other mitochondrial clearance mechanisms apart from autophagy. The labeling of Snx9-dependent MDVs by Parkin suggests such a mechanism, whereby reactive lipid species (oxidized lipids) and/or damaged products could be removed from the mitochondria. This would prevent the build up of damaging oxidized products in the mitochondria and would be especially helpful in primary neurons which unlike immortalized cell lines (e.g. HeLa cells)

depend heavily on mitochondrial oxidative phosphorylation for energy. It would be important to note that the production of Snx9-dependent whorls/vesicles in HeLa cells which do not have endogenous Parkin signals that there may be other E3 ubiqutin ligases involved. In addition to Parkin, another Parkinson's Disease related protein namely, VPS35 was found to label Snx9-dependent MDVs. This was a significant finding as it demonstrated a potential role for the retromer in the transport of Snx9 dependent MDVs.

This work has led to the formulation of a working hypothesis which integrates the known functions of Snx9, VPS35 and Parkin as well as their interacting partners, whereby localized mitochondrial damage e.g. ROS would prompt Pink 1- dependent accumulation of Parkin. Subsequently Parkin would ubiquitinate substrates on the mitochondrial surface and aid in the recruitment of Snx9 to mitochondria potentially through an SH3 (Snx9)- Ubl (Parkin) interaction. Snx9 would aid in the sculpting of the mitochondrial membranes as well as potentially interact with VPS35 in order to enrich cargo into the vesicle. Additionally, Snx9 may act as a scaffold, coordinating with the actin regulating proteins Arp2/3 and WASP for actin polymerization. The actin polymerization at the vesicle neck would potentially provide the additional torsion needed for the scission event to release the vesicle **(Figure, 4.1)**.

The presence of concentric membranous whorls of similar shape and architecture in the lysosome as those found at the mitochondria hinted at the lysosomes as a possible destination for Snx9-dependent MDVs. This raised the possibility that the Snx9-dependent whorls could be delivered to the lysosomes via the autophagosome. In this way, the Snx9-dependent MDVs would be encapsulated by the pre-autophagosome for subsequent fusion with the lysosome. Confocal imaging studies showed that Cherry-Snx9 colocalizes with the

Figure 4.1: Working hypothesis for the formation and release of whorls at the mitochondria. Localized mitochondrial damage would trigger the accumulation of Parkin at the mitochondria in a Pink1 dependent manner. Once at the mitochondrial surface, Parkin would ubiquitinate substrates and aid in the efficient recruitment of Snx9 to mitochondria. Snx9, would then use its lipid binding and sculpting properties to shape the mitochondrial membranes. Additionally, Snx9's interaction with VPS35 would facilitate enrichment of cargo into the vesicle. The release of the budding vesicle from the outer mitochondrial membrane would be mediated by Snx9's interaction with actin regulators. Actin polymerization at the neck of the vesicle would provide the torsion needed to release the Snx9-dependent whorl/vesicle.

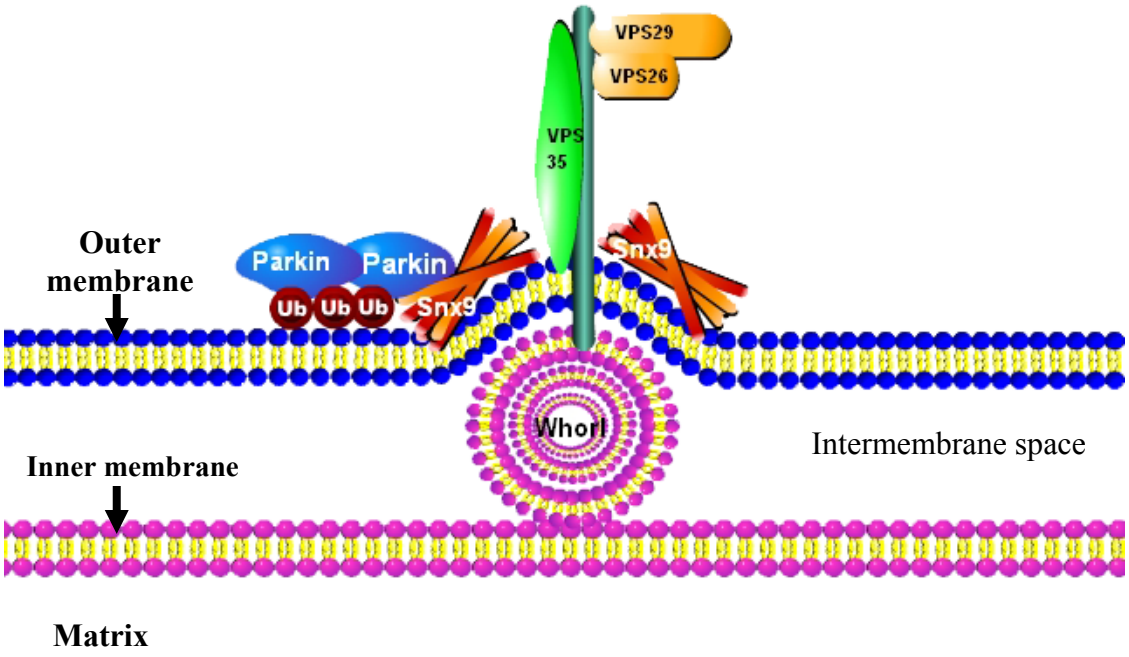
VPS29
VPS26
VPS
35
Outer
membrane
Parkin
Parkin
Ub
Ub
Ub
Snx9
Snx9
Whorl
Intermembrane space
Inner membrane
Matrix

late autophagosome marker, GFP-LC3 (Light chain 3) (not shown). However, the Cherry-Snx9 and GFP-LC3 molecules colocalized in the cytosol and not at the mitochondria. Alternatively, the Snx9-dependent MDVs could be delivered to the lysosome via multi-vesicular bodies, as noted in Tom20 containing mitochondrial vesicles which have been shown to travel to the lysosomes in this way (Soubannier et al, 2012). Future work will continue to examine Snx9-dependent whorls/vesicles in both the autophagy and multi-vesicular body pathways.

The characterization of the Snx9-dependent MDVs extended to the possible ways in which these vesicles achieve their striking architecture. There are two schools of thought on this: The first model is inspired by the formation of mesosomes in bacteria e.g. *E. coli* (Greenwalt and Whiteside, 1975), whereby a crista (inner mitochondrial membrane fold/sac) would collapse into a crescent shaped structure. This would be followed, by the growth and in-folding of either of the two end points on the collapsed crista. The continuous coiling of the growing endpoint would then culminate in the formation of a concentric membranous whorl **(Figure, 4.2)**. Conversely, the second model would be characterized by the elongation of cristae into "septae" like structures. Having run out of room for further extension, the extended crista would fold on itself, coiling into a concentric membranous whorl **(Figure, 4.3)**. The jury is still out on the two models, further analysis of the electron micrographs of Snx9-dependent MDVs will be required in order to determine the model which best represents the way in which these whorls form.

Snx9's distribution in the cytosol is largely diffuse, however Snx9 molecules also form foci/puncta which are mobile and thereby allow Snx9 to exert its functions at different sites in the cell. Aside from its (Snx9) well known role at the cell surface in clathrin

Figure 4.2: An illustration of a potential model for the formation of multi-membrane whorls, inspired by the formation of mesosomes in bacteria e.g. *E. coli* (Greenwalt and Whiteside, 1975).

Collapsed crista model for the formation of mitochondrial whorls

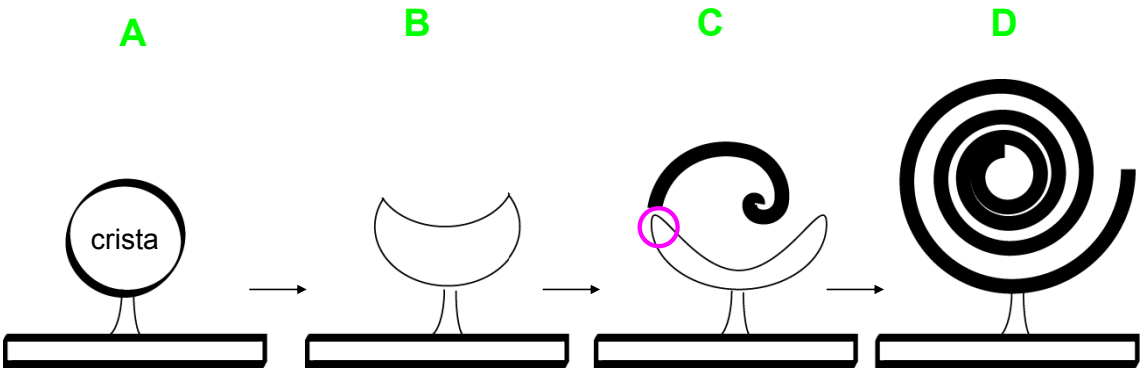

Crista = Inner mitochondrial membrane fold/sac

Crista collapses into a crescent shaped structure

Growth and in-folding of one of the two end points of the collapsed crista.

Note: Endpoint circled in **magenta**

Continuous coiling of the growing endpoint would then result in the formation of a concentric membranous whorl

Figure 4.3: An illustration of a potential model for the formation of membranous whorls in mitochondria. Briefly, newly formed membrane growing out of the base of a cristae junction would cause the continuous extension of a crista into a "septae" like structure. Having run out of room for further elongation the crista would fold on itself, coiling into a concentric membranous whorl.

Extended crista model for the formation of mitochondrial whorls

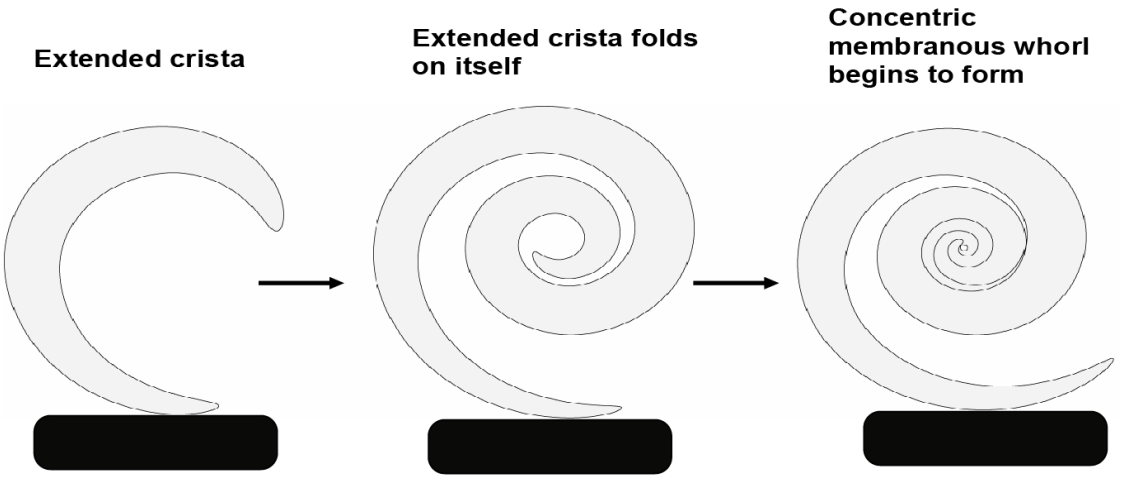

mediated endocytosis, this work has demonstrated that there is a sub-population of Snx9 molecules which translocate from the cytosol to mitochondria. However, the level of Snx9 enrichment at the mitochondria is variable as indicated in the results section under Aim2. In order to further substantiate the evidence for the localization of Snx9 to mitochondria it would have been important to fractionate mitochondria and probe for Snx9. However, the variable recruitment of Snx9 to mitochondria makes this approach less promising. Alternatively, immunogold labeling of Snx9 molecules could have been used to visualize and quantify Snx9 recruitment to the mitochondria.

In conclusion, the results presented in this thesis with respect to Snx9's role in mitochondrial derived vesicles and the larger area of mitochondrial quality control have provided evidence that endocytic proteins affect mitochondrial morphology and function. Moreover, the identification of Snx9 as a molecular engineer for mitochondrial vesicle budding and release serves as a rosetta stone "key" to unlocking the mystery behind the molecular pathways and interactions required for the formation of mitochondrial derived vesicles.

References:

Altmann, R. Die Elementarorganismeni uad ilue Beziehungen zu den Zellen. *Leipzig (von Veit)* (1890).

Arimura, S., Yamamoto, J., Aida, G. P., Nakazono, M. & Tsutsumi, N. Frequent fusion and fission of plant mitochondria with unequal nucleoid distribution. *Proc Natl Acad Sci U S A* **101**, 7805-8 (2004).

Arimura, S., Aida, G. P., Fujimoto, M., Nakazono, M. & Tsutsumi, N. Arabidopsis dynamin-like protein 2a (ADL2a), like ADL2b, is involved in plant mitochondrial division. *Plant Cell Physiol* **45**, 236-42 (2004).

Basurmanova, O. K. [Electron microscopic and electron histochemical study of mitochondrial inclusions in insect intestine epithelial cells]. *Tsitologiia* **17**, 98-100 (1975).

Benda, C. Ueber die Spermatogenese der Vertebraten und höherer Evertebraten, II. Theil: Die Histiogenese der Spermien. *Arch. Anat. Physiol.* **73**, 393-398 (1898).

Bereiter-Hahn, J. & Voth, M. Dynamics of mitochondria in living cells: shape changes, dislocations, fusion, and fission of mitochondria. *Microsc Res Tech* **27**, 198-219 (1994).

Birky, C. W., Jr. Relaxed cellular controls and organelle heredity. *Science* **222**, 468-75 (1983).

Braschi, E., Zunino, R. & McBride, H. M. MAPL is a new mitochondrial SUMO E3 ligase that regulates mitochondrial fission. *EMBO Rep* **10**, 748-54 (2009).

Braschi, E. et al. Vps35 mediates vesicle transport between the mitochondria and peroxisomes. *Curr Biol* **20**, 1310-5 (2010).

Chen, H. et al. Mitofusins Mfn1 and Mfn2 coordinately regulate mitochondrial fusion and are essential for embryonic development. *J Cell Biol* **160**, 189-200 (2003).

Chen, H. & Chan, D. C. Mitochondrial dynamics--fusion, fission, movement, and mitophagy--in neurodegenerative diseases. *Hum Mol Genet* **18**, R169-76 (2009).

Collins, B. M. The structure and function of the retromer protein complex. *Traffic* **9**, 1811-22 (2008).

Dajkovic, A., Mukherjee, A. & Lutkenhaus, J. Investigation of regulation of FtsZ assembly by SulA and development of a model for FtsZ polymerization. *J Bacteriol* **190**, 2513-26 (2008).

Dauer, W. & Przedborski, S. Parkinson's disease: mechanisms and models. *Neuron* **39**, 889-909 (2003).

Deitch, A. D. & Godman, G. C. Cytology of cultured cells surviving actinomycin D. *Proc Natl Acad Sci U S A* **57**, 1607-10 (1967).

Delettre, C. et al. Nuclear gene OPA1, encoding a mitochondrial dynamin-related protein, is mutated in dominant optic atrophy. *Nat Genet* **26**, 207-10 (2000).

Fawcett, D. W. *An atlas of fine structure: the cell, its organelles, and inclusions* (W. B. Saunders Co. (Philadelphia), 1966).

Gandre-Babbe, S. & van der Bliek, A. M. The novel tail-anchored membrane protein Mff controls mitochondrial and peroxisomal fission in mammalian cells. *Mol Biol Cell* **19**, 2402-12 (2008).

Gilson, P. R. et al. Two Dictyostelium orthologs of the prokaryotic cell division protein FtsZ localize to mitochondria and are required for the maintenance of normal mitochondrial morphology. *Eukaryot Cell* **2**, 1315-26 (2003).
Gomes, L. C., Di Benedetto, G. & Scorrano, L. During autophagy mitochondria elongate, are spared from degradation and sustain cell viability. *Nat Cell Biol* **13**, 589-98 (2011).
Gorsich, S. W. & Shaw, J. M. Importance of mitochondrial dynamics during meiosis and sporulation. *Mol Biol Cell* **15**, 4369-81 (2004).
Greenawalt, J. W. & Whiteside, T. L. Mesosomes: membranous bacterial organelles. *Bacteriol Rev* **39**, 405-63 (1975).
Griparic, L. & van der Bliek, A. M. The many shapes of mitochondrial membranes. *Traffic* **2**, 235-44 (2001).
Gutierrez, J., Ballinger, S. W., Darley-Usmar, V. M. & Landar, A. Free radicals, mitochondria, and oxidized lipids: the emerging role in signal transduction in vascular cells. *Circ Res* **99**, 924-32 (2006).
Hackenbrock, C. R. & Caplan, A. I. Ion-induced ultrastructural transformations in isolated mitochondria. The energized uptake of calcium. *J Cell Biol* **42**, 221-34 (1969).
Hales, K. G. & Fuller, M. T. Developmentally regulated mitochondrial fusion mediated by a conserved, novel, predicted GTPase. *Cell* **90**, 121-9 (1997).
Harder, Z., Zunino, R. & McBride, H. Sumo1 conjugates mitochondrial substrates and participates in mitochondrial fission. *Curr Biol* **14**, 340-5 (2004).
Jeyaraju, D. V. et al. Phosphorylation and cleavage of presenilin-associated rhomboid-like protein (PARL) promotes changes in mitochondrial morphology. *Proc Natl Acad Sci U S A* **103**, 18562-7 (2006).
Knott, A. B. & Bossy-Wetzel, E. Impairing the mitochondrial fission and fusion balance: a new mechanism of neurodegeneration. *Ann N Y Acad Sci* **1147**, 283-92 (2008).
Kuwana, T. et al. Bid, Bax, and lipids cooperate to form supramolecular openings in the outer mitochondrial membrane. *Cell* **111**, 331-42 (2002).
Lackner, L. L., Horner, J. S. & Nunnari, J. Mechanistic analysis of a dynamin effector. *Science* **325**, 874-7 (2009).
Laszlo, J., Miller, D. S., McCarty, K. S. & Hochstein, P. Actinomycin D: inhibition of respiration and glycolysis. *Science* **151**, 1007-10 (1966).
Lewis MR, L. W. Mitochondria (and other cytoplasmic struc- tures) in tissue cultures. *American Journal of Anatomy* **17**, 339-401 (1914).
Liesa, M., Palacin, M. & Zorzano, A. Mitochondrial dynamics in mammalian health and disease. *Physiol Rev* **89**, 799-845 (2009).
Lundmark, R. & Carlsson, S. R. Sorting nexin 9 participates in clathrin-mediated endocytosis through interactions with the core components. *J Biol Chem* **278**, 46772-81 (2003).
Lundmark, R. & Carlsson, S. R. SNX9 - a prelude to vesicle release. *J Cell Sci* **122**, 5-11 (2009).
Lutkenhaus, J. & Addinall, S. G. Bacterial cell division and the Z ring. *Annu Rev Biochem* **66**, 93-116 (1997).

Manczak, M. et al. Mitochondria are a direct site of A beta accumulation in Alzheimer's disease neurons: implications for free radical generation and oxidative damage in disease progression. *Hum Mol Genet* **15**, 1437-49 (2006).
Martens, S. & McMahon, H. T. Mechanisms of membrane fusion: disparate players and common principles. *Nat Rev Mol Cell Biol* **9**, 543-56 (2008).
McBride, H. M., Neuspiel, M. & Wasiak, S. Mitochondria: more than just a powerhouse. *Curr Biol* **16**, R551-60 (2006).
Meeusen, S., McCaffery, J. M. & Nunnari, J. Mitochondrial fusion intermediates revealed in vitro. *Science* **305**, 1747-52 (2004).
Meeusen, S. L. & Nunnari, J. How mitochondria fuse. *Curr Opin Cell Biol* **17**, 389-94 (2005).
Messerschmitt, M. et al. The inner membrane protein Mdm33 controls mitochondrial morphology in yeast. *J Cell Biol* **160**, 553-64 (2003).
Mozdy, A. D. & Shaw, J. M. A fuzzy mitochondrial fusion apparatus comes into focus. *Nat Rev Mol Cell Biol* **4**, 468-78 (2003).
Nakada, K. et al. Inter-mitochondrial complementation: Mitochondria-specific system preventing mice from expression of disease phenotypes by mutant mtDNA. *Nat Med* **7**, 934-40 (2001).
Nakada, K., Sato, A. & Hayashi, J. Mitochondrial functional complementation in mitochondrial DNA-based diseases. *Int J Biochem Cell Biol* **41**, 1907-13 (2009).
Narendra, D., Tanaka, A., Suen, D. F. & Youle, R. J. Parkin is recruited selectively to impaired mitochondria and promotes their autophagy. *J Cell Biol* **183**, 795-803 (2008).
Neuspiel, M. et al. Cargo-selected transport from the mitochondria to peroxisomes is mediated by vesicular carriers. *Curr Biol* **18**, 102-8 (2008).
Olichon, A. et al. Loss of OPA1 perturbates the mitochondrial inner membrane structure and integrity, leading to cytochrome c release and apoptosis. *J Biol Chem* **278**, 7743-6 (2003).
Ono, T., Isobe, K., Nakada, K. & Hayashi, J. I. Human cells are protected from mitochondrial dysfunction by complementation of DNA products in fused mitochondria. *Nat Genet* **28**, 272-5 (2001).
Otera, H. et al. Mff is an essential factor for mitochondrial recruitment of Drp1 during mitochondrial fission in mammalian cells. *J Cell Biol* **191**, 1141-58 (2010).
Pannese, E. Structures possibly related to the formation of new mitochondria in spinal ganglion neuroblasts. *J Ultrastruct Res* **15**, 57-65 (1966).
Rambold, A. S., Kostelecky, B., Elia, N. & Lippincott-Schwartz, J. Tubular network formation protects mitochondria from autophagosomal degradation during nutrient starvation. *Proc Natl Acad Sci U S A* **108**, 10190-5 (2011).
Schauss, A. C. et al. A novel cell-free mitochondrial fusion assay amenable for high-throughput screenings of fusion modulators. *BMC Biol* **8**, 100 (2010).
Scott I, L. D. in *Plant Mitochondria* (ed. Kempken, F.) (Springer, Berlin, Germany, 2010).
Sesaki, H. & Jensen, R. E. UGO1 encodes an outer membrane protein required for mitochondrial fusion. *J Cell Biol* **152**, 1123-34 (2001).

Sherer, T. B. et al. An in vitro model of Parkinson's disease: linking mitochondrial impairment to altered alpha-synuclein metabolism and oxidative damage. *J Neurosci* **22**, 7006-15 (2002).
Smallridge, R. Membrane trafficking: Mitochondria–peroxisome connection. *Nature Reviews Molecular Cell Biology* **9**, 186-187 (2008).
Smith, M. A. et al. Cytochemical demonstration of oxidative damage in Alzheimer disease by immunochemical enhancement of the carbonyl reaction with 2,4-dinitrophenylhydrazine. *J Histochem Cytochem* **46**, 731-5 (1998).
Soubannier, V. et al. A vesicular transport pathway shuttles cargo from mitochondria to lysosomes. *Curr Biol* **22**, 135-41 (2012).
Soulet, F., Yarar, D., Leonard, M. & Schmid, S. L. SNX9 regulates dynamin assembly and is required for efficient clathrin-mediated endocytosis. *Mol Biol Cell* **16**, 2058-67 (2005).
Sterky, F. H., Lee, S., Wibom, R., Olson, L. & Larsson, N. G. Impaired mitochondrial transport and Parkin-independent degeneration of respiratory chain-deficient dopamine neurons in vivo. *Proc Natl Acad Sci U S A* **108**, 12937-42 (2011).
Suzuki, H. Protein-protein interactions in the mammalian brain. *Journal of physiology* **575 (Pt2)**, 373-377 (2006).
Taguchi, N., Ishihara, N., Jofuku, A., Oka, T. & Mihara, K. Mitotic phosphorylation of dynamin-related GTPase Drp1 participates in mitochondrial fission. *J Biol Chem* **282**, 11521-9 (2007).
Tanaka, A. et al. Proteasome and p97 mediate mitophagy and degradation of mitofusins induced by Parkin. *J Cell Biol* **191**, 1367-80 (2010).
Tatsuta, T. & Langer, T. Quality control of mitochondria: protection against neurodegeneration and ageing. *Embo J* **27**, 306-14 (2008).
Tondera, D. et al. SLP-2 is required for stress-induced mitochondrial hyperfusion. *Embo J* **28**, 1589-600 (2009).
Trempe, J. F. et al. SH3 domains from a subset of BAR proteins define a Ubl-binding domain and implicate parkin in synaptic ubiquitination. *Mol Cell* **36**, 1034-47 (2009).
Twig, G. et al. Fission and selective fusion govern mitochondrial segregation and elimination by autophagy. *Embo J* **27**, 433-46 (2008).
Van Laar, V. S. et al. Bioenergetics of neurons inhibit the translocation response of Parkin following rapid mitochondrial depolarization. *Hum Mol Genet* **20**, 927-40 (2011).
Vander Heiden, M. G., Chandel, N. S., Williamson, E. K., Schumacker, P. T. & Thompson, C. B. Bcl-xL regulates the membrane potential and volume homeostasis of mitochondria. *Cell* **91**, 627-37 (1997).
Vander Heiden, M. G. & Thompson, C. B. Bcl-2 proteins: regulators of apoptosis or of mitochondrial homeostasis? *Nat Cell Biol* **1**, E209-16 (1999).
Walensky, L. D. BCL-2 in the crosshairs: tipping the balance of life and death. *Cell Death Differ* **13**, 1339-50 (2006).
Wasiak, S., Zunino, R. & McBride, H. M. Bax/Bak promote sumoylation of DRP1 and its stable association with mitochondria during apoptotic cell death. *J Cell Biol* **177**, 439-50 (2007).
Westermann, B. Merging mitochondria matters: cellular role and molecular machinery of mitochondrial fusion. *EMBO Rep* **3**, 527-31 (2002).

Westermann, B. Mitochondrial fusion and fission in cell life and death. *Nat Rev Mol Cell Biol* **11**, 872-84 (2010).
Whitworth, A. J. et al. Rhomboid-7 and HtrA2/Omi act in a common pathway with the Parkinson's disease factors Pink1 and Parkin. *Dis Model Mech* **1**, 168-74; discussion 173 (2008).
Yoshii, S. R., Kishi, C., Ishihara, N. & Mizushima, N. Parkin mediates proteasome-dependent protein degradation and rupture of the outer mitochondrial membrane. *J Biol Chem* **286**, 19630-40 (2011).
Youle, R. J. & Karbowski, M. Mitochondrial fission in apoptosis. *Nat Rev Mol Cell Biol* **6**, 657-63 (2005).
Youle, R. J. & Narendra, D. P. Mechanisms of mitophagy. *Nat Rev Mol Cell Biol* **12**, 9-14 (2011).
Zick, M., Rabl, R. & Reichert, A. S. Cristae formation-linking ultrastructure and function of mitochondria. *Biochim Biophys Acta* **1793**, 5-19 (2009).
Zimprich, A. et al. A mutation in VPS35, encoding a subunit of the retromer complex, causes late-onset Parkinson disease. *Am J Hum Genet* **89**, 168-75 (2011).
Zuchner, S. et al. Mutations in the mitochondrial GTPase mitofusin 2 cause Charcot-Marie-Tooth neuropathy type 2A. *Nat Genet* **36**, 449-51 (2004).
Zunino, R., Schauss, A., Rippstein, P., Andrade-Navarro, M. & McBride, H. M. The SUMO protease SENP5 is required to maintain mitochondrial morphology and function. *J Cell Sci* **120**, 1178-88 (2007).
Zunino, R., Braschi, E., Xu, L. & McBride, H. M. Translocation of SenP5 from the nucleoli to the mitochondria modulates DRP1-dependent fission during mitosis. *J Biol Chem* **284**, 17783-95 (2009).

Contributions of Collaborators:

The embedding and sectioning of transmission electron microscopy samples was carried out by Peter Rippstein (University of Ottawa Heart Institute, Canada).

The genome wide siRNA (GWsiRNA) screen was carried out in collaboration with Robert Screaton (Children's Hospital of Eastern Ontario- Research Institute, Canada).

Lerato Magosi, Highest Hons. B.Sc

EDUCATION

Master of Science, Biochemistry

University of Ottawa 2010 - Present

- Admission scholarship ($8,960 x 2 years)
- Excellence scholarship ($15,398)
- Ontario Graduate Scholarship in Science and Technology, 2010 ($ 16,000)
- Poster Prize – Faculty of Medicine Graduate Studies Biochemistry, 2011 ($ 50)
- Graduation date: June 2012

Highest Honours Bachelor of Science, Biochemistry & Biotechnology, Minor in Chemistry

Carleton University 2006-2010

- Completed, 11.35 out of 12.00 CGPA, corresponding letter grade: A
- Dean's list, 2007-2008
  2008-2009
- Senate Medal for Outstanding Academic Achievement, 2010
- Merit Award: Biochemistry from the Society of Chemical Industry (SCI) of Canada, 2010

HIGHLIGHTS OF QUALITIES

- Eager, creative, and hard-working for complex challenges and projects
- Experience with Instruments - High Pressure Capillary Electrophoresis (HPCE)
  - High Performance Liquid Chromatography (HPLC)
  - Scanning Electron Microscopy (SEM)
  - Transmission Electron Microscopy (TEM)
  - Confocal Microscopy
- Experience with Techniques - Western blot, PEG assay, Mitochondrial fractionation, Immunoprecipitation, live- cell imaging
- Molecular biology techniques - Gradient PCR, Cloning
- Cell culture - transfection, siRNA, growing and maintenance of HeLa, Hek293 and Cos 7 mammalian cell lines
- Experience with Software - ExPASy **:** protparam tool, CPH models, Prosite, ELM (Smart server), Netphos 2.0 server and Jpred3, Gentle

WORK EXPERIENCE

Research assistant (Official title: Summer student) May-Aug 2010
Dr McBride's lab, University of Ottawa Heart Institute

- Performed PCR based sub-cloning of target DNA sequences from parent recombinant plasmid transcription vectors into destination plasmid expression vectors (pEYFP-N1 and pEYFP-C1)
- Transformed competent cells (DH5α and XL-1 blue) with the recombinant destination plasmid expression vector in order to amplify the vector.
- Co-transfected Cos 7 and HeLa cells with mini-prep purified recombinant destination plasmid expression vector and OCT-CFP.
- Maintained Cos 7 and HeLa cell lines (passaging)
- Performed immunostaining of the transfected cells to characterize the gene expression product (protein) of the target DNA sequence and how it affected mitochondrial morphology through confocal microcopy.

Lab assistant (Official title: Student volunteer) Sept08-Apr09
Biochemistry 3rd year laboratory
Lab coordinator: Mihaela Flueraru, Carleton University

- Assisted in setting up for experiments before lab sessions
- Assisted in clearing up after laboratory sessions
- Provided support for experiments which outlasted the standard laboratory session period.

Research assistant (Official title: Student volunteer) Apr-Aug 2008
Dr Lai's lab, Carleton University

- Acquired the first protocol in the Lai lab for synthesizing magnetic particles and optimized the protocol for use in the removal of estrogen (*17 β-estradiol*) from water at the ppm level.
- Characterized the bare magnetic particles with High Pressure Capillary Electrophoresis
- The optimized magnetic particle protocol and characterized magnetic particles were then used as a starting base for the projects of new MSc (Master of Science) students in the Lai lab.
- Analyzed molecularly imprinted polymers and their non-imprinted counter parts with solid state NMR (**Instrument:** Bruker avance 400- solid state NMR , University of Ottawa).

RESEARCH EXPERIENCE

Graduate research:

1. I presented a poster at the 2011 uOttawa Biochemistry Immunology and Microbiology poster day entitled: From endocytosis to mitochondrial fission? Role of snx9 in mitochondrial morphology. Mitochondria have a plastic physique which allows them to fragment into small spherical organelles for separation during cell division. Alternatively, they can fuse into a tubular network for the spread of metabolic energy around the cell.

Mitochondrial fragmentation is important for the regulation of cell death and dysregulation of mitochondrial division has been implicated in heart failure. Mitochondrial fission is primarily governed by the GTPase Drp1 (dynamin related protein 1) with the aid of MFF (mitochondrial fission factor) and Fis1 (fission protein 1) as adaptors. Although the central regulator of mitochondrial fission (Drp1) has been identified, the molecular mechanism of mitochondrial fragmentation in mammals is unknown. We have identified Snx9 (sorting nexin 9) as a novel player in mitochondrial fission through a genome wide siRNA screen monitoring mitochondrial morphology. Genes, that when silenced afforded fused mitochondria were identified as fission candidates. Of those, the level of fusion measured upon silencing Snx9 emulated that obtained when silencing the key mitochondrial fission regulator Drp1, suggesting a role for Snx9 in fission. I demonstrated that Snx9 transiently associates with mitochondria in healthy cells and upon stimulation of death-induced mitochondrial fragmentation.

2. Undergraduate thesis:

My undergraduate thesis was entitled"(Methacrylic acid-co-ethynyl glycol dimethacrylic acid) ferrimagnetic polymer beads for binding and extraction of 17β-estradiol from water samples by magnetic separation". The steroid estradiol is a major sex hormone found in women and has been implicated as an endocrine disruptor in men; therefore its removal from drinking water is an important issue, however it is more abundant in females. I synthesized ferrimagnetic polymer beads that could be used for the extraction of *17β-estradiol* at low concentration levels (≤1 ppm). The beads were synthesized by a two–step polymerization process. The MAA-co-EGDMA magnetic polymer beads were demonstrated in a method for extraction of *17β-estradiol,* followed by magnetic separation. The magnetic polymer beads were capable of binding *17β-estradiol* at 99±1% recovery, as determined from HPLC measurements.

3.Undergraduate- Directed studies:

My directed studies report was titled "Sulphoximines: History, biochemistry, preparation, synthetic utility, general properties, and the biochemistry of sulfoxides and sulfones." Sulphoximines are highly versatile sulphur compounds that can be prepared from various synthetic reactions and can be employed as starting materials for synthetic reactions. Sulfoxides, sulfones, and sulphoximines have numerous medical applications. Sulphoximines have been used in construction of anti-tumor drugs and antiviral agents.

BIOCHEMISTRY FIELD 2007- Present

- Member of the Canadian Society of Biochemistry, Molecular and Cellular Biology
- Member of the Carleton Chemistry and Biochemistry Society (2007-2010)
- Member of the Society of chemical industry 2010-Present

LEADERSHIP ACTIVITIES

Educator (Volunteer)

Let's talk science, Ottawa

- Judge at the Westboro Academy Science Fair in June 2010 and June 2011

- Presented science activities for teachers at Ottawa teachers' college to aid in enhancing student's learning experiences in the class room in December 2008 and December 2009

EXTRA-CURRICULAR ACTIVITIES

Activities (Culture)

National Arts Centre, Ottawa

- Dance Subscriber, 08-09 and 09 - 10 seasons

100% Martial arts, Ottawa

- Jujitsu yellow belt, 2011

COURSES

Title	Code	Term	Grade
M.Sc			
Current Topics in RNA Molecular Biology	BCH 8310	Winter 2012	Current
Current Topics in Biological Imaging	CMM 7301	Winter 2011	6.0/6.0 (A^+)
B.Sc Hons:			
Protein Structure and Function	BCH 3125	Winter 2010	5.5/6.0 (A)
General Intermediary Metabolism	BCH 3120	Winter 2010	4.5/6.0(B+)
Low Intermediate French	FLS 1511	Winter 2010	6.0/6.0 (A^+)
Molecular Genetics	BIOL 3104	Fall 2009	6.0/6.0 (A^+)
Industrial Chemistry	CHEM 3700	Fall 2009	6.0/6.0 (A^+)
Plant Physiology and Biochemistry	BIO 3140	Fall 2009	5.5/6.0 (A)
Directed Special Studies	BIOC 4901	Summer 2009	6.0/6.0 (A^+)
Introduction to Inorganic and Bioinorganic Chemistry	CHEM 2501	Winter 2009	6.0/6.0 (A^+)
Practical Biochemistry	BIOC 3006	Fall 2008 - Winter 2009	12.0/12.0 (A^+)
Honours Project	BIOC 4908	Fall 2008 - Winter 2009	12.0/12.0 (A^+)
Elementary French	FLS 1510	Winter 2009	6.0/6.0 (A^+)
Introduction to American Sign Language	ASLA 1000	Summer 2008	11.0/12.0 (A)
Methods in Molecular Genetics	BIOL 4106	Fall 2008	5.5/6.0 (A)
Advanced Organic Chemistry II	CHEM 3202	Winter 2008	6.0/6.0 (A^+)
Directed Special Studies	BIOL 4901	Winter 2008	6.0/6.0 (A^+)
Introductory Genetics	BIOL 2104	Winter 2008	5.5/6.0 (A)
Advanced Organic Chemistry I	CHEM 3201	Fall 2007	5.5/6.0 (A)
Linear Algebra	MATH 1107	Fall 2007	6.0/6.0 (A^+)
Plants: Form and Function	BIOL 2002	Fall 2007	5.0/6.0 (A^-)
Organic Chemistry II	CHEM 2208	Winter 2007	6.0/6.0 (A^+)
Microbiology	BIOL 2303	Winter 2007	5.0/6.0 (A^-)

Analytical Chemistry	CHEM 2303	Winter 2007	5.5/6.0 (A)
Cell Physiology and Biochemistry	BIOC 2200	Fall 2006	5.0/6.0 (A^-)
Organic Chemistry I	CHEM 2203	Fall 2006	5.5/6.0 (A)
Introduction to Statistical Modeling I	STAT 2507	Fall 2006	6.0/6.0 (A^+)